

Abundance, growth and respiration rates of the cold-water scleractinian *Tethocyathus endesa* in the Chilean Fjord region



Master Thesis

in the subject Biological Oceanography

Mathematisch-Naturwissenschaftliche Fakultät
Christian-Albrechts-Universität zu Kiel

Submitted by

Susann Diercks

Olshausenstraße 23, 24118 Kiel

Matrikel: 997870

November 2015

1 Content

Cover picture: *Tethocyathus endesa*

Reviewer: Prof. Dr. Ulf Riebesell
GEOMAR-Helmholtz Centre for Ocean Research Kiel
Düsternbrooker Weg 20, D-24105 Kiel, Germany

Second Reviewer: Dr. Jürgen Laudien
Alfred Wegener Institute Helmholtz Center for Polar and Marine Research
Am Alten Hafen 26, D-27568 Bremerhaven, Germany

1 CONTENT

1	Content.....	3
2	List of figures.....	6
3	List of tables.....	8
4	List of abbreviations.....	9
5	Abstract.....	11
5.1	Abstract.....	11
5.2	Kurzfassung.....	12
6	Introduction.....	13
6.1	Ocean acidification (OA).....	13
6.2	Study site.....	14
6.2.1	The Chilean Fjord region.....	14
6.2.2	Comau Fjord.....	14
6.2.3	Piti-Palena Fjord.....	16
6.3	Cold-water corals (CWC).....	17
6.4	The cold-water scleractinian <i>Tethocyathus endesa</i>	17
7	State of the art.....	19
7.1	CWC and ocean acidification.....	19
7.1.1	CWC in the fjord Comau and ocean acidification.....	20
8	Aim of work and work strategies.....	21
9	Material and methods.....	22
9.1	Sampling sites.....	22
9.1.1	Comau Fjord.....	22
9.1.2	Piti-Palena Fjord.....	23
9.2	Physical parameters.....	24
9.2.1	Carbonate chemistry.....	24
9.3	Abundance regarding depth and substrate inclination.....	25
9.4	Cross-transplantation experiment.....	27
9.4.1	Setup.....	27

1	Content	
9.4.2	Mass increase	28
9.4.3	Respiration	28
9.5	Data processing	32
10	Results	33
10.1	Hydrology	33
10.1.1	CTD profiles	33
10.1.2	Long-term temperature data measurements	36
10.1.3	Sea water pH	38
10.1.4	Sea water TA.....	39
10.2	Abundance in relation to depth and substrate inclination	40
10.2.1	Abundance in relation to depth.....	40
10.2.2	Abundance regarding substrate inclination	42
10.3	Mass increase	45
10.4	Respiration.....	46
10.4.1	Correlation of the calyx surface area and DM.....	46
10.4.2	Respiration rates.....	47
11	Discussion.....	49
11.1	Oceanographic measurements.....	49
11.2	Abundance regarding depth and substrate inclination	51
11.2.1	Methodological considerations	51
11.2.2	Abundance in relation to water depth.....	51
11.2.3	Abundance regarding substrate inclination	53
11.3	Mass increase	54
11.3.1	Methodological considerations	54
11.3.2	Influence of carbonate chemistry on <i>in situ</i> growth rates	55
11.4	Respiration rates	56
11.4.1	Methodological considerations	56
11.4.2	Influence of carbonate chemistry on respiration rates.....	57
12	Conclusion.....	59
13	Outlook.....	60
14	Acknowledgements.....	61

1	Content	
15	References.....	62
16	Appendix	69
17	Declaration of Academic Integrity (Selbstständigkeitserklärung).....	78

2 LIST OF FIGURES

Figure 1: Multi-model simulated time series (Coupled Model Intercomparison Project; CMIP5) from 1950 to 2100 for global mean ocean surface pH (IPCC, 2013).....	13
Figure 2: Overview of Patagonia and Comau Fjord	15
Figure 3: High and low tide at the Huinay Scientific Field Station	16
Figure 4: Overview on Patagonia and Piti-Palena Fjord.....	16
Figure 5: The cold-water scleractinian <i>Tethocyathus endesa</i>	17
Figure 6: Morphology of a solitary scleractinian. Modified after Stolzenberger-Ramirez (2014).	18
Figure 7: Global distribution of corals.....	19
Figure 8: Map of Comau Fjord with sampling sites Lilliguapi and XHuinay North	22
Figure 9: Piti-Palena Fjord and sampling station Ensenada de Las Islas	23
Figure 10: Sampling frame to measure abundance and substrate inclination (Wendländer, 2014).....	26
Figure 11: Photos of sampling frame with enumeration of <i>T. endesa</i> with PhotoScape and measurement of substrate inclination with MB Ruler.	26
Figure 12: Experimental setup for cross-transplantation experiment with <i>T. endesa</i>	27
Figure 13: Coral glued on a screw, screwed-in the lid of a 100ml Schott bottle.	29
Figure 14: Schematic drawing of water bath setup for incubation.	30
Figure 15: Schematic drawing of respiration chamber with coral glued on screw.....	31
Figure 16: Optical needle-type Oxygen Micro sensor and PVC block with inlet, flow-through, sealed micro sensors and outlet (Wurz, 2014).	32
Figure 17: CTD profiles for salinity at XHuinay North at different sampling dates.....	33
Figure 18: CTD profiles for temperature [°C] at XHuinay North at different sampling dates. Red lines represent casts at rising tide; blue lines represent casts at falling tide.	34
Figure 19: CTD profiles for salinity at Lilliguapi at different sampling dates..	34
Figure 20: CTD profiles for temperature [°C] at Lilliguapi at different sampling dates..	35
Figure 21: CTD profiles for salinity and temperature [°C] at Ensenada de Las Islas..	35
Figure 22: Boxplots showing monthly water temperatures at sampling site XHuinay North from a water depth of 20m.....	36
Figure 23: Boxplots showing monthly water temperatures at sampling site Lilliguapi from a water depth of 20m..	37

2 List of figures

Figure 24: Boxplots showing monthly water temperatures at sampling site Ensenada de Las Islas from a water depth of 22m..	37
Figure 25: Sea water pH at sampling site Lilliguapi (7.87 ± 0.06) and XHuina North (7.66 ± 0.04)..... Fehler! Textmarke nicht definiert.	
Figure 26: Boxplots of TA (mmol/l) measured at Lilliguapi (2.219 ± 0.020 mmol/l) and XHuina North (2.241 ± 0.031 mmol/l) and Ensenada de Las Islas (2.182 ± 0.004 mmol/l)..	39
Figure 27: Boxplots showing population density [n/m^2] of <i>T. endesa</i> in different water depths (16m, 19m, 22m and 25m) at sampling site XHuina North..	40
Figure 28: Boxplots, showing population density in individuals (n) per m^2 at a water depth of 21/22m at sampling station Ensenada de Las Islas and XHuina North .	41
Figure 29: Photo of sampling frame at Lilliguapi with maximum observed abundance of <i>T. endesa</i> .	41
Figure 30: Boxplots, representing the population density of <i>T. endesa</i> in individuals (n) per m^2 for different substrate inclinations at XHuina North..	43
Figure 31: Boxplots, representing the population density of <i>T. endesa</i> in individuals (n) per m^2 for different substrate inclinations at Ensenada de Las Islas.....	44
Figure 32: Boxplots showing mass increase of control groups in $\% y^{-1}$..	45
Figure 33: Boxplots showing mass increase of control groups and transplanted groups in $\% y^{-1}$	46
Figure 34: Scatterplot with regression line of calyx surface area in cm^2 and DM in g.....	46
Figure 35: Boxplots showing respiration rates [$\mu Mol O_2 \times cm^2 \times d^{-1}$] of all treatments.....	48
Figure 36: Schematic drawing of a rocky overhang, colonized by <i>T. endesa</i> and <i>C. huinayensis</i> .	53

3 LIST OF TABLES

Table 1 TA values (mmol/l with SD) at XHuainay North, Lilliguapi and Ensenada de Las Islas between 26.01.2015 and 21.02.2015.....	39
Table 2 Population densities [n/m^2] of <i>T. endesa</i> in four different depth zones at XHuainay North.....	40
Table 3 Groups of inclination angles and related population densities at XHuainay North calculated to $1m^2$	42
Table 4 Groups of inclination angles and related population densities at Ensenada de Las Islas calculated to $1m^2$	43
Table 5 Respiration rates (RR) of all treatments, given in $\mu\text{Mol O}_2 \times \text{cm}^2 \times \text{d}^{-1}$ with SD. Respiration rates were measured with a manual and an automatical method.....	47
Table 6 Respiration rates (RR) of all treatments, given in $\mu\text{Mol O}_2 \times \text{cm}^2 \times \text{d}^{-1}$ with SD. Values of manual and automatical measurements are amalgamated.....	47
Table A1.1 Logged temperature [$^{\circ}\text{C}$] at XHuainayNorth (Feb. 2014-Feb. 2015), depth: 20m.....	69
Table A1.2 Logged temperature [$^{\circ}\text{C}$] at Lilliguapi (February 2014-January 2015), depth: 20m.....	69
Table A2.1 Manually pH measurements at Lilliguapi and XHuainay North.....	70
Table A2.2 Statistical report for ANOVA of manually measured pH values at Lilliguapi and XHuainay North	70
Table A3.1 Total Alkalinity at XHuainay North, Lilliguapi and Ensenada de Las Islas in mmol l^{-1}	71
Table A3.2 Statistical report for ANOVA of Total Alkalinity values at XHuainay North and Ensenada de Las Islas.....	71
Table A4.1 Abundancy in different depth zones at XHuainay North.....	72
Table A4.2 Abundancy in different depth zones at Ensenada de Las Islas.....	74
Table A4.3 Statistical report for ANOVA of abundancy of <i>T.endesa</i> in 21/22m depth at Ensenada de Las Islas and XHuainay North.....	75
Table A5.1 Mass increase (mg y^{-1} and $\% \text{d}^{-1}$). Treatments: L and X (Controls), LtoX (transplanted from high to low pH), XtoL (transplanted from low to high pH).....	75
Table A6.1 Respiration rates [$\mu\text{Mol O}_2 \text{cm}^{-2} \text{d}^{-1}$] measured via handheld Luminescent/Optical Dissolved Oxygen Probe.....	76
Table A6.2 Respiration rates [$\mu\text{Mol O}_2 \text{cm}^{-2} \text{d}^{-1}$] measured via optodes and respiration chambers.....	77

4 LIST OF ABBREVIATIONS

A	Area
ANOVA	Analysis of variance
AWI	Alfred Wegener Institute Helmholtz Center for polar and marine research
°C	Degree Celsius
<i>C. huinayensis</i>	<i>Caryophyllia huinayensis</i>
CaCO ₃	Calcium carbonate
CMIP5	Coupled Model Intercomparison Project
CTD probe	Conductivity-temperature-depth probe
CO ₂	Carbon dioxide
pCO ₂	Partial pressure of Carbon dioxide
CWC	Cold-water coral
d	Day
<i>D. dianthus</i>	<i>Desmophyllum dianthus</i>
DM	dry mass
Fig.	Figure
<i>in situ</i>	"on site"; an observed phenomenon exactly in place where it occurs
<i>in vitro</i>	observed phenomenon in an artificial environment
kg	kilogram
km	kilometer
LED	Light-emitting diode
l	Liter
LAT	lowest astronomical tide
M	Molar mass (kg/mol)
ml	Milliliter
<i>M. oculata</i>	<i>Madrepora oculata</i>
mol	number of atoms in precisely 12 thousandths of a kilogram (0.012 kg) of C ⁻¹²
mmol	1/1000 of a mol
MSAAW	Modified Sub-Antarctic Water
n	Number of specimen
OA	Ocean Acidification
O ₂	Oxygen
pH	the negative of the logarithm to base 10 of the activity of the hydrogen ion

4 List of abbreviations

R	Respiration rate [$\mu\text{Mol/L}$]
SCUBA	Self-contained underwater breathing apparatus
SD	Standard deviation
t	time [h]
TA	Total Alkalinity
V	Volume
yr	Year
XHuinay North	Cross Huinay North

5 ABSTRACT

5.1 ABSTRACT

Many cold-water corals act as bioengineers, forming complex, three-dimensional habitats that are beneficial for other species. Whether the cold-water coral biocenosis in the Patagonian fjord region has a comparable ecological importance is yet not clear. *Tethocyathus endesa* (Cairns *et al.*, 2005) is a recently discovered solitary scleractinian and besides *Desmophyllum dianthus* and *Caryophyllia huinayensis* one of the most frequent cold-water coral species thriving in the Chilean fjord region. In two Chilean fjords, year-round temperature measurements and a frame based census have been carried out to describe the temperature environment and to quantify abundance in relation to water depth and substrate inclination. *T. endesa* thrives in water temperatures between 9.61°C and 15.30°C and can reach maximum abundancies up to 1,161 individuals per m². It settles at substrates with an inclination between 71° and 145°. This study aims for a better understanding of the reaction of this cold-water coral in a changing ocean. Besides ocean warming, especially ongoing ocean acidification may have extensive impacts on all calcifying organisms. The fjord Comau exhibits horizontal and vertical pH-gradients, which resemble the values that are forecasted by the recent IPCC-report for the end of the next century. These conditions allow experiments along the natural horizontal pH-gradient that can provide estimations on the influence of changing water parameters on *T. endesa*. Two parameters, which can be used to predict the influence of these environmental changes, are growth and respiration rates. The long-term study (12 months) revealed an *in situ*-growth rate of $10.34 \pm 4.34\% \text{ yr}^{-1}$ ($0.03 \pm 0.01\% \text{ d}^{-1}$), which is comparable to other cold-water coral species of this region. In the present *in situ* experiment, *T. endesa* specimens have been cross transplanted between a location with high pH of 7.87 ± 0.06 and a Total Alkalinity (TA) of $2.219 \pm 0.020 \text{ mmol/l}$ and a location with a low pH of 7.66 ± 0.04 and a TA of $2.241 \pm 0.031 \text{ mmol/l}$, respectively. Corals moved to low pH-conditions showed mass increases of $10.51 \pm 1.14\% \text{ yr}^{-1}$ ($0.03 \pm 0.00\% \text{ d}^{-1}$), which is comparable to the control group under high pH conditions with $9.82 \pm 4.38\% \text{ yr}^{-1}$ ($0.03 \pm 0.01\% \text{ d}^{-1}$). This may indicate physiological adaptations of *T. endesa*, enabling this species to up-regulate internal pH in tissues where biologically induced calcification takes place. Specimens from the cross-transplantation experiment, which have been transplanted from high to low pH conditions showed no statistical difference in respiration rates ($9.88 \pm 4.52 \mu\text{mol O}_2 \times \text{cm}^2 \times \text{d}^{-1}$) compared to their control group ($8.05 \pm 2.93 \mu\text{mol O}_2 \times \text{cm}^2 \times \text{d}^{-1}$). As shown by the present study, the scleractinian cold-water coral *T. endesa* has the ability to thrive in conditions with future acidified sea water. Although cold-water corals reveal the potential of calcification under decreased sea water pH, the underlying balancing mechanisms are suggested to be accompanied by energetic effort, leading to a reduction of energy for other physiological important processes.

5.2 KURZFASSUNG

Viele Kaltwasserkorallenarten bilden komplexe, dreidimensionale Strukturen und sind als Bioingenieure Habitatbildner für andere Meeresorganismen. Inwiefern die Kaltwasserkorallen der patagonischen Fjordregion eine ähnlich wichtige, ökologische Rolle für die ansässige Lebensgemeinschaft einnehmen ist bisher ungeklärt. Die erst kürzlich beschriebene solitäre Steinkoralle *Tethocyathus endesa* (Cairns *et al.*, 2005), ist nach *Desmophyllum dianthus* und *Caryophyllia huinayensis*, die dritthäufigste Kaltwasserkorallenart in der chilenischen Fjordregion. In zwei chilenischen Fjorden wurden ganzjährige Temperaturmessungen vorgenommen und die Abundanz von *T. endesa* im Bezug zur Wassertiefe und des Neigungswinkels des besiedelten Substrats bestimmt. *T. endesa* erreicht dort maximale Abundanzen von 1161 Individuen pro m² und siedelt in Wassertemperaturen zwischen 9,61°C und 15,30°C. Das besiedelte Substrat weist Neigungswinkel zwischen 71° und 145° auf. Alle kalzifizierenden Organismen sind von voranschreitender Ozeanversauerung und globaler Erwärmung beeinflusst. Ziel dieser Arbeit ist daher ein besseres Verständnis der Reaktionen von *T. endesa* auf diese Veränderungen des Ozeans. Der Comau Fjord weist bereits heute vertikale und horizontale pH-Gradienten auf, die von dem IPCC für das Ende dieses Jahrhunderts für alle Ozeane vorhergesagt werden. Daher eignet sich der natürliche, horizontale pH-Gradient des Fjords, Vorhersagen über die Reaktionen von *T. endesa* gegenüber dem Einfluss wechselnder Wasserparameter zu treffen. Untersuchte Parameter hierfür waren Wachstums- und Respirationsraten. Die experimentell ermittelte langzeit *in situ* Wachstumsrate von *T. endesa* entspricht $10,34 \pm 4,43\% \text{ y}^{-1}$ ($0,03 \pm 0,01\% \text{ d}^{-1}$) und ist vergleichbar mit anderen Kaltwasserkorallenarten dieser Region. Im Rahmen eines Kreuztransplantationsexperiments wurden Individuen von *T. endesa* aus einem Habitat mit einem hohen pH von $7,87 \pm 0,06$ und einer Alkalinität von $2,219 \pm 0,020 \text{ mmol/l}$ und einem Habitat mit niedrigem pH von $7,66 \pm 0,04$ und einer Alkalinität von $2,241 \pm 0,031 \text{ mmol/l}$ jeweils an den anderen Standort versetzt. Korallen die von einem Standort mit hohem pH in ein saureres Milieu transplantiert wurden, wiesen Wachstumsraten von $10,51 \pm 1,14\% \text{ yr}^{-1}$ ($0,03 \pm 0,00\% \text{ d}^{-1}$) und damit vergleichbare Werte zur Kontrollgruppe am Standort mit hohem pH auf ($9,82 \pm 4,38\% \text{ d}^{-1}$). Dies weist auf die physiologische Anpassungsfähigkeit von *T. endesa* hin den internen pH-Wert zu regulieren. Auch bezüglich der Respirationsraten gab es keinen statistischen Unterschied zwischen der Kontrollgruppe am Standort mit hohem pH ($8,05 \pm 2,93 \mu\text{mol O}_2 \times \text{cm}^2 \times \text{d}^{-1}$) und jenen die im Rahmen des Kreuztransplantationsexperiments an einen Standort mit niedrigerem pH versetzt wurden ($9,88 \pm 4,52 \mu\text{mol O}_2 \times \text{cm}^2 \times \text{d}^{-1}$). Die vorliegende Studie zeigt, dass *T. endesa* in der Lage ist auch in den künftigen Bedingungen eines versauernden Ozeans physiologisch aktiv und erfolgreich zu bleiben. Kaltwasserkorallen zeigen auch unter Abnahme des pH-Werts das Potential zur Kalzifizierung, gleichwohl können die zugrundeliegenden Ausgleichsmechanismen zu einem gesteigerten Energiebedarf führen, welcher andere physiologisch bedeutende Prozesse hemmen könnte.

6 INTRODUCTION

6.1 OCEAN ACIDIFICATION (OA)

Since the industrial revolution, the pH of surface oceans has dropped by 0.1 units and will probably drop another 0.3 to 0.4 units by 2100 (Guinott *et al.*, 2006; Hennige *et al.*, 2013) (Fig. 1). This is due to the fact that the increasing amount of atmospheric carbon dioxide (CO_2) absorbed by the ocean extensively affects sea water carbonate chemistry (e.g. Caldeira and Wickett, 2003; Feely *et al.*, 2004). Increased concentrations of anthropogenic CO_2 are reflected in an elevated concentration of hydrogen ions (H^+), which lowers the pH and the available carbonate (CO_3^{2-}) ions (Orr *et al.*, 2005). An impairing effect is therefore predicted for marine calcifying organisms forming biogenic calcium carbonate (CaCO_3) in general (e.g. Orr *et al.*, 2005; Guinott *et al.*, 2006; Comeau *et al.*, 2009) and for cold-water corals (CWC) in specific (e.g. Boehmer, 2013; Jantzen *et al.*, 2013a and b; McCulloch *et al.*, 2013).

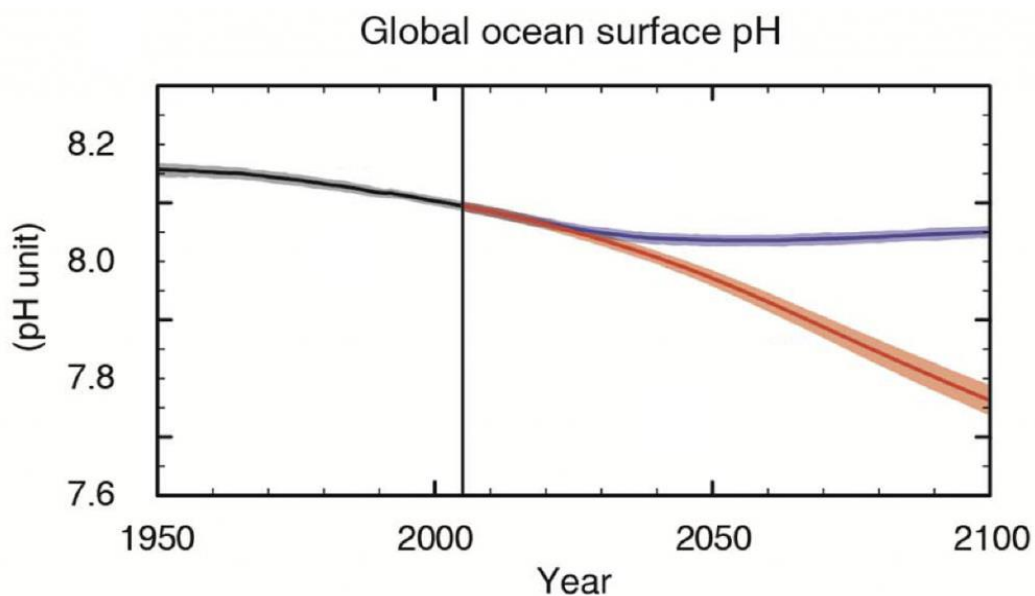


Figure 1: Multi-model simulated time series (Coupled Model Intercomparison Project; CMIP5) from 1950 to 2100 for global mean ocean surface pH. Time series of projections and a measure of uncertainty (shading) are shown for a ‘best-case’ (blue) and ‘worst-case’ (red) scenario (IPCC, 2013).

The central focus of OA research is on the calcification process, although it may alter other processes such as acid-base regulation (Pörtner, 2008), reproduction and development (Kurihara, 2008), respiration (Rosa and Seibel, 2008) and tolerances of other stressors (Hoegh-Guldberg *et al.*, 2007; Hutchins *et al.*, 2009).

6 Introduction

6.2 STUDY SITE

6.2.1 THE CHILEAN FJORD REGION

With an area of 240,000km² and a total length of 1,500km, the Chilean Fjord system is one of the largest connected fjord systems on earth (Pantoja *et al.*, 2011). This area is highly structured through various channels, islands, fjords and archipelagos and therefore comprises different regions, which are inhabited by a diverse biocenosis. In terms of oceanography, the Chilean Fjords and surrounding oceanic waters have been unexplored till 1995 (Silva, 2008). Although the Chilean Fjord ecosystem constitutes one of the major fjord systems in the subpolar margin, still only little is known about the local oceanography (Pantoja *et al.*, 2011). The channels and estuaries of southern Chile receive freshwater discharges and organic material originating from the rivers and continental run-off (Bustamante, 2009). The fresh water influence generates large vertical and horizontal gradients of density (Bustamante, 2009). These density gradients often cause restricted exchange of waters or restricted mixing which drives the eutrophication of the environment (Bustamante, 2009). The exponentially growing economic interest in the fjord region increases the anthropogenic pressure on its marine systems. Nutrient input, sediment production due to an intensified land use as well as pharmaceutical and anti-fouling substances mainly introduced by the salmon-farming industry might present a serious threat to its sensitive communities. This restricted exchange of water masses also favors ecological isolation and influences areas which are particularly sensitive to over-fishing or to the introduction of new species for human activities (Bustamante, 2009). During the last years efforts have been increased on extending existing and announcing new marine protected areas in the Patagonian Fjord region (Vila *et al.*, 2015). However, today only a neglectable portion (about 4.3%) of the Chilean Sea is protected (Friedlander *et al.*, 2013; Vila *et al.*, 2015).

6.2.2 COMAU FJORD

The fjord Comau is located in the northernmost part of the Chilean Fjord region, near the island Chiloé (42°10' to 42°50'N and 72°40' to 72°60'W) (Fig. 2). In total it has a length of 45km and reaches a maximum width of 8.5km (Häussermann *et al.*, 2012). The fjords' orientation is predominantly north to south in a straight direction and it is turning towards the West before it empties into the Gulf of Ancud, directly connected to the Pacific Ocean through the Comau channel (Reichel, 2012). Comau Fjord receives freshwater from precipitation (1,800mm yr⁻¹) and rivers, mainly during winter and early spring (September - October). This freshwater influx produces a low salinity surface layer (0.5 - 8m) with salinities as low as 2 (Pantoja *et al.*, 2011; Häussermann *et al.*, 2012), while below 18m, salinity is rather constant at 32 (Galea *et al.*, 2007). As typical for fjords in the northern Patagonian region (Silva, 2008) Comau Fjord is characterized by a strong vertical stratification. The intermediate layer is constituted by Modified Sub-Antarctic Water (MSAAW), which compensates the freshwater outflow (Palma and Silva, 2004; Valle-Levinson *et al.*, 2007).

6 Introduction

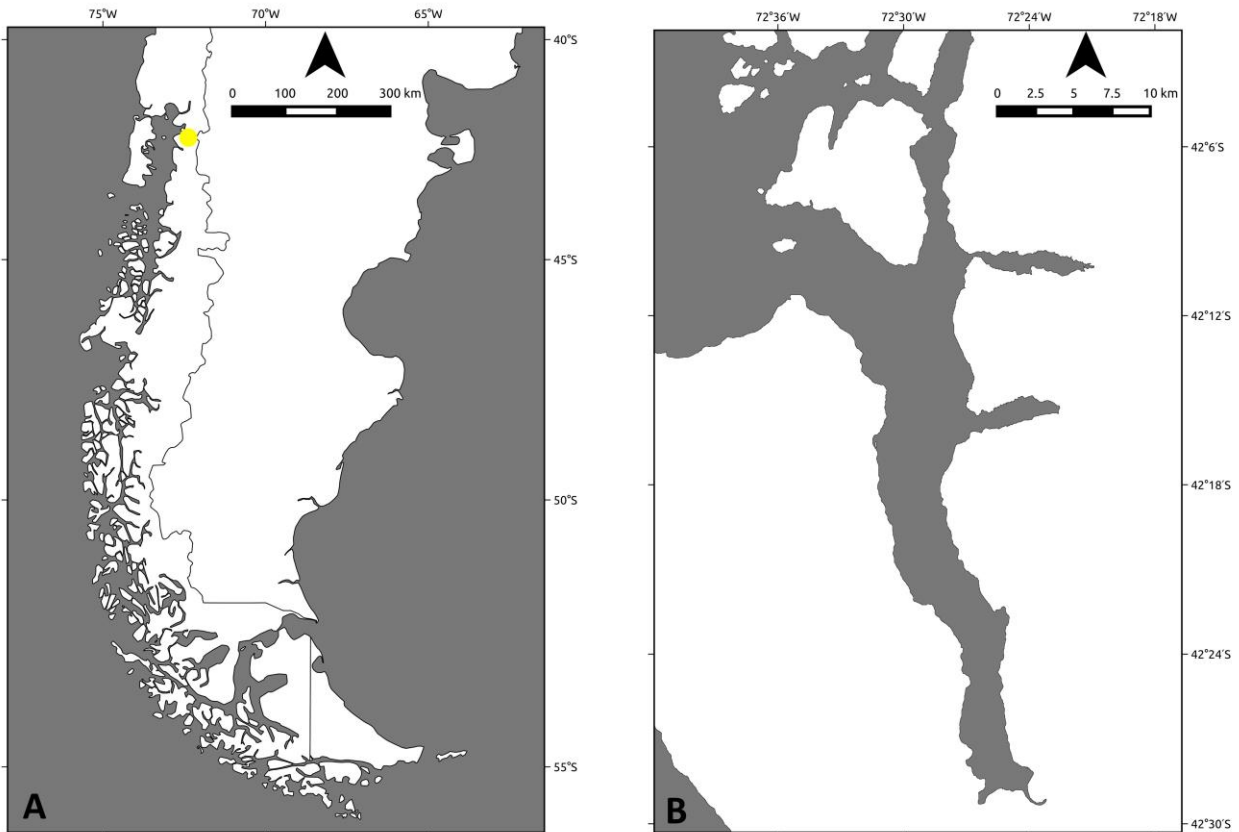


Figure 2: (A) Overview of Patagonia, yellow dot • represents the location of Comau Fjord; (B) Comau Fjord.

Fillinger and Richter (2013) reported from a water mass below 300m, which has a longer resilience time in the fjord and shows higher salinities and temperatures as well as a lower pH and oxygen. They conclude that the reasons for the latter are decomposition processes in the lower water column and in the basin of the fjord. Häussermann and colleagues (2012) mention water temperatures at the surface between 6°C and 23°C and a seasonal variation below the pycnocline between 8°C and 12°C.

Comau Fjord may be used as a model for actual ‘future ocean scenario’ experiments (e.g. Fillinger and Richter, 2013; Jantzen *et al.*, 2014; Wurz, 2014) with decreasing pH, because the fjord’s pH value is particularly low with a current aragonite saturation horizon at about 150m depth (Jantzen *et al.*, 2011). Due to this high acidity values especially calcifying species are challenged to maintain their physiological virility and even grow under these conditions. Tides are diurnal, with maximum amplitude of 7m (Galea, 2007) (Fig. 3). With the tidal amplitude the halocline changes relative to the substratum. Below the halocline various types of flourishing benthic communities can be found, often dominated by sessile filtering organisms such as cnidarians, sponges and brachiopods (Försterra, 2004). The fjord Comau is structured by hard rock walls with various slopes and steep overhangs (Reichel, 2012), leading to a vast number of habitats. This structural diversity is reflected in a highly diverse benthic community.

6 Introduction



Figure 3: High and low tide at the Huinay Scientific Field Station

It is one of the most sampled fjords in this region, mainly due to the resident ‘Huinay Scientific Field Station’, currently known for studies on the abundant benthic macrofauna (e.g. Försterra and Häussermann, 2003, 2005 and 2007) and revealing new species (e.g. Breedy *et al.*, 2015). A characteristic of the fjord Comau is the observed eurybathy, meaning the occurrence of deep sea species in surface waters, a feature that has been also observed for other fjord regions (Häussermann, 2004).

6.2.3 PITI-PALENA FJORD

Piti-Palena Fjord is about 300km south of the fjord Comau and enters into the Southern-East Pacific (Fig. 4). It exhibits a length of 19km, width of 4km and a maximum depth of 145m (Wurz, 2014). At its mouth sediments, which are deposited by the river Palena, form a natural boundary between the water exchange of the fjord and the Pacific. As the fjord Comau, Piti-Palena Fjord therefore exhibits a brackish surface water layer.

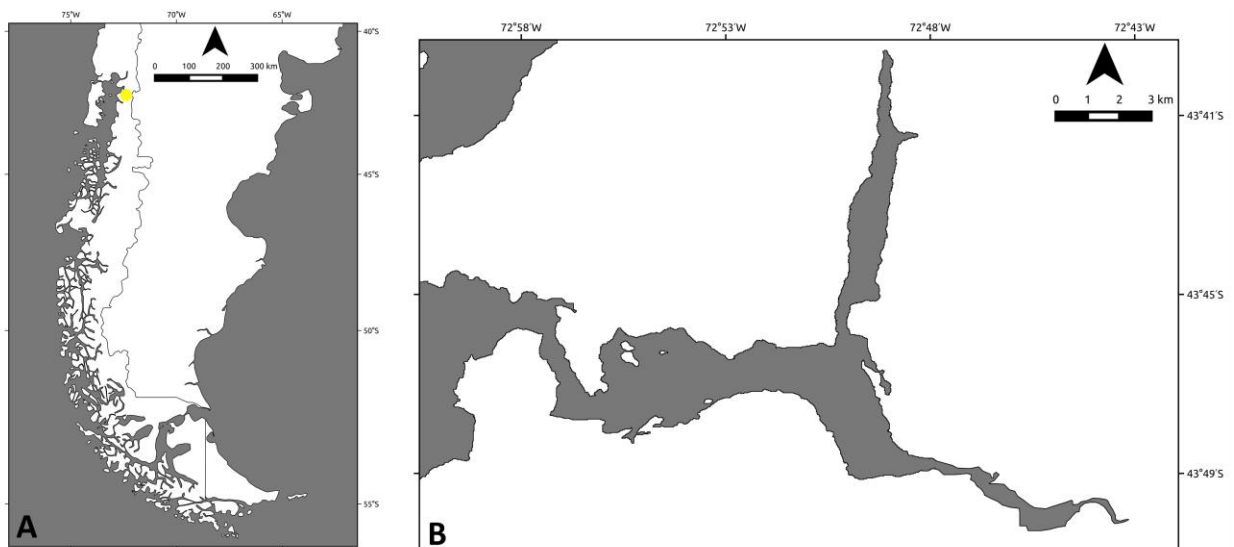
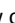


Figure 4: A) Overview on Patagonia, yellow dot  represents the location of the fjord Piti-Palena; (B) Piti-Palena Fjord.

6 Introduction

6.3 COLD-WATER CORALS (CWC)

More than 50% of the approximately 5,100 recent coral species are deep and cold-water corals (CWC) (Roberts *et al.*, 2009). Contrary to their tropical counterparts, CWC are typically lacking photoautotrophic symbionts (Freiwald *et al.*, 2004) and therefore have the potential to thrive in depths below the euphotic zone. CWC often inhabit hard substrates in dark, cold deep regions of the oceans and make up complex reefs with a high degree of biodiversity (Freiwald *et al.*, 2004). The three important CWC taxa include: Hydrocorallia, Octocorallia (including soft corals and gorgonians) and Hexacorallia, with the orders Zoanthidae, Antipatharia and Scleractinia (Cairns, 2007). In the Patagonian fjord region, shallow and dense azooxanthellate cold-water coral banks were described in the last decade (Försterra *et al.*, 2003).

6.4 THE COLD-WATER SCLERACTINIAN *TETHOCYATHUS ENDESA*

The recently discovered cold-water scleractinian *Tethocyathus endesa* (Cairns *et al.*, 2005) (Fig. 5) is one of the 23 CWC species that have been described in the Chilean Fjord Region (Cairns *et al.*, 2005).



Figure 5: The cold-water scleractinian *Tethocyathus endesa*

T. endesa is a solitary stony coral (Fig. 6), which occurs in shallow waters in association with the scleractinians *Desmophyllum dianthus* and *Caryophyllia huinayensis*. It is regularly found on rocky surfaces that are covered by crustose red algae (Cairns *et al.*, 2005). In the fjord Comau it also settles on top of other species, such as the slipper limpets *Crepidula* (own personal experience). The coral can reach up to 11mm in diameter and 8mm height and is separated in a corallite and polyp part (Cairns *et al.*, 2005). The polyp part is segmented in 48 septa, which are hexamerally arranged in four cycles. In some individuals, the pharynx is slightly orange, contrary to the distinct and whitish spherulae (Cairns *et al.*, 2005). The colour appearance is thought to vary due to endolithic algae (Cairns *et al.*, 2005).

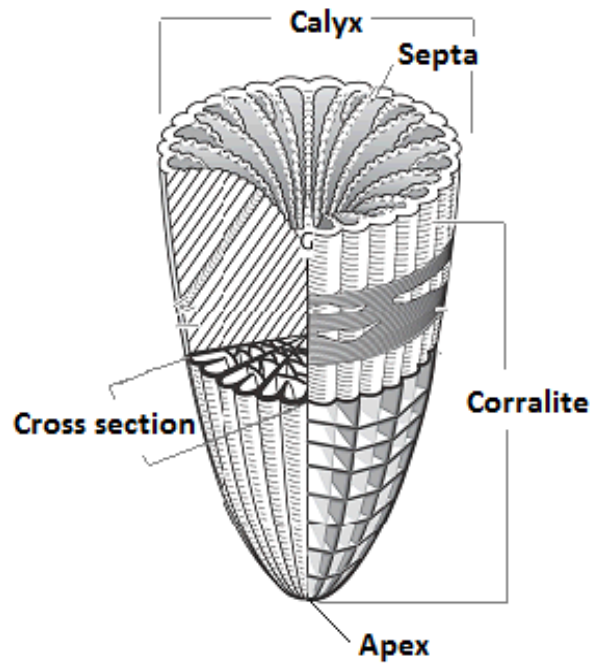


Figure 6: Morphology of a solitary scleractinian. Modified after Stolzenberger-Ramirez (2014).

In the fjord Comau the upper distribution limit of *T. endesa* is at a depth of about 15m (own personal experience) – but always below the influence of the low salinity layer (Cairns *et al.*, 2005). The lower distribution limit has not been examined so far, but the species was found in a depth of 240m (Häussermann and Försterra, 2007).

7 STATE OF THE ART

7.1 CWC AND OCEAN ACIDIFICATION

Already the first publications about the influence of OA dealt with the impact on corals (e.g. Kleypas *et al.*, 1999) and also the first manipulative experiments explored the influence of pCO₂ on calcification processes (e.g. Gattuso *et al.*, 1998; Langdon *et al.*, 2000). Detrimental effects are foreseen for tropical coral reef systems, which are predicted to decline in their reef growth (Langdon and Atkinson, 2005; Kleypas *et al.*, 2009) and shifts in species composition due to a decrease in diversity (Hoegh-Guldberg *et al.*, 2007; Fabricius *et al.*, 2011). However, the response to OA was also shown to be highly variable for different taxonomic groups (Ries *et al.*, 2009b). Initially CWC were expected to be earlier and more affected by OA than their tropical relatives. The regions they inhabit are deeper and colder and therefore the aragonite saturation state there is lower than in shallower, warmer regions (Orr *et al.*, 2005) (Fig. 7). According to Maier *et al.* (2013), more than 70% of CWC communities live in regions that will be undersaturated with respect to aragonite by the end of the century. This is particularly important as the aragonite saturation state is considered to be one of the main drivers of the distribution of CWC (Davies and Guinotte, 2011).

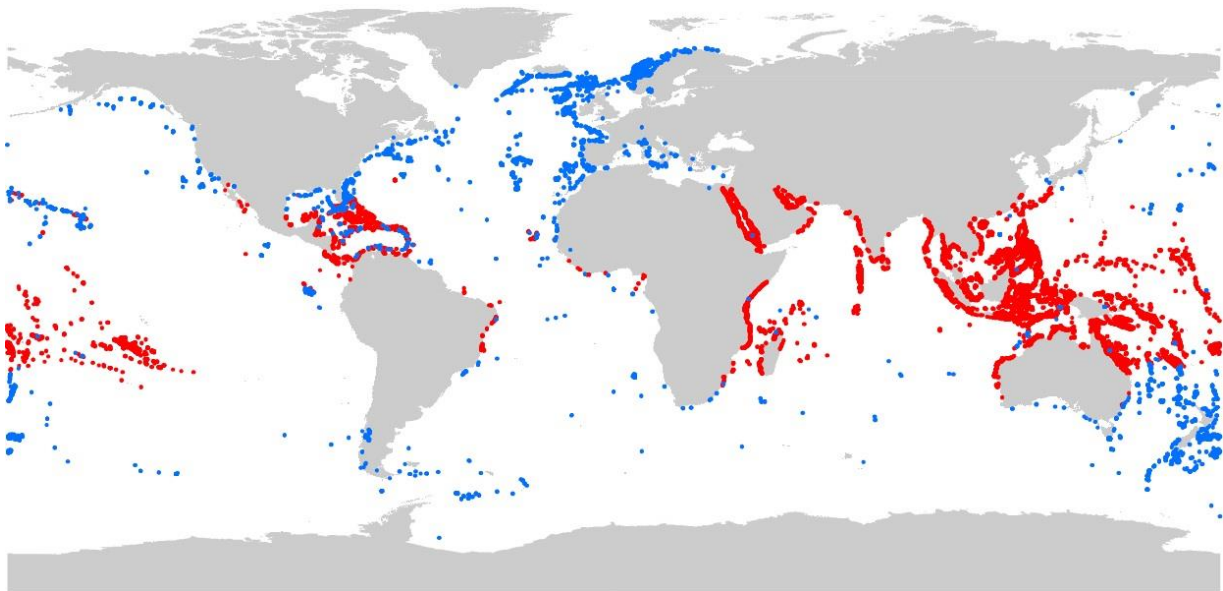


Figure 7: Global distribution of corals; Data: Pörtner *et al.* 2014; IPCC 2014; Map: Laura Fillinger

● Warm-water corals ● Cold-water corals

There are few long-term studies (but see Form and Riebesell, 2012; Maier *et al.*, 2013) conducted on the main reef-building CWC *Lophelia pertusa* and *Madrepora oculata*. These corals seem to be quite unaffected by experimental future pH levels. Also Thresher *et al.* (2011) found several cold-water coral

8 Aim of work and work strategies

species to show no correlation of the skeletal density to the carbonate saturation of the surrounding water. A possible explanation could be the capacity to regulate the internal pH, as it has been shown for the solitary coral *Caryophyllia smithii* (McCulloch *et al.*, 2012a). This species is able to regulate the internal pH in its tissues up to 0.78 units above the surrounding sea water pH. This active physiological adaptation to changing pH values in the surrounding water is due to the regulation of the internal pH through Ca^{+2} -ATPase activity (McCulloch *et al.*, 2012a). However, pH elevation is suggested to be accompanied by energetic effort, leading to a reduction of energy for other physiological important processes. Therefore, a decrease of sea water pH of 0.1 units leads to a 10% increased energy budget (McCulloch *et al.*, 2012a). However, species specific responses to abiotic environmental factors might be different and the extrapolation and prediction of physiological responses of different species is of limited suitability. The ecological niche of CWC is therefore yet not defined and needs further investigations, especially concerning their performance with respect to sea water carbonate chemistry.

7.1.1 CWC IN THE FJORD COMAU AND OCEAN ACIDIFICATION

Beside *T. endesa*, there are some more CWC, which occur in shallow waters in the fjord Comau. The most abundant and at this time best studied coral is *D. dianthus*. Thresher *et al.* (2011) detected *D. dianthus* in waters largely undersaturated with regard to aragonite. Also Fillinger and Richter (2013) recorded *D. dianthus* appearing in aragonite undersaturated water. These observations support the hypothesis that some scleractinian corals possess mechanisms to adapt their internal pH relative to the sea water pH thus facilitating their calcification rates.

So far there is only little knowledge about the *in situ* long-term growth rates (but see e.g. Jantzen *et al.*, 2013a for *D. dianthus*; Wurz 2014 for *C. huinayensis*) and the respiration rates of CWC (e.g. for *L. pertusa* by Form and Riebesell, 2012; and Hennige *et al.*, 2014). Respiration measurements for *D. dianthus* (Böhmer, 2013) and for *C. huinayensis* (Wurz, 2014; Wendländer, 2014) under different CO_2 concentrations were conducted in artificial sea water in the laboratory.

8 AIM OF WORK AND WORK STRATEGIES

Aim of this study was to determine the abundance of *T. endesa* in different depths of the shallow water zone (0m - 30m), as well as the observation of the preferred substrate inclination. The connection of observations on *T. endesa* from the current study and observations from previous studies on other solitary CWC (such as *C. huinayensis* and *D. dianthus*) aimed to understand the spatial distribution pattern of CWC communities in Comau Fjord. In order to describe the physical conditions at the sampling sites related to the fjord Comau (XHuinay North and Lilliguapi) and in Piti-Palena Fjord (Ensenada de Las Islas), temperature and carbonate chemistry (pH and Total Alkalinity) were determined. To detect whether the carbonate chemistry has an influence on the growth of *T. endesa*, long-term (one year) *in situ*-growth rates were determined for specimen living in different sea water pH regimes. As increased respiration rates in scleractinians are an indicator for stress (Telesnicki *et al.*, 1995) respiration rates of *T. endesa* were also examined under different pH-regimes.

Hypothesis 1: Between 0m and 30m water depth, the inclination of the substrate determines the abundance of *T. endesa*.

Nullhypothesis 1: Between 0m and 30m water depth, the abundance of *T. endesa* is not determined by the substrate inclination.

Hypothesis 2: *T. endesa* occurs on substrates with a different range of inclination angles compared to *D. dianthus* and *C. huinayensis*.

Nullhypothesis 2: *T. endesa* occurs on substrate with the same range of inclination angles as *D. dianthus* and *C. huinayensis*.

Hypothesis 3: The carbonate chemistry in the fjord Comau and Piti-Palena Fjord influences the long-term *in situ*-growth rates of *T. endesa*.

Nullhypothesis 3: Long-term *in situ*-growth rates of *T. endesa* are not influenced by the carbonate chemistry in the fjord Comau and Piti-Palena Fjord.

Hypothesis 4: The carbonate chemistry in the fjord Comau and Piti-Palena influences the respiration rate of *T. endesa*.

Nullhypothesis 4: Respiration rates of *T. endesa* are not influenced by the carbonate chemistry in the fjord Comau and Piti-Palena.

9 MATERIAL AND METHODS

9.1 SAMPLING SITES

9.1.1 COMAU FJORD

The main experiment took place at two sampling sites. One in the central fjord Comau, the other one outside the fjord, located close to its mouth. At both sampling stations samples for Total Alkalinity (TA) measurements were collected and the abiotic factors temperature, salinity, conductivity and depth were logged with a conductivity-temperature and depth multi sensor (CTD). Specimens of *T. endesa* from both stations were used for a cross-transplantation experiment, which already started in 2014. The conditions of this experiment will be explained hereinafter.

The first sampling site was Lilliguapi, which is located outside Comau Fjord, at the western region of the Lilliguapi Island (Fig. 8) ($42^{\circ} 09' 43''\text{S}$; $72^{\circ} 35' 27''\text{W}$) at about 20m water depth. It is characterized by rocky walls, overhangs and steeply increasing basaltic hard bottom. In addition to the cross-transplantation experiment, samples on abiotic factors were collected at this sampling site. At this sampling site, the abundance survey was only carried out at one overhang.

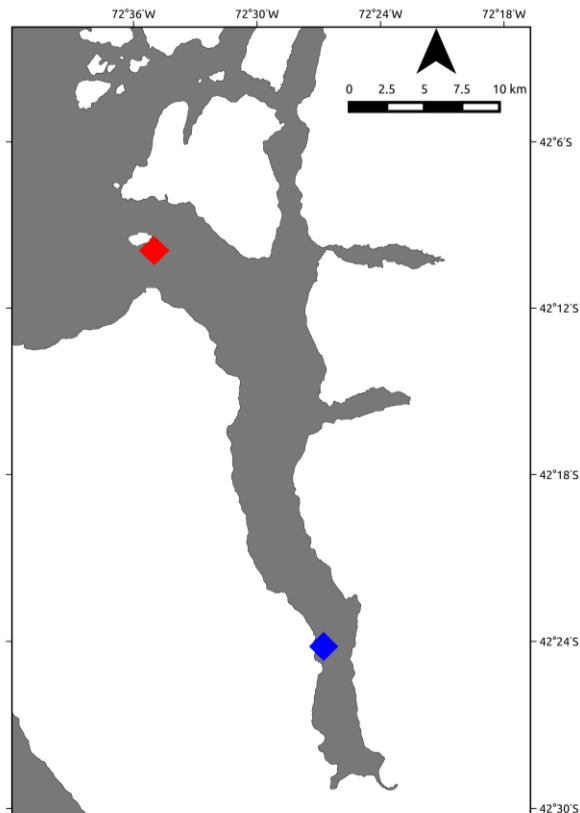


Figure 8: Map of Comau Fjord with sampling sites Lilliguapi ◆ and XHuinay North ◆

9 Material and methods

The second sampling site was XHuinay North (see Fig. 8) ($42^{\circ} 23' 25''\text{S}$; $72^{\circ} 27' 32''\text{W}$), located inside the fjord Comau at its western coast, also at about 20m water depth. Likewise Lilliguapi, this sampling site is characterized by vertical rock walls and overhangs. In addition to the data collection of abiotic factors and the cross-transplantation experiment at this sampling site, an abundance survey was carried out with respect to water depth and substrate inclination.

Fillinger and Richter (2013) examined the natural, vertical pH gradient, present in Comau Fjord. They identified a general decrease in sea water pH from the mouth of the fjord towards its end. At XHuinay, a sampling site which is located very close to XHuinay North, studies of recent years (e.g. Jantzen *et al.*, 2013b; Wurz, 2014) also examined the sea water pH and detected XHuinay to be more acidic than Lilliguapi.

9.1.2 PITI-PALENA FJORD

The sampling site Ensenada de Las Islas in the fjord Piti-Palena is located close to the Jaime Island ($43^{\circ} 46' 31.26''\text{S}$, $72^{\circ} 55' 14.988''\text{W}$). At this site, samples for TA and CTD data were collected, as well as an abundance- and substrate inclination survey was carried out.



Figure 9: Piti-Palena Fjord and sampling station Ensenada de Las Islas ◆

9 Material and methods

9.2 PHYSICAL PARAMETERS

To determine the abiotic conditions at the sampling sites XHuinay North, Lilliguapi and Ensenada de Las Islas, the physical parameters temperature, oxygen and salinity were measured with aid of a CTD-probe (SBE 19plus-SEACAT Profiler [Conductivity, Temperature and Pressure with RS 232 Interface], Sea-Bird Electronics Inc., Washington, USA). To cover potential fluctuations of the water parameters due to the distinct tidal amplitude (see Fig. 3) samples at both of the sampling sites XHuinay North and Lilliguapi were taken several times at falling and rising tide, each. At Ensenada de Las Islas samples were only taken once. At the sampling sites XHuinay North and Lilliguapi, pH was determined manually with a portable device (PHC301, Hach Lange Company, Düsseldorf, Germany) and temperature data were collected for one year with the aid of data loggers (TidbT V2 Temp Logger, Onset Computer Corporation, Bourne, USA). Those were installed at all three sampling sites, where they performed temperature measurements every 15 minutes to assure the best resolution possible.

9.2.1 CARBONATE CHEMISTRY

In order to describe the carbonate chemistry at the sampling sites, TA data were collected additionally to the pH data. Changes of TA can be an indicator for various biogeochemical processes such as the formation and remineralization of organic matter, precipitation and dissolution of calcium carbonate (Wolf-Gladrow *et al.*, 2007). In surface ocean waters, TA variability is mainly controlled by freshwater input (precipitation and sea-ice melting) or removal (evaporation and sea-ice formation), which is also changing salinity (Brewer *et al.*, 1986; Millero *et al.*, 1998). Sea water samples were taken with a 500ml Schott bottle (Schott AG, Mainz, Germany) during SCUBA diving or with a 2.5l Niskin-type plastic water sampler (Hydrobios GmbH, Altenholz, Germany) aboard. Each measurement comprised three replicates. For the TA determination sea water was filtered with glass microfibre filters (Whatman GF/F 25mm, GE Healthcare Europe GmbH, Freiburg, Germany) to remove most of the particulate organic matter. Analysis was then performed with potentiometric titration (TitroLine alpha plus + TA05plus, SIAnalytics GmbH, Mainz, Germany and TitriSoft 2.72, Schott Instruments, Mainz, Germany) (after Gran, 1952).

TA can be calculated with the following equation:

$$\text{TA} \approx [\text{HCO}_3^-] + 2[\text{CO}_3^{2-}] + [\text{OH}^-] - [\text{H}_3\text{O}^+] + [\text{B}(\text{OH})_4^-] + 2[\text{PO}_4^{3-}] + [\text{HPO}_4^{2-}] - [\text{H}_3\text{PO}_4]$$

Formula 1

The ion concentration is represented by Bicarbonate $[\text{HCO}_3^-]$, Carbonate $[\text{CO}_3^{2-}]$, Hydroxide $[\text{OH}^-]$, Hydronium $[\text{H}_3\text{O}^+]$ and Tetrahydroxyborate $[\text{B}(\text{OH})_4^-]$, Phosphate $[\text{PO}_4^{3-}]$, Hydrogenphosphate $[\text{HPO}_4^{2-}]$ and

9 Material and methods

Phosphoric acid [H_3PO_4]. Calibration was conducted with Dickson standard batches (Scripps Institution of Oceanography, San Diego). Total Alkalinity was then determined by plotting the total number of protons (calculated using the respective pH and total sample volume (start volume (V_0) plus volume of titrant (HCl) added to the sample) against the volume of the titrant (HCl) added to the samples respectively (Gran, 1952).

$$\text{TA} = [(b/a) \times c (\text{HCl})]/V_0$$

Formula 2

b = axis intercept of the Gran plot ($^{\circ}$) (ml M^{-1})

a = slope of the Gran plot (ml M ml^{-1})

c (HCl) = concentration of hydrochloric acid (mol l^{-1})

V_0 = initial volume of sea water (standard) sample (ml)

9.3 ABUNDANCE REGARDING DEPTH AND SUBSTRATE INCLINATION

A frame based census of *T. endesa* at the sampling stations XHuinay North and Ensenada de Las Islas was carried out to describe the abundance regarding depth and substrate inclination in the fjord Comau and Piti-Palena. For this purpose, water depths for sampling were always correlated to the lowest astronomical tide (LAT). Photos were taken during SCUBA dives (Fig. 10). A rectangular sampling frame ($19.5\text{cm} \times 29.6\text{cm}$) was used as reference and equipped with a board, fixed in a right angular to the frame. Here, a rope with a metal nut was attached to serve as an angle meter (Fig. 10). Pictures of the sampling frame and the angle meter were taken with a digital camera (Canon, G11 Powershot, Krefeld, Germany) at 16m, 19m, 22m and 25m water depth. The shallow limit was set because *T. endesa* was not found in shallower water depths as 16m, the deep limit of 25m was set due to the insurance regulations for scientific SCUBA diving. To ensure random sampling, photos were taken along a horizontal line transect in a 2m interval. For the analysis, only photos with at least one specimen of *T. endesa* were considered. The determined numbers of individuals per sampling frame was then used to calculate the abundance of *T. endesa* per m^2 using the following equation:

$$n = (n_{\text{frame}}/A_{\text{frame}}) \times 10,000$$

Formula 3

Where the population density (n) is given in numbers of individuals within the sampling frame (n_{frame}) per sampling frame area (A_{frame} in cm^2) and extrapolated to m^2 .

9 Material and methods

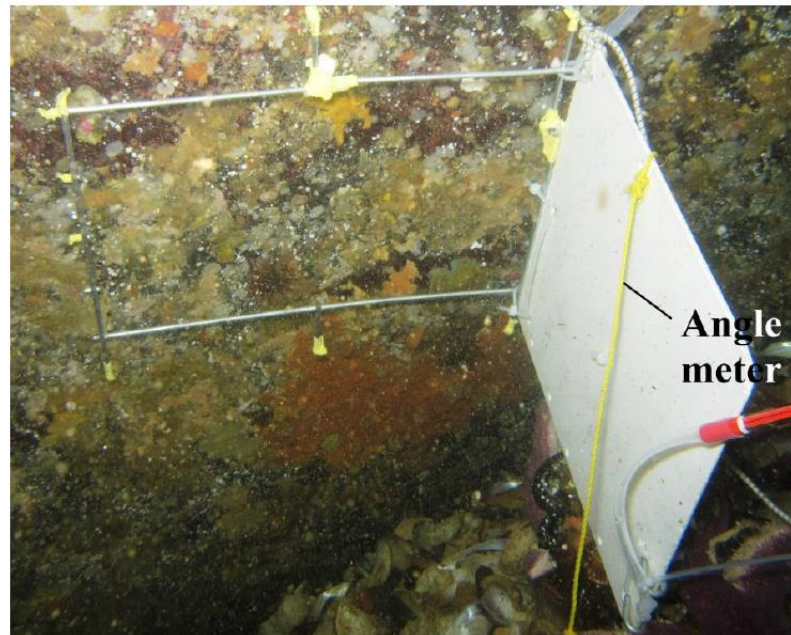


Figure 10: Sampling frame to measure abundance and substrate inclination. Photos of the frame were used for abundance calculations. Photos of the white side plate and angle meter for the determination of the substrate inclination (Wendländer, 2014).

Abundance calculations were conducted via enumeration with PhotoScape (Mooii Tech, Version 3.7). Substrate inclinations were determined with MB Ruler (Markus Bader, Version 5.3) (Fig. 11). Substrate inclinations were related to the inclination of the rocky substratum only and not to potentially overgrown animals, such as *Crepidula*.

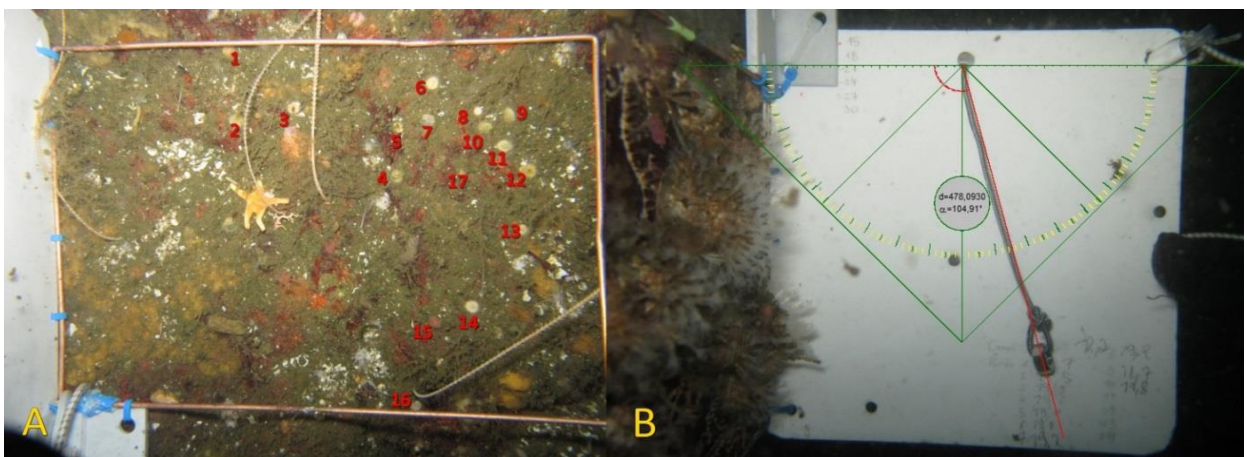


Figure 11: Photos of sampling frame. A: Enumeration of *T. endesa* with PhotoScape (note red numbers), B: Measurement of substrate inclination with MB Ruler.

9 Material and methods

9.4 CROSS-TRANSPLANTATION EXPERIMENT

9.4.1 SETUP

The cross-transplantation experiment took place at the sampling sites XHuinay North and Lilliguapi. At each site, two coral holders (capacity per holder = ten corals) were installed. These holders were mounted on the substratum at a depth of 20m. The experimental corals were glued onto polyethylene screws and installed onto the coral holders (Fig. 12).

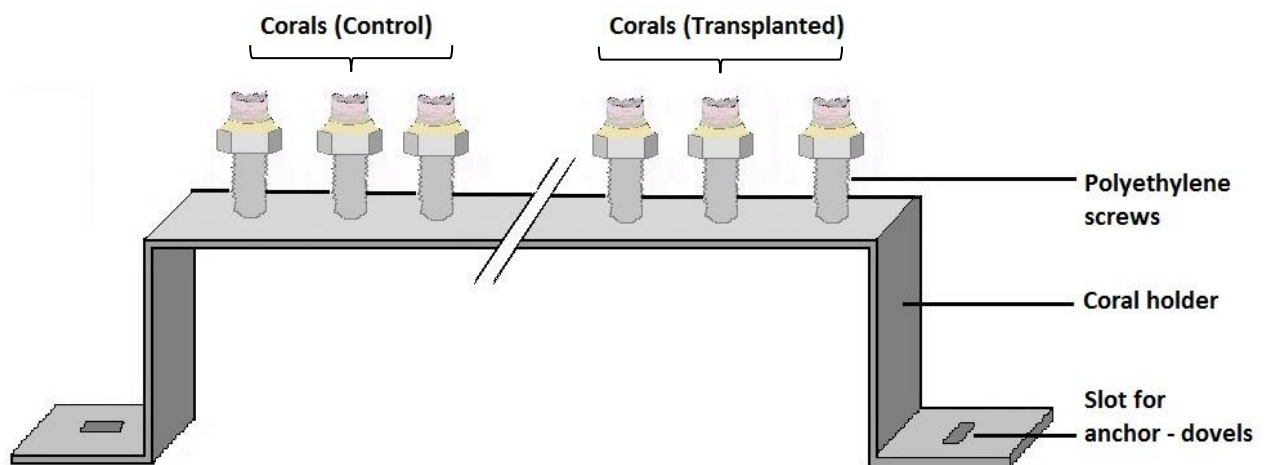


Figure 12: Experimental setup for cross-transplantation experiment with *T. endesa*; Sketch is not true to scale.

At each study site ten specimens of *T. endesa* were used to determine the general *in situ*-growth rate (one year). They also served as a control for the cross transplantation experiment in which, additionally ten specimens of *T. endesa* were exchanged to the other study site respectively, in 2014. All in all, 40 corals were therefore located at the sampling sites XHuinay North and Lilliguapi. Ten controls and ten transplanted corals at each station, respectively. Experimental groups were composed of specimens of different size classes and corals were distributed randomly. Before their installation at the coral holders in 2014 the mass of all 40 corals was determined using the buoyancy weight technique (Jokiel *et al.*, 1978). In 2015, scientific SCUBA divers collected the corals and brought them instantly to the aquarium laboratory of the Huinay Scientific Field Station (Huinay, Chile). Respiration measurements took place immediately after retrieving and arrival at the laboratory. After that, corals were maintained in aquaria, which were supplied with water constantly pumped from 25m depth at the Huinay Scientific Field Station (Comau Fjord). After buoyant weighing corals were returned to the sampling sites and reinstalled at the coral holders for long-term measurements.

9 Material and methods

9.4.2 MASS INCREASE

Skeletal growth rates of *T. endesa* were determined using the buoyant weight technique (Davies, 1989). On the basis of Archimedes' principle-theory, mass of the coral skeleton can be determined from its mass in sea water, which is accounting for the density of the coral skeleton plus the density of sea water (Davies, 1989). This method has already been shown to be efficient for other CWC (e.g. Jantzen *et al.*, 2013a; Wendländer, 2014; Wurz, 2014). All corals were weighted three times with an analytical balance (Sartoris CP 225D-OCE, Germany, 220g - 1mg ± 0.1mg). The obtained values were averaged to determine the buoyant weight (skeletal mass in water (m_{water} in g). Having determined m_{water} the skeletal mass in air (m_{air}) was calculated after Jokiel *et al.* (1978), using the following equation:

$$m_{\text{air}} = m_{\text{water}} / (1 - (\rho_{\text{water}} / \rho_{\text{aragonite}}))$$

Formula 4

where ρ_{water} is the sea water density (in g/cm^3) and $\rho_{\text{aragonite}}$ the skeleton density of the coral (in g/cm^3). In order to calculate the sea water density (after Bialek, 1966) temperature and salinity were measured with a temperature sensor (WTW ama-digit, 40°C - 120°C ± 0.1°C, Wissenschaftlich-Technische Werkstätten GmbH, Weilheim, Germany) and a refractometer (Salinity 20-40 ppm ± 0.1% (1ppt), Sinokit Enterprise Limited, Hong Kong) during the weighing process. Sea water temperature was kept at 12 ± 0.5°C. The difference between the coral mass in 2014 and 2015 was assumed to be the mass increase per year.

9.4.3 RESPIRATION

Respiration rates were determined during closed incubations, using two different methods. Firstly, via a manual method, using a handheld Luminescent/Optical Dissolved Oxygen Probe. Secondly, via an automatically measurement with optodes in a flow-through system with respiration chambers. Aim of this two-part measurement was to determine whether the manual method is valid for respiration measurements of *T. endesa* since it is much easier to implement, especially in field expeditions. The respiration rates of *T. endesa* were measured *in vitro*, but the sea water was sampled at the sampling sites and was brought to the laboratory. Temperature matched with the natural ambient temperature (12.5 ± 0.5°C) and measurements started immediately after the arrival at the field station. The measurement period was 12h in order to ensure still saturated oxygen conditions (O_2 saturation > 70%). Daily respiration rates R ($\text{O}_2 \times \text{cm}^{-2} \times \text{d}^{-1}$) expressed in μmol ($1\text{mol O}_2 \triangleq 32\text{g} \triangleq 32\mu\text{g} \mu\text{mol}^{-1}$) were normalized to the volume of the respiration chamber ($V_{\text{incubation}}$ in L), incubation time ($T_{\text{incubation}}$ in min) and calyx surface area (A_{calyx} in cm^2) for each coral and calculated with the following equation:

$$R (\text{O}_2 \text{ cm}^{-2} \text{ d}^{-1}) = [((\Delta \text{O}_2 \times V_{\text{incubation}}) / T_{\text{incubation}}) / A_{\text{calyx}}] \times (1.000/32) \times 24$$

Formula 5

9 Material and methods

In addition to all measurements, respiration of a blank water sample was determined. Using the data from the blank replicate, it was possible to derive the bacterial background respiration from the measured values in order to calculate the actual respiration rates of the corals.

9.4.3.1 CALYX SURFACE

Top view-scaled photos were taken with a digital camera (OLYMPUS Digital Camera EM3, Olympus Deutschland GmbH, Hamburg, Germany), in order to calculate the 'calyx surface area' (after Kanwisher and Wainwright, 1967). The diameter was measured using a calliper (precision ± 0.01 mm). This 'calyx surface area' was used for the calculation of the respiration rates.

9.4.3.2 CORRELATION OF DRY MASS AND CALYX SURFACE AREA

In an additional experiment, ten specimen of *T. endesa* were used to determine a potential correlation between the 'calyx surface area' and the dry mass (DM). This was necessary for the subsequent normalisation of respiration rates. In a first step, the calyx surface area (see 9.4.3.1) was measured and corals were dried in a compartment dryer at 50°C for 48h. After that, they were weighed with an analytical balance (Sartoris CP 225D-OCE, Germany, 220g - 1mg \pm 0.1mg) to obtain the dry mass (DM). In case of a correlation, corals with a larger 'calyx surface area' can be assumed to have a higher amount of living – and therefore respiring polyp tissue.

9.4.3.3 MANUAL O₂ MEASUREMENTS

For the manual measurement of respiration, corals were attached with their screws to the lids of 100ml Schott (Schott AG, Mainz, Germany) bottles (Fig. 13). The screws were fixated by screwing them into a mounting that has been implemented to the lid of the Schott bottle. The procedure of attaching the coral to the lid took place underwater, directly at the coral holders. The bottles were equipped with a stirring bar and closed airtight underwater.



Figure 13: Coral glued on a screw, screwed-in the lid of a 100ml Schott bottle.

9 Material and methods

Additionally, water samples were taken to determine the start value of dissolved oxygen. The measurements were conducted with a handheld Standard Luminescent/Optical Dissolved Oxygen Probe (LDO 101, Hach Lange GmbH, Düsseldorf, Germany). In the laboratory, the Schott bottles were placed in a water bath with a constant water flow, provided by the in-house pumping system of the Huinay Scientific Field Station. Below the water bath a magnetic stirrer was located (RH Basic, IKA-Werke GmbH & Co. KG, Staufen, Germany), which provided a constant water movement within the bottles (Fig. 14).

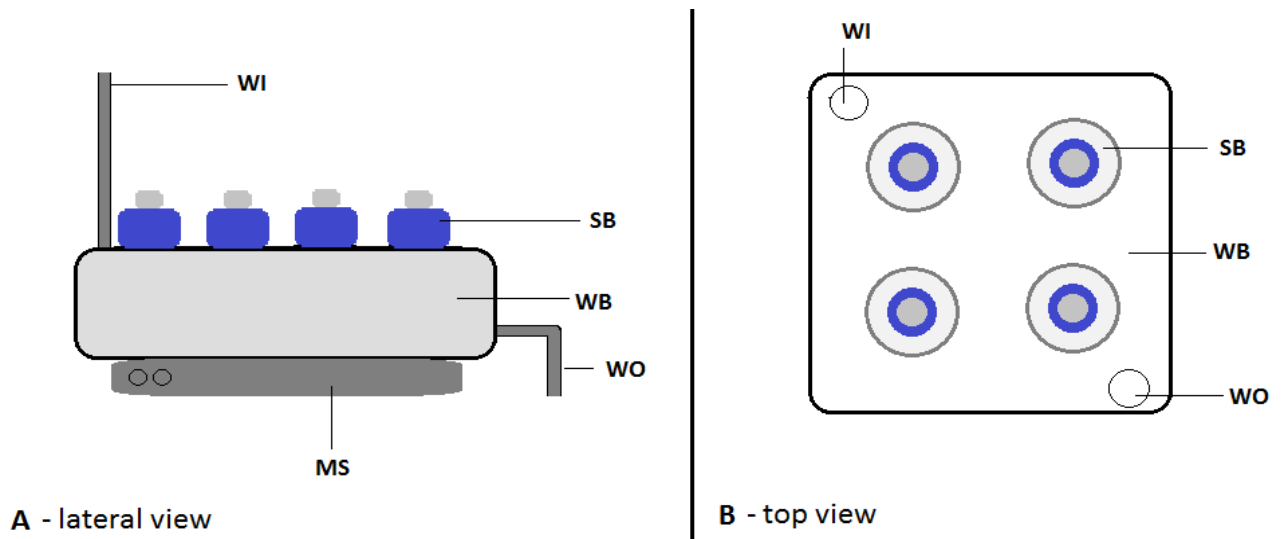


Figure 14: Schematic drawing of water bath setup for incubation. A) Lateral view of water bath with Schott bottles B) Top view of water bath. WI (water inlet), WO (water outlet), WB (water bath), SB (Schott bottles with corals), MS (magnetic stirrer).

Dissolved oxygen content in the Schott bottles was measured after 12 hours of incubation. Oxygen consumption (ΔO_2) was calculated by the delta between start (oxygen concentration of initial sea water sample) and end values.

$$\Delta O_2 = (O_2^{\text{Initial}} - O_2^{\text{End}}) - O_2^{\text{BBR}}$$

Formula 6

O_2^{Initial} = oxygen concentration of initial sea water sample

O_2^{End} = oxygen concentration in Schott bottle after incubation time

O_2^{BBR} = Bacterial background respiration

9 Material and methods

9.4.3.4 AUTOMATICAL MEASUREMENTS OF OXYGEN CONCENTRATION

In a second measurement setup, respiration rates were determined via optodes in a flow-through setup with respiration chambers. This measurement took place in a large water bath ($60 \times 25 \times 14$ cm). The water bath was supplied with water from 25m water depth constantly pumped by the in-house system of the Huinay Scientific Field Station. Temperature was constantly logged in a five-second interval during the whole measurement using a temperature sensor connected to the Oxygenic meter (MICROX TX3 Fibre-optic oxygenic meter, PreSens GmbH, Regensburg, Germany). Inside the water bath two Perspex cylindrical respiration chambers (Volume: 96 - 114 ml) (Fig. 15) were positioned. The respiration chambers were equipped with Tygon tubes (T3603-23, Tygon, Lima, Ohio, USA), which were attached to a peristaltic pump (MASTERFLEX, Cole-Palmer Instrument Company, Kehl, Germany). This ensured a constant water movement inside the respiration chamber-tube system.

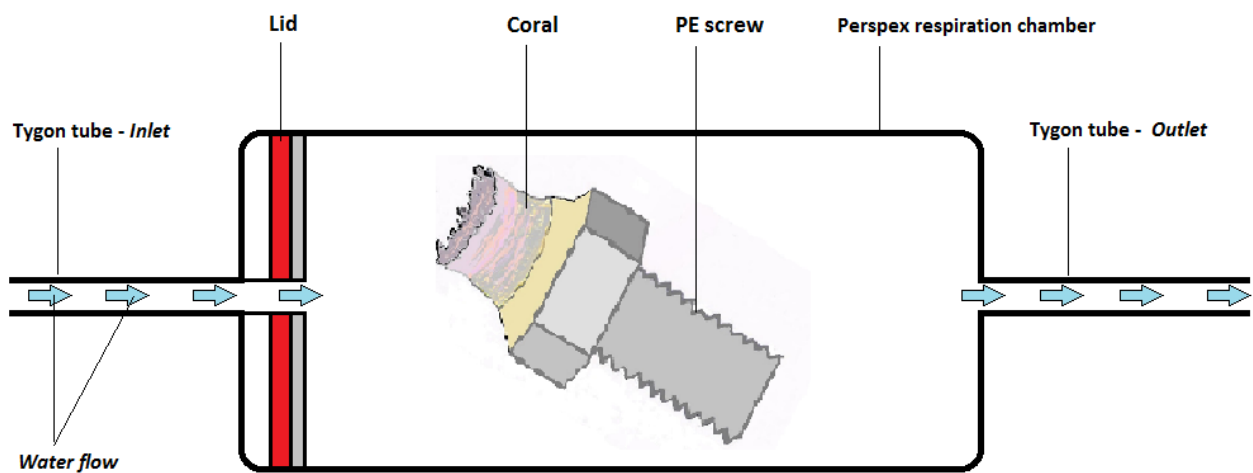


Figure 15: Schematic drawing of respiration chamber with coral glued on screw.

Optical needle-type Oxygen Micro sensors (PreSens, Regensburg, Germany) were inserted to a housing, which was connected to the tubes (Fig. 16). Optodes consist of a fluorophore, whose fluorescence is quenched by the O_2 molecules. Embedded in a gas-permeable membrane the O_2 -sensitive fluorescent compound is stimulated by a signal light-emitting diode (LED). The resulting fluorescence signal is amplified by a photomultiplier. Quantified signals are the fluorescence amplitude and the phase angle, whose fluorescence decay time is affected by O_2 (Schumann, 2012). The measurement was started without closing the respiration chambers and ran for one hour for two reasons: First, to grant the coral time for acclimatization and to assure the expansion of their tentacles. Polyp extension was assumed to be a visual indicator for 'good condition', as corals extend their polyps to capture particles (Boehmer, 2013). Second, to determine the measurement drift of the oxygen sensors (optodes). After one hour, the lids were closed airtight underwater and the measurement continued without interruption.

10 Results

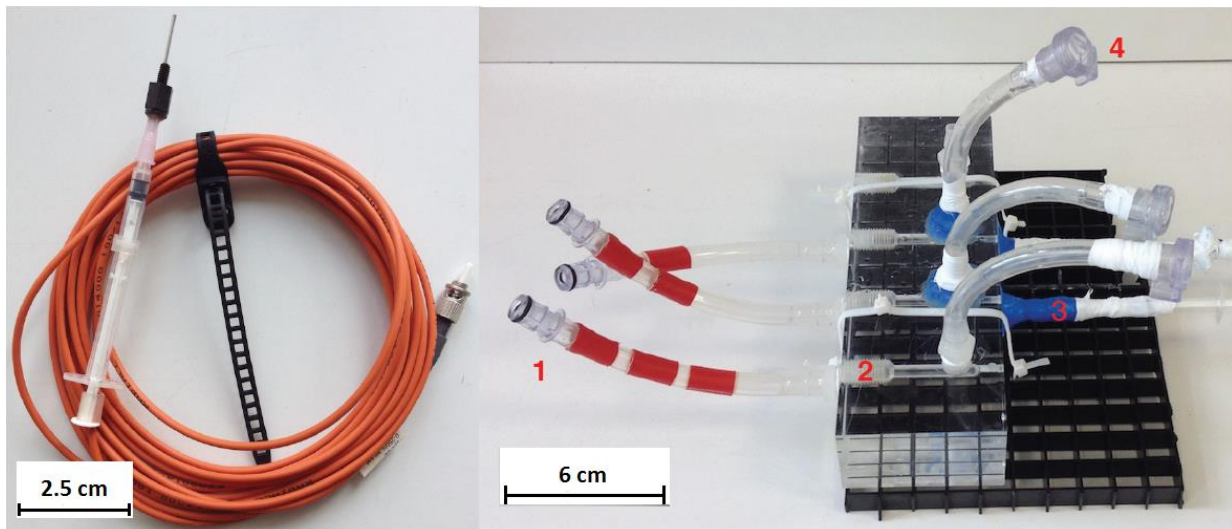


Figure 16: Left picture: optical needle-type Oxygen Micro sensor. Right picture: PVC block with inlet (1), flow-through (2), sealed micro sensors (3) and outlet (4) (Wurz, 2014).

The data acquisition during the measurements was performed with the OxyView_TX3_V5.31 software (PreSens, Regensburg, Germany). The oxygen content of the water body was constantly logged at an interval of five seconds. Oxygen consumption (ΔO_2) was calculated by the delta between start and end values. These values were later corrected for bacterial background respiration measured with the manual method.

9.5 DATA PROCESSING

All statistical analyses were performed using the statistical computing and graphics program R (Foundation for Statistical Computing, Vienna, Austria, Version 3.2.0). Graphs for CTD data were produced with Microsoft Excel (Microsoft Corporation, Redmond, USA, Version 2010). For statistical comparisons of different groups an analysis of variance (ANOVA) was used, measured data with nonparametric distribution were tested with the Kruskal-Wallis test for significant differences. Statistical test for correlations was a Tukey multiple comparison of means. For all tests the set level for significance was $p < 0.05$. If not otherwise specified, values are given as means \pm standard deviation (SD). Significant effects between measured values of different locations are marked by capital letters (A, B, etc.). Treatments with the same letter do not differ significantly.

10 RESULTS

10.1 HYDROLOGY

Hydrological data were collected at all three sampling sites. Temperature and salinity were determined by using a CTD. In addition the sea water pH was determined using a portable sampling probe and TA was measured in the laboratory. At XHuinay North and Lilliguapi sampling was conducted at falling and rising tide, each. At Ensenada de Las Islas sampling took place only once.

10.1.1 CTD PROFILES

10.1.1.1 XHUINAY NORTH

At XHuinay North, four CTD casts were conducted at falling and rising tide each. Maximum sampling depth was between 17.2m and 31.3m. The brackish surface layer, with varying salinities between 15 and 31.5 extended between 0 and 10m water depth. Lowest salinity value (15.6 at 0.6m) was measured during falling tide at 22.01.2015. Highest salinity (32.2) was measured from 26.5m on, at 23.02.2015. Below 10m, the salinity was always higher than 31. The variability in salinity within the surface layer was higher during rising tide than during falling tide (Fig. 17).

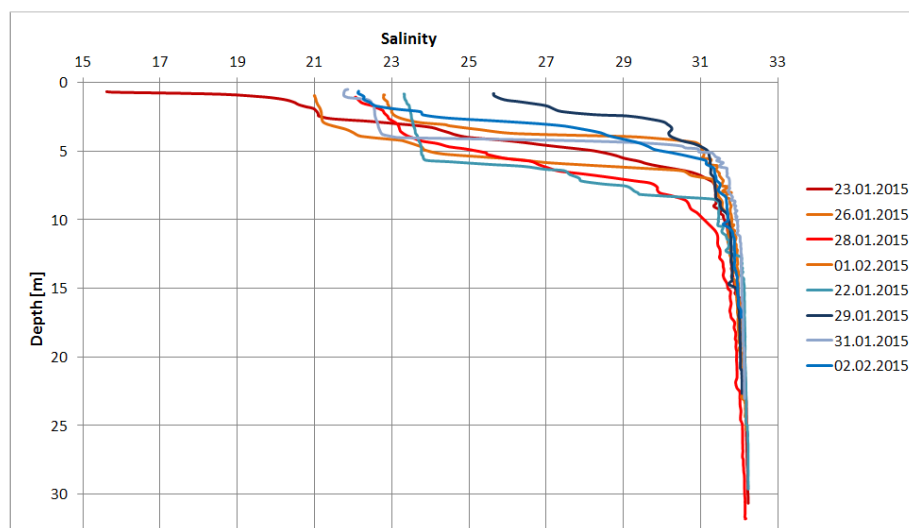


Figure 17: CTD profiles for salinity at XHuinay North at different sampling dates. Red lines represent casts at rising tide; blue lines represent casts at falling tide.

Water temperatures decline at XHuinay North was less distinct (Fig. 18). Steepest temperature decline was between 0m and 20m with a range between 19.6°C and 12.07°C at falling tide (28.02.2015). From about 25m all temperature measurements were akin to each other at about 11°C.

10 Results

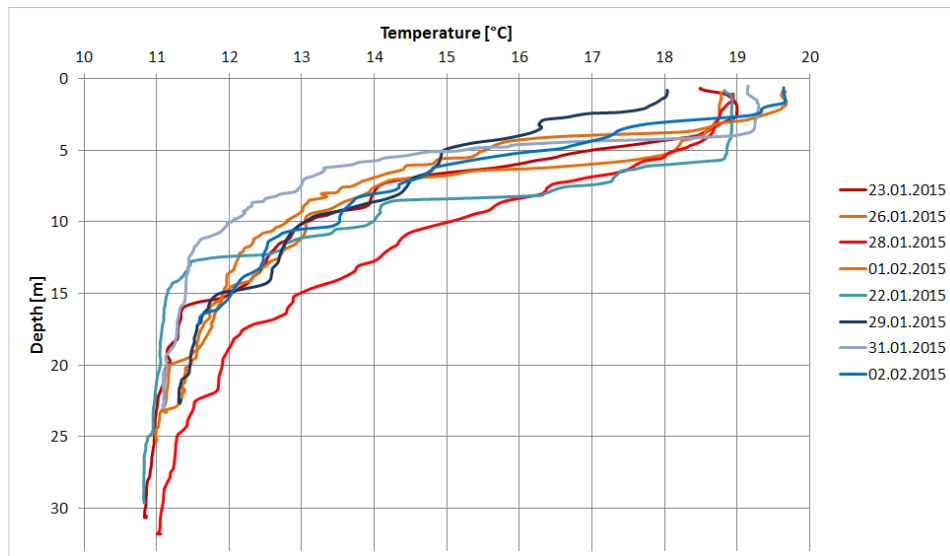


Figure 18: CTD profiles for temperature [°C] at XHuinay North at different sampling dates. Red lines represent casts at rising tide; blue lines represent casts at falling tide.

10.1.1.2 LILLIGUAPI

At sampling site Lilliguapi CTD casts were carried out for three times at rising and three times at falling tide. Maximum sampling depth was between 14.5m and 24.6m. The low salinity surface layer only extended to 5m (Fig. 19).

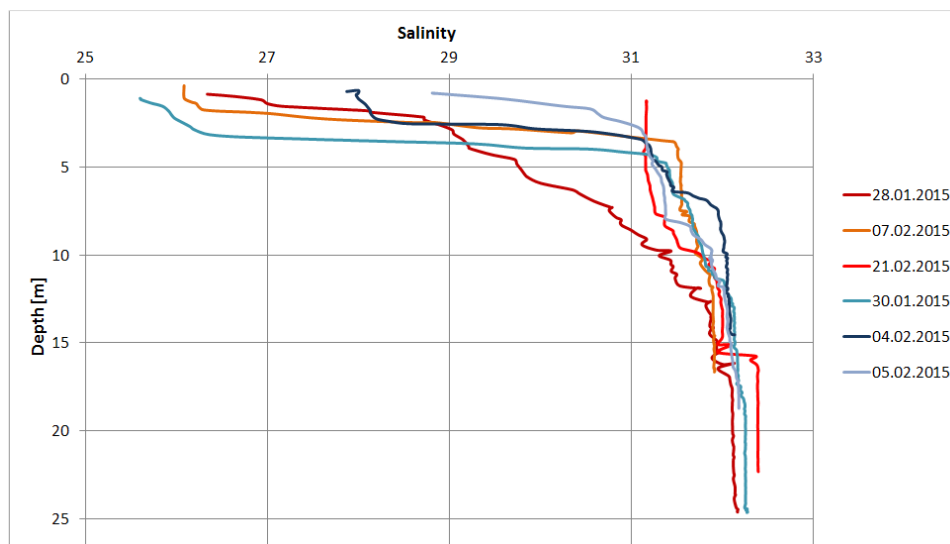


Figure 19: CTD profiles for salinity at Lilliguapi at different sampling dates. Blue lines represent measurements at falling tide; red lines represent values at rising tide.

Also the difference between the surface layer and the deeper water was much smaller. Lowest salinity was measured at falling tide (30.01.2015) at 1m depth with 25.6, highest at rising tide (21.02.2015) with 32.4 from 21.6m on. There was no difference in salinity between rising and falling tide. Water temperature fluctuated up to a depth of about 20m with a mean change between 18°C to 12°C (Fig. 20).

10 Results

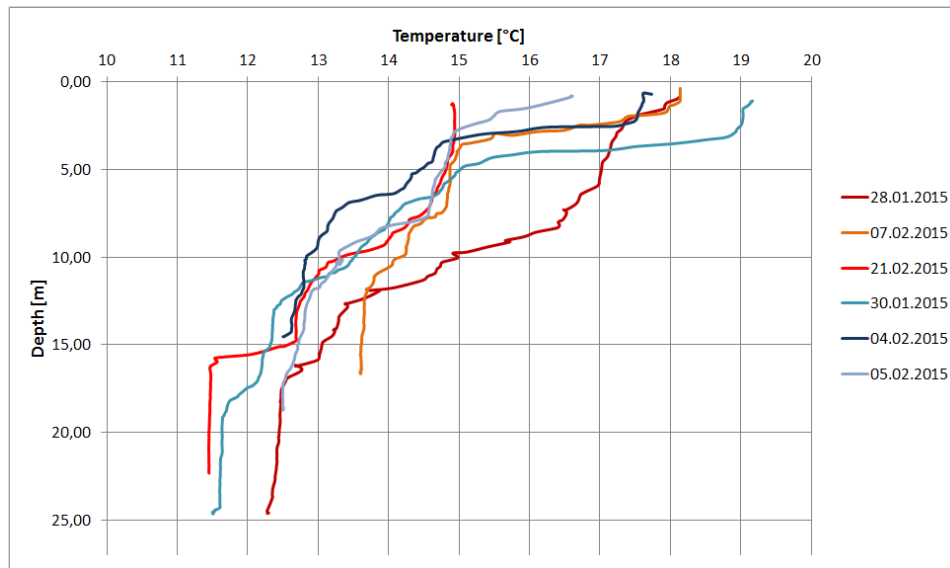


Figure 20: CTD profiles for temperature [°C] at Lilliguapi at different sampling dates. Red lines represent casts at rising tide; blue lines represent casts at falling tide.

Highest surface water layer temperature was measured at 1m (30.01.2015) with 19.17°C, lowest at 1.3m (21.02.2015) with 14.89°C. There was no difference between rising and falling tide.

10.1.1.3 ENSENADA DE LAS ISLAS

At sampling site Ensenada de Las Islas, CTD data were only collected once at rising tide on the 12.02.2015. Maximum sampling depth was 26.9m. Figure 21 shows logged data for temperature and salinity.

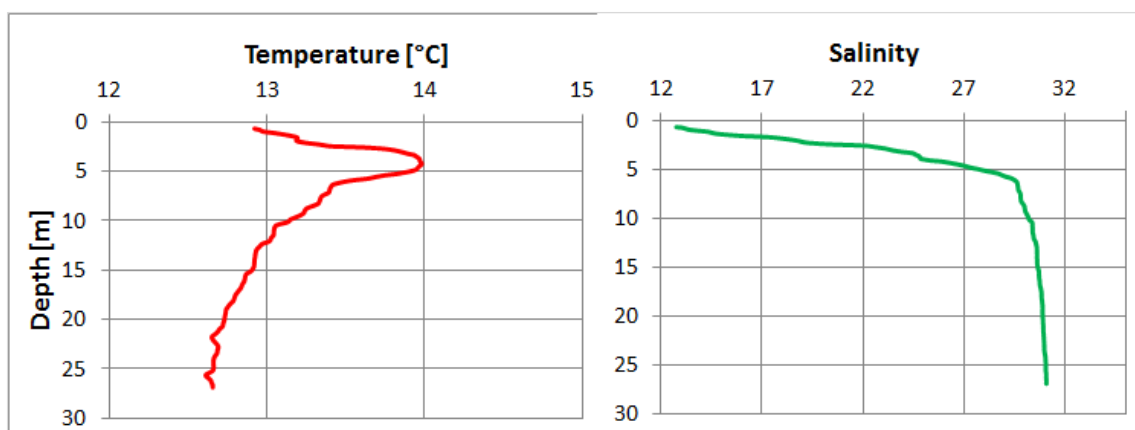


Figure 21: CTD profiles at Ensenada de Las Islas. Data were logged for temperature (red) and salinity (green).

At this sampling site a clear surface layer is identifiable, which extends to 5m depth. In this surface layer, the water temperature first increases with increasing depth, from 12.9°C to 13.97°C. Below this depth the temperature starts to decrease again to the lowest measured value of 12.60°C at 25.5m. This surface layer

10 Results

is also pronounced concerning the salinity. Within the first 5m the salinity increases from brackish 12.7 to 28.5. Below the 5m horizon the salinity increases further to a maximum of 31.1.

10.1.2 LONG-TERM TEMPERATURE DATA MEASUREMENTS

Temperatures are given in degree Celsius and were measured with an interval of 15 minutes. Measured data were averaged for a mean diurnal temperature. Figure 22 shows the monthly water temperatures in 20m depth at XHuinay North during the course of one year (February 2014 - February 2015). Averaged monthly temperatures alternated between $10.55 \pm 0.15^\circ\text{C}$ in August 2014 and $12.64 \pm 0.89^\circ\text{C}$ in March 2014. The highest water temperature was documented on a day in December 2014 with 15.30°C , the lowest in August 2014 with 9.93°C . Maximum temperature fluctuations of $\Delta 0.89^\circ\text{C}$ and $\Delta 0.77^\circ\text{C}$ were recorded in March 2014 and December 2014 (Appendix 1, Table A1.1).

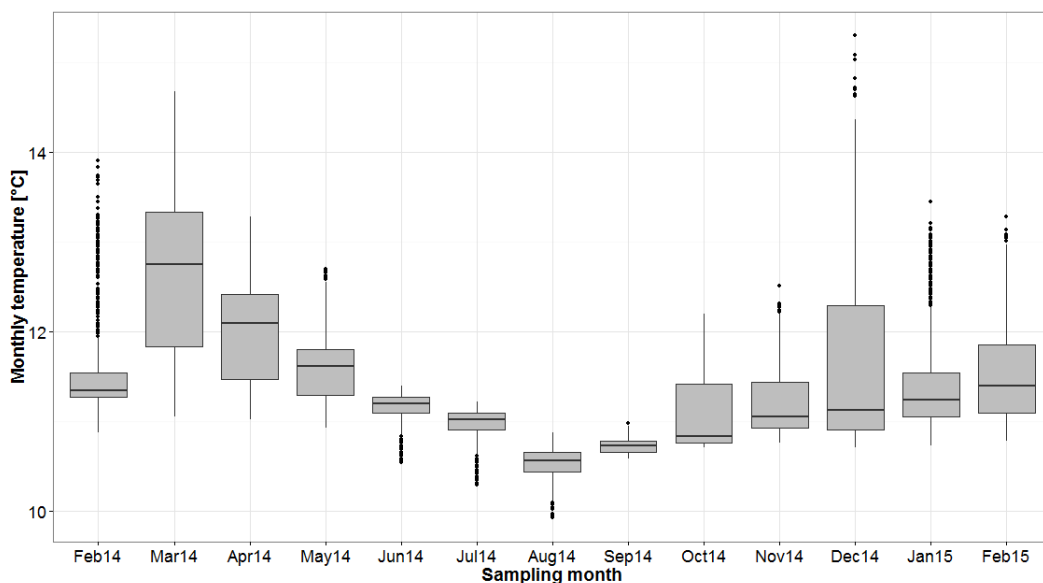


Figure 22: Boxplots showing monthly water temperatures at sampling site XHuinay North from a water depth of 20m. Boxplots are given with median line (horizontal), SD (vertical lines) and outliers (dots). Measurements were conducted every 15 minutes and were averaged for a diurnal temperature. Measurements are shown from February 2014 till February 2015. Averaged monthly temperatures alternated between $10.55 \pm 0.15^\circ\text{C}$ in August 2014 and $12.64 \pm 0.89^\circ\text{C}$ in March 2014. Minimum temperature was recorded in August 2014 (9.93°C), maximum temperature in December 2014 (15.30°C).

Monthly water temperature (February 2014 - January 2015) in 20m depth for site Lilliguapi are shown in Figure 23. Averaged monthly temperatures alternated between $10.41 \pm 0.17^\circ\text{C}$ in August 2014 and $12.85 \pm 0.93^\circ\text{C}$ in February 2014. The highest water temperature 15.53°C was documented on a day in February 2014, the lowest 9.46°C in August 2014. Maximum temperature fluctuations of $\Delta 0.93^\circ\text{C}$ were recorded in February and December 2014 (Appendix 1, Table A1.2).

10 Results

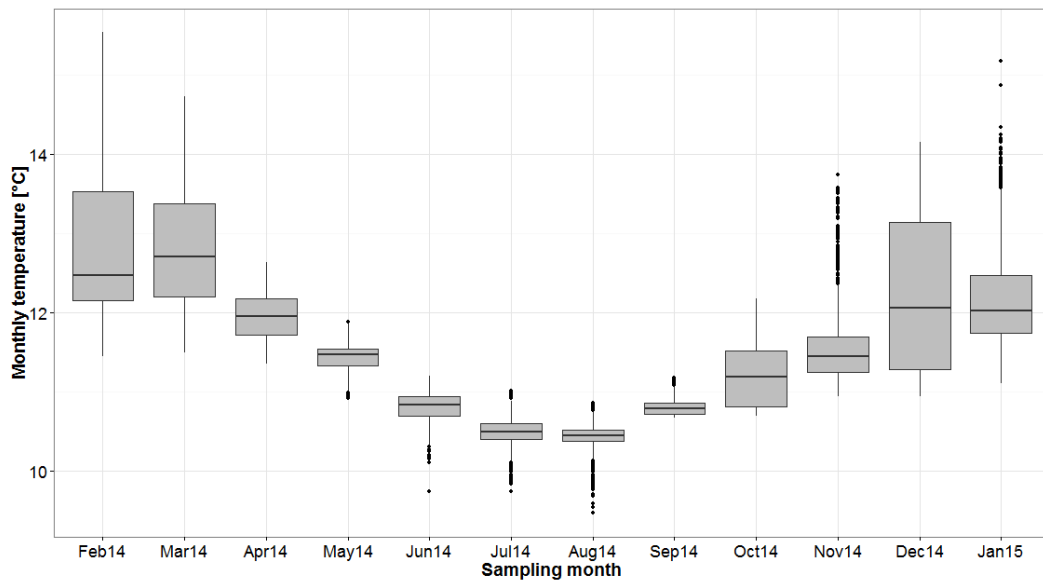


Figure 23: Boxplots showing monthly water temperatures at sampling site Lilliguapi from a water depth of 20m. Boxplots are given with median line (horizontal), SD (vertical lines) and outliers (dots). Measurements were conducted every 15 minutes and were averaged for a diurnal temperature. Measurements are shown from February 2014 till January 2015. Averaged monthly temperatures alternated between $10.41 \pm 0.17^\circ\text{C}$ in August 2014 and $12.85 \pm 0.93^\circ\text{C}$ in February 2014. Minimum temperature was recorded in August 2014 (9.93°C), maximum temperature in February 2014 (15.53°C).

Figure 24 shows the monthly water temperatures at sampling station Ensenada de Las Islas in a water depth of 22m.

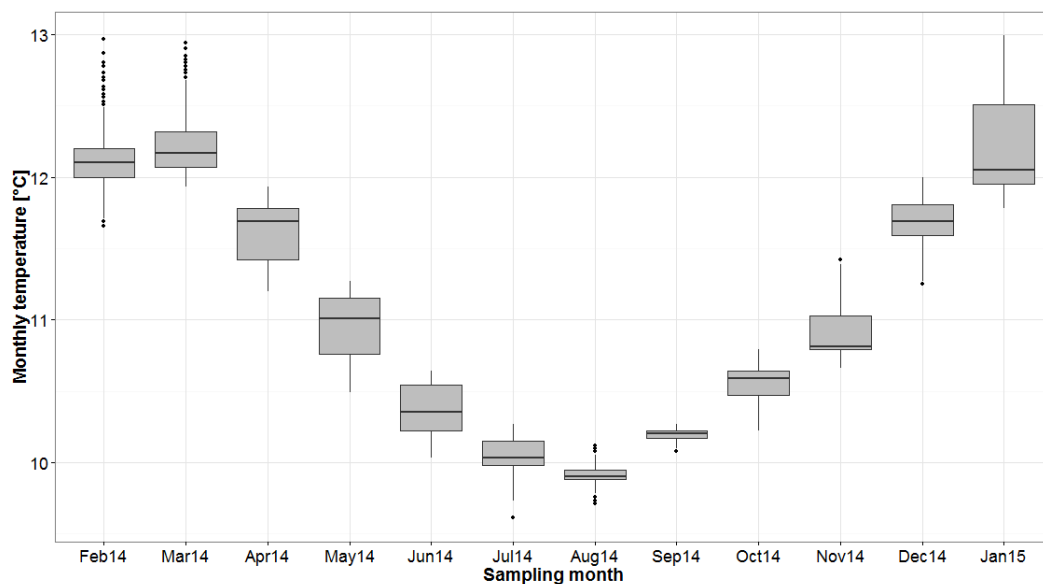


Figure 24: Boxplots showing monthly water temperatures at sampling site Ensenada de Las Islas from a water depth of 22m. Boxplots are given with median line (horizontal), SD (vertical lines) and outliers (dots). Measurements were conducted every 15 minutes and were averaged for a diurnal temperature. Measurements are shown from February 2014 till January 2015. Averaged monthly temperatures alternated between $9.92 \pm 0.07^\circ\text{C}$ in August 2014 and $12.59 \pm 0.72^\circ\text{C}$ in February 2014. Minimum temperature was recorded in July 2014 (9.61°C), maximum temperature in February 2015 (12.99°C).

10 Results

Mean water temperatures were between $9.92^{\circ}\text{C} \pm 0.07^{\circ}\text{C}$ in August 2014 and $12.59^{\circ}\text{C} \pm 0.72^{\circ}\text{C}$ in January 2015. The highest temperature was measured on a day in January 2015 with 12.99°C , lowest temperature in July 2014 with 9.61°C . Maximum fluctuations took place in May 2014 with $\Delta 0.83^{\circ}\text{C}$ and January 2015 with $\Delta 0.72^{\circ}\text{C}$ (Appendix 1, Table A1.3).

10.1.3 SEA WATER PH

At sampling site Lilliguapi the averaged sea water pH (7.87 ± 0.06) was significantly higher ($p = 0.00002$, $R^2 = 0.8$) than at XHuinay North (7.66 ± 0.04) (Fig. 25) (see also Appendix 2).

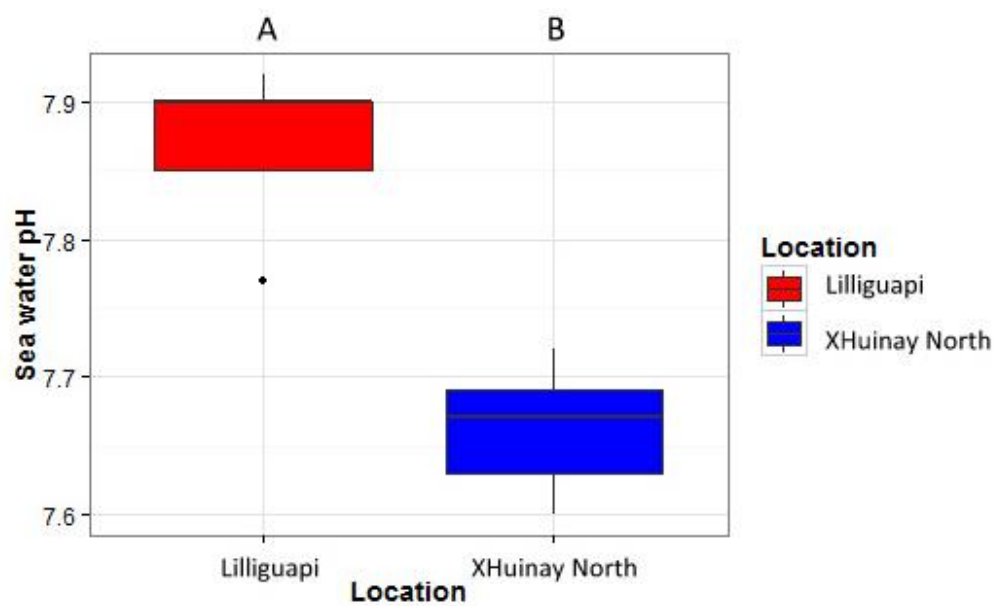


Figure 25: Sea water pH at sampling site Lilliguapi (red) (7.87 ± 0.06) and XHuinay North (blue) (7.66 ± 0.04). Boxplots are given with median line (horizontal), SD (vertical lines) and outliers (dots). A and B symbolize statistically differences between both groups (ANOVA; $p = 0.00002$, $R^2 = 0.8$).

10 Results

10.1.4 SEA WATER TA

At the sampling sites XHuainay North and Lilliguapi TA measurements took place between 26.01.2015 and 21.02.2015 and at Ensenada de Las Islas at 19.02.2015. Highest TA was measured at sampling site XHuainay North (2.241 ± 0.032 mmol/l). At Lilliguapi it was 2.219 ± 0.020 mmol/l and at Ensenada de Las Islas TA was 2.182 ± 0.004 mmol/l (Table 1) (Appendix 3.1) (see also: Diercks *et al.*, 2015a, b, c).

Table 1 TA values (mmol/l with SD) at XHuainay North, Lilliguapi and Ensenada de Las Islas between 26.01.2015 and 21.02.2015

Location	TA [mmol/l]
XHuainay North	2.241 ± 0.031
Lilliguapi	2.219 ± 0.020
Ensenada de Las Islas	2.182 ± 0.004

TA was significantly lower ($p = 0.038$, $R^2 = 0.11$) at sampling site Lilliguapi than at XHuainay North and significantly higher than at sampling site Ensenada de Las Islas ($p = 0.011$, $R^2 = 0.36$). Likewise the difference between XHuainay North and Ensenada de Las Islas was significant ($p = 0.005$, $R^2 = 0.31$) (Appendix 3.2, A3.3, A3.4).

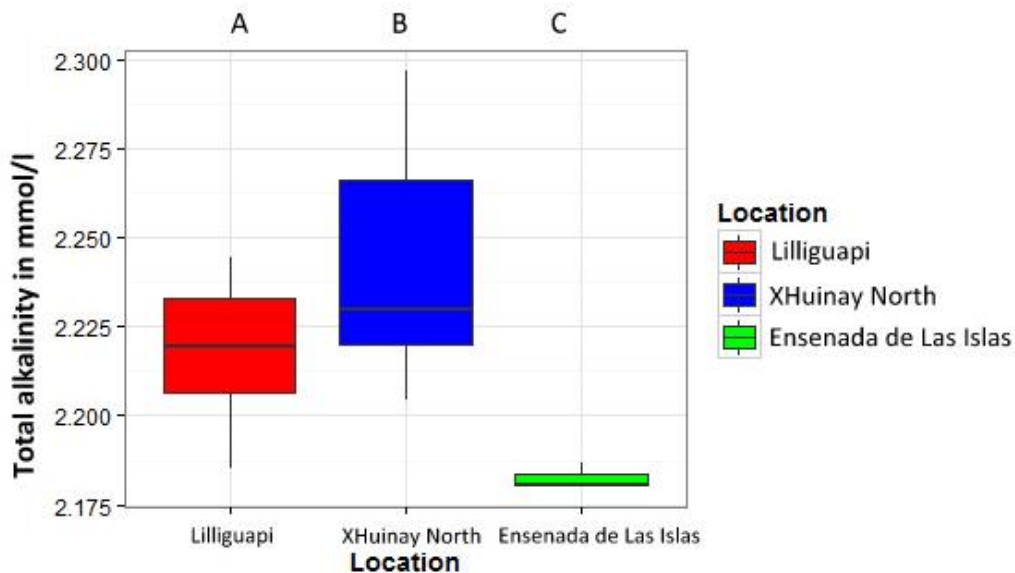


Figure 26: Boxplots of TA (mmol/l) measured at Lilliguapi (red) (2.219 ± 0.020 mmol/l) and XHuainay North (blue) (2.241 ± 0.031 mmol/l) and Ensenada de Las Islas (green) (2.182 ± 0.004 mmol/l). Boxplots are given with median line (horizontal) and SD (vertical lines). Different capital letters indicate statistical difference in TA between locations: Statistical significant difference between XHuainay North and Lilliguapi (ANOVA; $p = 0.038$, $R^2 = 0.11$), significant difference between Lilliguapi and Ensenada de Las Islas (ANOVA; $p = 0.011$, $R^2 = 0.36$) and significant difference between XHuainay North and Ensenada de Las Islas (ANOVA; $p = 0.005$, $R^2 = 0.31$).

10 Results

10.2 ABUNDANCE IN RELATION TO DEPTH AND SUBSTRATE INCLINATION

10.2.1 ABUNDANCE IN RELATION TO DEPTH

The abundance of *T. endesa* in relation to different depth zones was determined exemplarily for a sub-population in XHuainay North. *T. endesa* was not found at depths shallower as 16m. Therefore, pictures for abundance measurements were taken in four different depth zones, which are referred to the LAT: 16m, 19m, 22m and 25m. Due to a patchy distribution only pictures with at least one specimen of *T. endesa* were analysed (Appendix 4). The average abundance of *T. endesa* at sampling site XHuainay North was 69 ± 45 individuals per m^2 . For the analysis, population densities recorded in pictures taken in the same depth and with the same inclination angle, values were averaged and are given with standard deviation (\pm SD) (Table 2).

Table 2 Population densities [n/m^2] of *T. endesa* in four different depth zones at XHuainay North.

Depth	Population density [n/m^2]
16m	55 ± 30
19m	71 ± 41
22m	76 ± 28
25m	67 ± 44

There was no significant difference ($p = 0.424$) in population density within the four depth zones (Fig. 27).

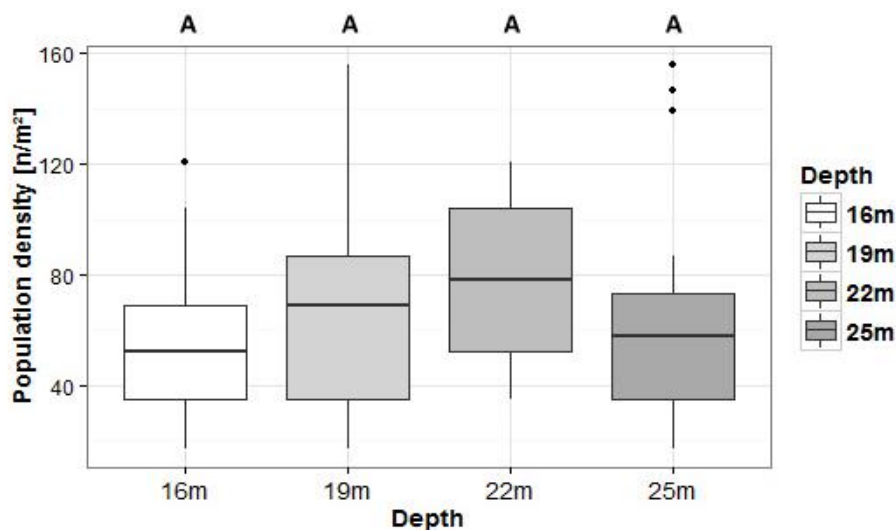


Figure 27: Boxplots showing population density [n/m^2] of *T. endesa* in different water depths (16m, 19m, 22m and 25m) at sampling site XHuainay North. Boxplots are given with median line (horizontal), SD (vertical lines) and outliers (dots). Increased shading of boxplots indicates increased depth. Identical capital letters indicate that there is no statistical difference (ANOVA; $p = 0.424$) in population density of *T. endesa* in depth zones between 16m and 25m.

10 Results

Population densities in water depth 21/22m were compared between the sampling site XHuinay North, located in the fjord Comau and Ensenada de Las Islas in the fjord Piti-Palena. The population density at a depth of 22m at XHuinay North is 76 ± 28 individuals (n) per m^2 , whereas at Ensenada de Las Islas it is 159 ± 71 n per m^2 at 21m (Fig. 28). There is a significantly ($p = 0.0002$, $R^2 = 0.3473$) (Appendix 4.3) higher population density of *T. endesa* at the sampling site Ensenada de Las Islas.

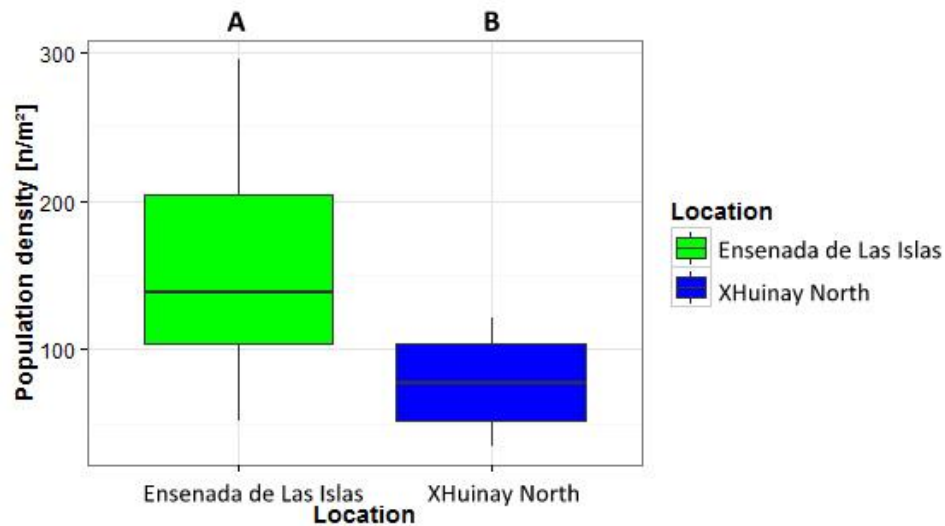


Figure 28: Boxplots, showing population density in individuals (n) per m^2 at a water depth of 21/22m at sampling station Ensenada de Las Islas (green) and XHuinay North (blue). Boxplots are given with median line (horizontal) and SD (vertical lines). Capital letters A and B symbolize statistical differences between both groups (ANOVA, $p = 0.0002$; $R^2 = 0.3473$).

Maximum abundance of *T. endesa* was observed in a small niche at sampling site Lilliguapi (Fig. 29). The extrapolated maximum population density was 1,161 individuals per m^2 .

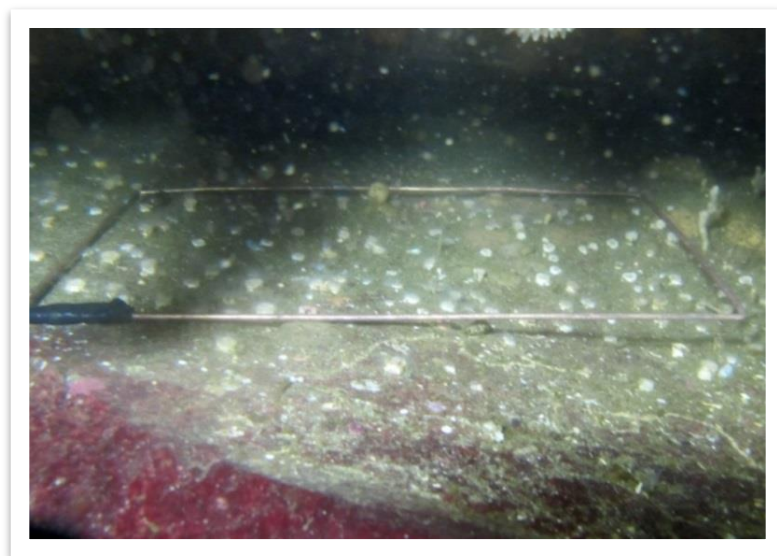


Figure 29: Photo of sampling frame in a niche at Lilliguapi with maximum observed abundance of *T. endesa*.

10 Results

10.2.2 ABUNDANCE REGARDING SUBSTRATE INCLINATION

The abundance of *T. endesa* related to the substrate inclination was calculated for a sub-population at XHuinay North and Ensenada de Las Islas. Pictures were taken at different substrate inclination angles but only analysed when at least one specimen of *T. endesa* was present within the sampling frame area (c.f. Appendix 4). For pictures with identical inclination angle values were averaged. Pictures were pooled to groups in 10° steps. Population densities related to substrate inclination were calculated to m² and are given in total numbers with standard deviation. At XHuinay North *T. endesa* appears at substrates with inclination angles between 71° and 145°. During the survey at XHuinay North it was not found at substratum flatter or steeper than this. Pictures were categorized in eight groups: >70-80°, >80°-90°, >90°-100°, >100°-110°, >110°-120°, >120°-130°, >130°-140° and >140°-145°. As no photo was taken at an inclination between 80° and 90°, this group is neglected in the following (Table 3).

Table 3 Groups of inclination angles and related population densities at XHuinay North calculated to 1m². Number of photos represents number of pictures analyzed. Values are given in total numbers with standard deviation.

Substrate Inclination [°]	Number of photos	Population density [n/m ²]
>70° - 80°	4	48 ± 17
>90° - 100°	1	87 ± 0
>100° - 110°	16	59 ± 32
>110° - 120°	34	73 ± 26
>120° - 130°	13	74 ± 38
>130° - 140°	1	52
>140° - 145°	3	48 ± 18

In XHuinay North (Fig. 30) the substrate inclination had no significant effect (ANOVA; $p = 0.749$) on the population density of *T. endesa*.

10 Results

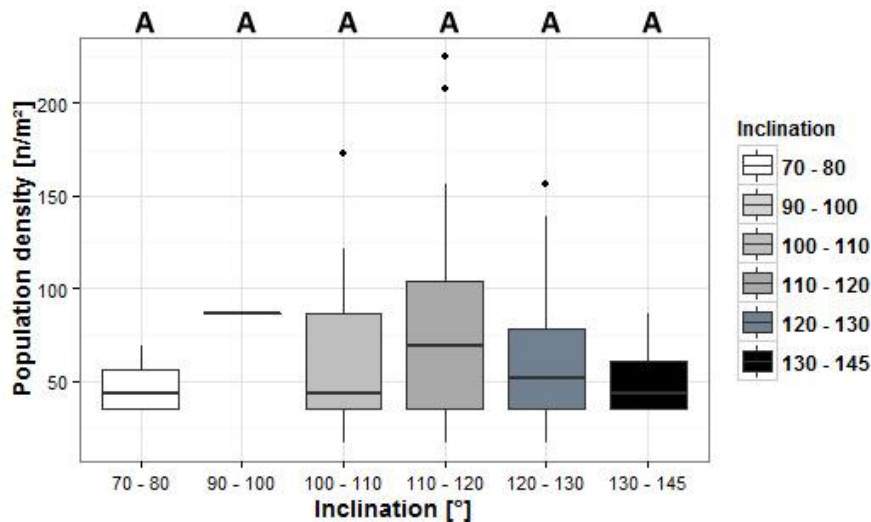


Figure 30: Boxplots, representing the population density of *T. endesa* in individuals (n) per m² for different substrate inclinations at XHuinay North. Boxplots are given with median line (horizontal), SD (vertical lines) and outliers (dots). Shadings of grey refer to steepness of the substratum with bright to dark shades symbolizing increasing steepness. Pictures were categorized in groups: >70-80°, >90-100°, >100-110°, >110-120°, >120-130°, >130-140° and >140-145°. Identical capital letters indicate that there was no statistical difference in population density between the groups ($p = 0.749$).

At sampling site Ensenada de Las Islas, *T. endesa* was found on substrates with an inclination of 71° - 122°. Here, pictures were grouped to >70° - 80°, >80° - 90°, >90° - 100°, >100° - 110°, >110° - 120° and >120° - 122° (Table 4).

Table 4 Groups of inclination angles and related population densities at Ensenada de Las Islas calculated to 1m². Number of photos represents number of pictures analyzed. Values are given in total numbers with standard deviation.

Substrate Inclination [°]	Number of photos	Population density [n/m ²]
>70° - 80°	3	76 ± 4
>80° - 90°	4	158 ± 33
>90° - 100°	4	178 ± 96
>100° - 110°	10	164 ± 62
>110° - 120°	22	125 ± 25
>120° - 122°	1	121

At sampling site Ensenada de Las Islas (Fig. 31), no statistical evidence for the relation between abundance of *T. endesa* and inclination of the settled substrate was found (ANOVA; $p = 0.075$).

10 Results

A pooled dataset of population densities and related inclinations for XHuinay North and Ensenada de Las Islas was also not significant (ANOVA; $p = 0.0552$).

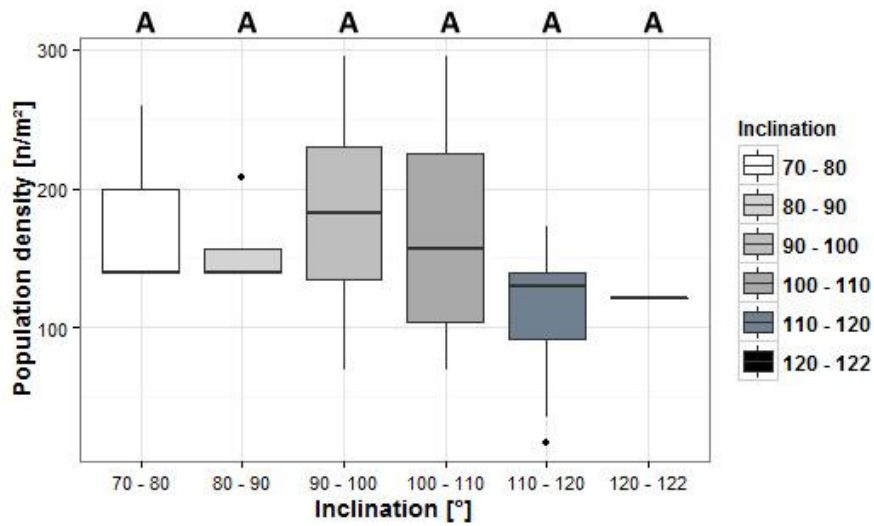


Figure 31: Boxplots, representing the population density of *T. endesa* in individuals (n) per m^2 for different substrate inclinations at Ensenada de Las Islas. Boxplots are given with median line (horizontal), SD (vertical lines) and outliers (dots). Shadings of grey refer to steepness of the substratum with bright to dark shades symbolizing increasing steepness. Pictures were grouped to $>70^\circ - 80^\circ$, $>80^\circ - 90^\circ$, $>90^\circ - 100^\circ$, $>100^\circ - 110^\circ$, $>110^\circ - 120^\circ$ and $>120^\circ - 122^\circ$. Identical capital letters indicate that there was no statistical difference in population density between the groups ($p = 0.075$).

10.3 MASS INCREASE

Size classes of *T. endesa* specimens in the cross-transplantation experiment ranged between 0.06cm^3 and 0.32cm^3 in volume. Using the statistical method of an ANOVA revealed that corals of different size classes were distributed randomly among the groups. There was no significant difference between the experimental groups (ANOVA; $p = 0.131$). Mass increase of the control treatment at sampling site Lilliguapi was $9.82 \pm 4.38\% \text{ yr}^{-1}$, or $0.03 \pm 0.01\% \text{ d}^{-1}$ respectively. At XHuainay North corals grew $10.87 \pm 4.4\% \text{ yr}^{-1}$ ($0.03 \pm 0.01\% \text{ d}^{-1}$). There was no significant difference (ANOVA; $p = 0.455$) between both groups (Fig. 32).

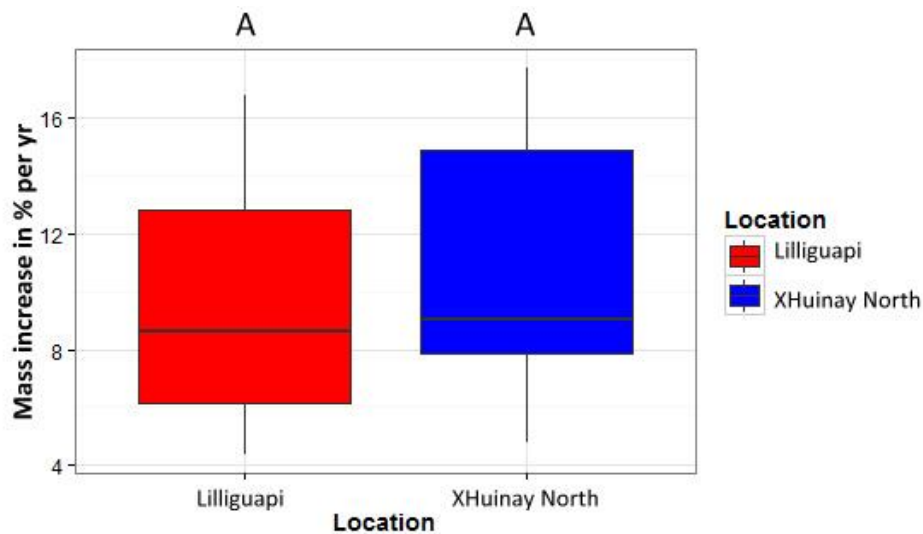


Figure 32: Boxplots showing mass increase of control groups in $\% \text{ yr}^{-1}$. Boxplots are given with median line (horizontal), SD (vertical lines). Red symbolizes control group in Lilliguapi (high pH) ($9.82 \pm 4.38\% \text{ yr}^{-1}$), blue symbolizes control group in XHuainay North (low pH) ($10.87 \pm 4.4\% \text{ yr}^{-1}$). Identic capital letters symbolize that there is no significant difference between both groups (ANOVA; $p = 0.445$).

General long-term *in situ* growth rate of *T. endesa* is therefore $10.34 \pm 4.34\% \text{ yr}^{-1}$ ($0.03 \pm 0.01\% \text{ d}^{-1}$). Corals, being transplanted from Lilliguapi to XHuainay North (LtoX) showed a mass increase of $10.51 \pm 1.14\% \text{ yr}^{-1}$ ($0.03 \pm 0.00\% \text{ d}^{-1}$). Those, which have been transplanted from XHuainay North to Lilliguapi (XtoL) grew $7.34 \pm 3.13\% \text{ yr}^{-1}$ ($0.02 \pm 0.01\% \text{ d}^{-1}$) (Fig. 33). There was no significant difference between both transplanted groups (XtoL and LtoX; ANOVA; $p = 0.581$) the control group in XHuainay North and the transplanted group (X and XtoL; ANOVA; $p = 0.290$) or the control group in Lilliguapi and the transplanted group (L and LtoX; ANOVA; $p = 0.980$) (Appendix 5).

10 Results

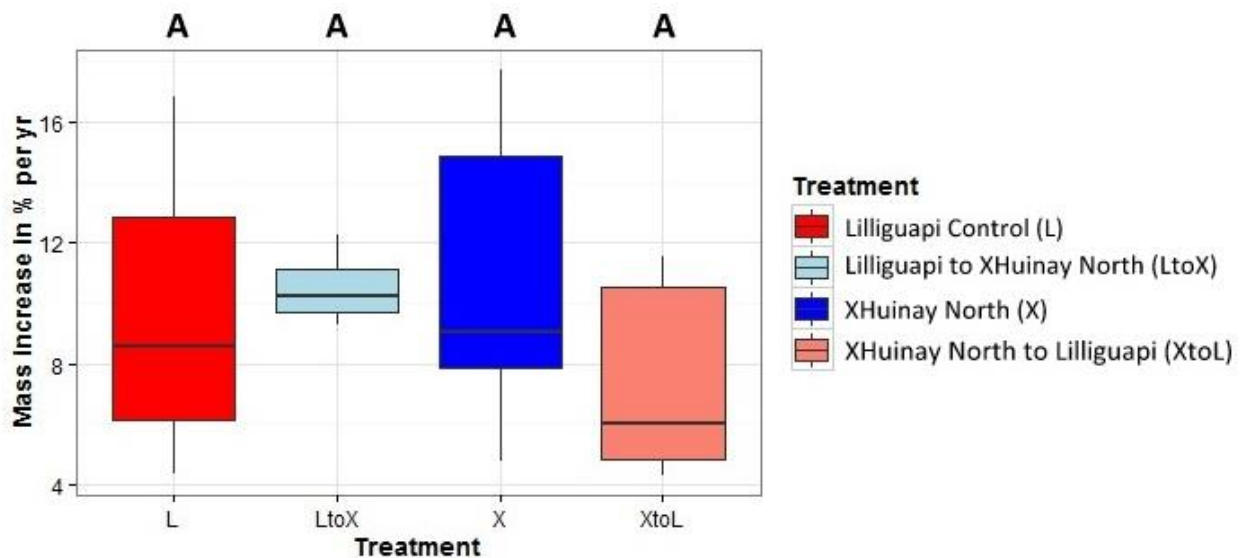


Figure 33: Boxplots showing mass increase of control groups and transplanted groups in % y^{-1} . Boxplots are given with median line (horizontal) and SD (vertical lines). Red color indicates high pH environment (Dark red symbolizes the control group in Lilliguapi, (L) ($9.82 \pm 4.38\% \text{ yr}^{-1}$) light red the corals coming from XHuainay North and being transplanted to Lilliguapi (XtoL) ($7.34 \pm 3.13\% \text{ yr}^{-1}$). Blue color indicates low pH environment (Dark blue symbolizes the control group in XHuainay North (X) ($10.87 \pm 4.4\% \text{ yr}^{-1}$), light blue the corals being transplanted from Lilliguapi to XHuainay North (LtoX) ($10.51 \pm 1.14\% \text{ yr}^{-1}$). Identical capital letters symbolize that there is no statistical difference between the groups.

10.4 RESPIRATION

10.4.1 CORRELATION OF THE CALYX SURFACE AREA AND DM

The comparison of the 'projected calyx surface area' and DM of *T. endesa* revealed a statistically significant correlation (Tukey; $p = 0.004$, correlation coefficient = 0.881) (Fig. 34) (Appendix A6.1). The calculations of respiration rates in the following chapter 10.4.2 are therefore referring to the calyx surface area.

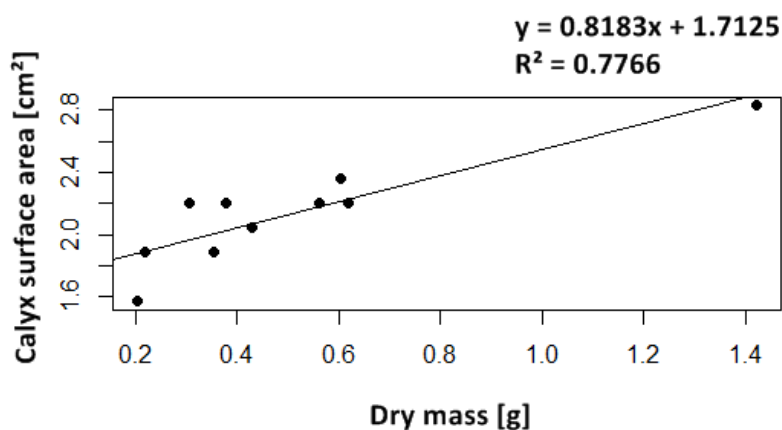


Figure 34: Scatterplot with regression line ($y = 0.8183x + 1.7125$) of calyx surface area in cm^2 and DM in g. Correlation is significant (Tukey; $p = 0.004$).

10 Results

10.4.2 RESPIRATION RATES

Respiration rates were measured with two methods: A manual method using a handheld Luminescent/Optical Dissolved Oxygen Probe and an automatical Optode measurement in a flow-through system (Table 5) (Appendix 6).

Table 5 Respiration rates (RR) of all treatments, given in $\mu\text{Mol O}_2 \times \text{cm}^2 \times \text{d}^{-1}$ with SD. Respiration rates were measured with a manual and an automatical method. Control group at Lilliguapi (L), corals transplanted from high pH (Lilliguapi) to low pH (XHuinay North) (LtoX), control group XHuina North (X) and corals being transplanted from low pH to high pH (XtoL).

Treatment	Respiration rates [$\mu\text{Mol O}_2 \times \text{cm}^2 \times \text{d}^{-1}$]	
	Manual measurement	Automatical measurement
L	9.20 ± 2.53	5.712 ± 2.148
L to X	10.57 ± 4.10	6.793 ± 6.799
X	8.23 ± 4.32	5.239 ± 3.666
X to L	7.24 ± 0.74	8.916 ± 1.844

Measurements with the automatical method revealed, that the oxygen decrease within the respiration chamber was consistent and linear. Therefore, only start and end values of oxygen saturation were used for determination of respiration rates. As the respiration rates for both measurements did not differ statistically (ANOVA; $p = 1.00$) from each other, values were amalgamated for further statistical analyses (Table 6, Fig. 34).

Table 6: Respiration rates (RR) of all treatments, given in $\mu\text{Mol O}_2 \times \text{cm}^2 \times \text{d}^{-1}$ with SD. Values of manual and automatical measurements have been amalgamated.

Treatment	RR [$\mu\text{Mol O}_2 \times \text{cm}^2 \times \text{d}^{-1}$]
L	8.05 ± 2.93
LtoX	9.88 ± 4.52
X	7.16 ± 4.23
XtoL	8.08 ± 1.50

10 Results

Respiration rates of all four different treatments did not differ significantly (ANOVA; $p = 0.398$) from each other. Corals being transplanted from a high to a low pH environment (LtoX) showed increased respiration rates of 22% compared to their control group, although this effect was not statistically significant.

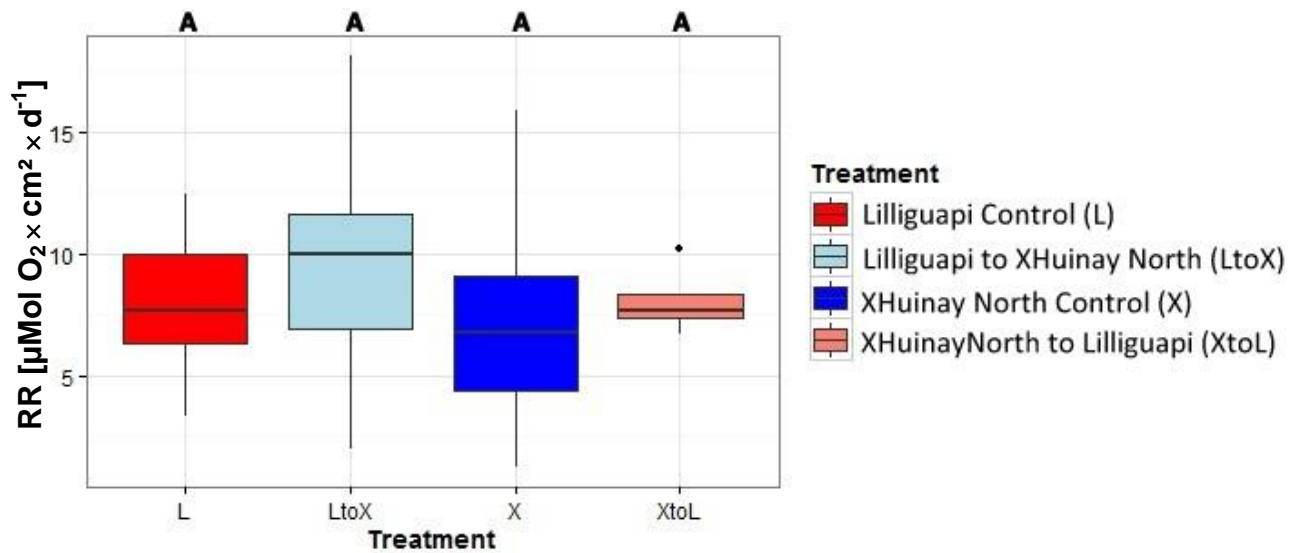


Figure 35: Boxplots showing respiration rates [$\mu\text{Mol O}_2 \times \text{cm}^2 \times \text{d}^{-1}$] of all treatments. Boxplots are given with median line (horizontal), SD (vertical lines) and outliers (dots). Red boxplot symbolizes control group in Lilliguapi (L) ($8.05 \pm 2.93 \mu\text{Mol O}_2 \times \text{cm}^2 \times \text{d}^{-1}$), lightblue corals being transplanted from Lilliguapi to XHuainay North (LtoX) ($9.88 \pm 4.52 \mu\text{Mol O}_2 \times \text{cm}^2 \times \text{d}^{-1}$), blue symbolizes control group in XHuainay North (X) ($7.16 \pm 4.23 \mu\text{Mol O}_2 \times \text{cm}^2 \times \text{d}^{-1}$) and lightred corals being transplanted from XHuainay North to Lilliguapi (XtoL) ($8.08 \pm 1.50 \mu\text{Mol O}_2 \times \text{cm}^2 \times \text{d}^{-1}$). Values are amalgamated from manual and automatical measurements. Identic capital letters indicate that there was so statistical difference in RR between the groups (ANOVA; $p = 0.389$).

11 DISCUSSION

The present study aimed to describe the physiological reactions of the solitary cold-water scleractinian *T. endesa* towards different physical environmental factors. For this purpose, its abundance – related to depth and substrate inclination and the autecological parameters growth and respiration were examined. The conducted oceanographic depth profiles of the fjords Comau and Piti-Palena illustrated different abiotic influences on the sampling stations of *T. endesa*. Findings of variations in abiotic environmental conditions at the sampling sites, such as the difference in the layering of the water column, can be linked to location-dependent, divergent abundances. *T. endesa* was not found in waters shallower than 16m, nonetheless between 16m and 25m there seems to be no distinct favoured depth for its settlement. Although it is not statistically verified, *T. endesa* seems to settle most commonly at substrates that are too shallow for other accompanied coral species such as *D. dianthus* and *C. huinayensis*. Corals transplanted along the natural pH gradient of the fjord Comau showed no significant effects concerning their growth rates compared to their control group, when exposed to lower pH values. Comparable growth and respiration rates of corals in the cross-transplantation experiment indicate the capability of *T. endesa* to adapt to environmental conditions, which locally exist already today and are predicted for the future ocean.

11.1 OCEANOGRAPHIC MEASUREMENTS

The oceanographic data revealed a stratification of the water body in the fjord Comau. Concerning salinity, this stratification is distinct at XHuinay North, the sampling site, which is located in the inner fjord. In the depth zone between 0m and 10m a brackish surface layer was evident, which has been demonstrated before by Försterra *et al.* (2010) and Wurz (2014). As the tidal amplitude can reach up to 7m, the brackish water layer can influence benthos communities down to 17m depth (Försterra *et al.*, 2010). The thickness of the surface layer is dependent on the input of freshwater through rivers and other swellings as of seasonal rainfall rates. It underlies seasonal variations (Pantoja *et al.*, 2011). At sampling station Lilliguapi the salinity gradient was less distinct. This might be because of the oceanic influence from the Gulf of Ancud. At Ensenada de Las Islas the brackish surface layer was far more pronounced than at the sampling stations XHuinay North and Lilliguapi. Within the first five meters salinity rises from 12.7 to 28.5.

In Comau Fjord, Fillinger and Richter (2013) revealed a vertical zoning with a warm surface layer up to a depth between 20m and 50m and a cold layer below it up to a depth of 250m. The temperature measurements of the present study at XHuinay North and Lilliguapi support these findings. Herein also a temperature horizon in a depth of about 20m was detectable. The ambient temperature for specimen of the cross-transplantation experiment at Lilliguapi and XHuinay North was between 10°C and 12.5°C. At Ensenada de Las Islas corals at a water depth of 22m experienced comparable ambient water temperatures between 9.9°C and 12.6°C.

11 Discussion

The increased concentration of stored anthropogenic CO₂ in the oceans is reflected in an elevation of the hydrogen ions (H⁺) concentration, which lowers the pH and the available carbonate (CO₃²⁻) ions (Orr *et al.*, 2005). Equilibrium constants are highly affected by temperature, salinity and pressure (Erez *et al.*, 2011) and determine the composition of chemicals. The carbonate ion pool in the present study is represented by pH and TA. Mean ocean pH has decreased from 8.2 to 8.1 since the industrial revolution and is expected to decrease further to 7.8 by the end of this century (Hilmi *et al.*, 2013). Compared to the Atlantic Ocean, the pH of the Pacific is relatively low and reveals a sharp drop within the first 500m with lowest pH values of even 7.4 at 1,000m (Millero, 2006). Wurz (2014) found a vertical pH gradient in the fjord Comau, with decreasing pH values from Lilliguapi, outside the fjord, to Leptepu at the end of the fjord. This is also reflected in the pH values measured in this study, with a pH of 7.87 ± 0.06 at Lilliguapi and a lower pH at XHuina North with 7.66 ± 0.04. Jantzen *et al.* (2013b) examined in 2011 higher pH values of 7.94 ± 0.11 at Lilliguapi and 7.76 ± 0.09 at XHuina, a sampling site located in close proximity to XHuina North. However, daily fluctuations in pH can be up to 0.2 units (i.e. by photosynthetic production, respiration or tide) (Jantzen *et al.*, 2013b). An enhanced CO₂ concentration in Comau Fjord and hence the generally low pH values is probably caused by the geological activity in the Patagonian fjord region and the resulting seepages of volcanic origin (Pantoja *et al.*, 2011; Jantzen *et al.*, 2013b, Muñoz *et al.*, 2014). TA changes with temperature, salinity and pressure (Wolf-Gladrow *et al.*, 2007) and is independent of pH. In 2010 and 2011 Jantzen *et al.* (2013b) recorded TA values of 2.193mmol L⁻¹ and 2.162 ± 3mmol L⁻¹ at Lilliguapi as well as 2.172 ± 41mmol L⁻¹ and 2.144 ± 13mmol L⁻¹ at XHuina. Those values are slightly lower than the ones measured in the recent study and they also show a somewhat higher TA outside the fjord, close to its mouth than in the inner fjord. Though, these variations might be caused by fluctuations over time. In 2015, a TA of 2.219 ± 0.022mmol L⁻¹ was measured at Lilliguapi and of 2.241 ± 0.032mmol L⁻¹ at XHuina North. These values are comparable to those currently expected for surface waters of the Southern Ocean (2.305 ± 0.525mmol L⁻¹) and the equatorial upwelling Pacific (2.294 ± 0.649mmol L⁻¹) (Lee *et al.*, 2006). TA concentrations in the oceans are mainly influenced by salinity, thus the respective Cl⁻ and Na⁺ concentrations and biogeochemical processes such as production of particulate organic matter by microalgae and the precipitation of calcium carbonate (Wolf-Gladrow *et al.*, 2007). Measured salinities in the recent study were comparable to those of Jantzen *et al.* (2013b). However, the amount of organic matter and the precipitation of calcium carbonate may have been different in 2015 compared to 2010 and 2011 and thus have led to other TA concentrations. Divergent values measured in the fjord Comau for different years may be a hint for the dynamics of abiotic environmental factors in this area. Compared to the sampling station XHuina North in Comau Fjord (2.241 ± 0.032 mmol/L), TA values were significantly (p = 0.019, R² = 0.51) lower at Ensenada de Las Islas (2.182 mmol/L). One explanation could be a general less precipitation or remineralization at Ensenada de Las Islas. Alternatively, organisms living in the surface layer of this sampling site and forming calcium carbonate structures, are leaving just a small portion of organic matter to descend to deeper waters. In addition or as a further theory, the pronounced stratification

11 Discussion

between surface layer and deeper waters at Ensenada de Las Islas may have prevented the descending of organic matter and other compounds comprising ions that would have increased the TA.

In 2014, Laudien *et al.* conducted additional oxygen measurements in the fjord Comau. In general, their measurements revealed a vertical zoning with a surface water layer with a thickness of 15 to 30m, oxygenated in concentrations of 280 - 400 $\mu\text{mol O}_2 \times \text{kg}^{-1}$. Below that a zone with 150 – 200 $\mu\text{mol O}_2 \times \text{kg}^{-1}$ extends at least up to the maximum sampling depth of 200m (Wurz, 2014). At sampling site Lilliguapi the averaged oxygen concentration of the surface layer in 2014 (0 - 25m) was $260.88 \pm 43.53 \mu\text{mol O}_2 \times \text{kg}^{-1}$, at sampling site XHuinay it was $258.87 \pm 74.65 \mu\text{mol O}_2 \times \text{kg}^{-1}$ (Laudien *et al.*, 2014).

11.2 ABUNDANCE REGARDING DEPTH AND SUBSTRATE INCLINATION

11.2.1 METHODOLOGICAL CONSIDERATIONS

The frame based census method, which has been used in the present study, has been already demonstrated to be an adequate method for analysing abundances and preferred substrate inclination angles of solitary CCWs (Wendländer, 2014; Wurz, 2014). Nevertheless, all statements are only based on a small section of the area and depth zones where *T. endesa* is abundant. The insurance regulations for scientific SCUBA divers restricted the operational depth to 30m. As the upper distribution limit of *T. endesa* is at about 15 m (own personal experience) and always below the influence of the low salinity layer (Cairns *et al.*, 2005), the examined area is quite narrow. Nevertheless, the high number of pictures taken and analysed and the comparison of two different sampling sites in different fjords provide a substantial overview of the distributional patterns of *T. endesa* in upper water layers of the Chilean fjord system.

11.2.2 ABUNDANCE IN RELATION TO WATER DEPTH

Although CWC are mainly known as deep-sea corals, some of them, such as *D. dianthus*, *C. huinayensis* or *L. pertusa* are also known to occur in shallow waters of the sublittoral (Roberts *et al.*, 2009). Therefore, the abundance of these corals is not primarily dependent on the water depth and the resulting hydrostatic pressure but on other abiotic environmental factors such as the ambient water temperature (Roberts *et al.*, 2009). The habitats of cold-water corals living in the deep sea underlie only minor fluctuations (Roberts *et al.*, 2006). In oceanographic conditions the Chilean fjord region seems to be favourable habitat for several CWCs such as *D. dianthus*, *C. huinayensis* and *T. endesa*, although it is characterized by more severe fluctuations concerning abiotic environmental factors, especially in the shallow water zones. *T. endesa* faces strong daily and seasonal fluctuations in temperature (up to 6°C) and sea water pH in Comau Fjord. Its abundance, despite these inconsistent environmental conditions, can be interpreted as a result of the ecophysiological tolerance against fluctuating abiotic conditions. Maximum abundance of *T. endesa* was documented in a small niche at sampling station Lilliguapi with 1,161 individuals per m^2 and is therefore comparable to the maximum abundance of *C. huinayensis*

11 Discussion

(at 18m depth) with 1,300 individuals per m² (Wurz, 2014). For *D. dianthus*, Försterra *et al.* (2003) recorded a maximum abundance to be 1,500 individuals per m². In Comau Fjord, the abundance of *T. endesa* could be limited by the massive and dense banks of *D. dianthus*, which start at a water depth of 20m and cover more than 1,000 m² (Häussermann and Försterra, 2007). Moreover, the slipper snail (*Crepidula*) can be found in large assemblages at the sampling site XHuinay North (own personal experience.) Their appearance could have two opposed impacts on the settlement of *T. endesa*. On one hand, they can serve as secondary hard bottom structure, as *T. endesa* also settles on the snails' shells. On the other hand, as *Crepidula* also settles at the rocky walls of the fjord, they could also constitute another potential spatial competitor. However, in the same depth at Piti-Palena Fjord, the abundance of *D. dianthus* was much lower and *Crepidula* was rarely found (own personal experience). This would leave more settlement area for other species such as *T. endesa* and *C. huinayensis*.

Abundances of *T. endesa* in 21/22m water depth were compared between XHuinay North in the fjord Comau and Ensenada de Las Islas in Piti-Palena Fjord. The average abundance of *T. endesa* at sampling station XHuinay North at a depth of 22m is 76 ± 28 individuals per m², at 21m at Ensenada de Las Islas it is 159 ± 71 individuals per m². Abundances of *T. endesa* in the fjord Comau are therefore comparable to *C. huinayensis* (XHuinay: 210 ± 310 n/m²; Wurz, 2014). At Ensenada de Las Islas their abundance is significantly higher compared to XHuinay North. This divergent pattern can be caused by location dependent factors. At XHuinay North the volatile surface layer extends to a depth of 10m for salinity and even 20m for temperature. Contingent on the tidal amplitude corals in 21m depth at this station can still be influenced by changing temperature and salinity. The long-term measurement of water temperatures at XHuinay North showed that corals there can be exposed to water temperatures of even 15.30°C, mean annual temperature was 11.4°C. The distinct brackish water layer and the resulting lowered salinity can induce osmotic reactions in the corals. This might reduce the physiological efficiency of *T. endesa* at this location and thus its competitiveness regarding spatial benthic competitors such as molluscs (e.g. *Crepidula*) and other CWC species. At Ensenada de Las Islas the brackish surface layer only extends to a water depth of 5m. Below, the abiotic conditions stay relatively stable. The tidal amplitude seems to have no influence on corals thriving in 22m depth. CWCs occur primarily in waters with temperatures between 4°C and 12°C (Roberts *et al.*, 2006). Significantly higher abundances of *T. endesa* in Piti-Palena Fjord could be favored by the lower water temperatures of 9.92°C up to 12.59°C and the minor appearance of spatial competitors. The highest temperature measured at 20m was 12.99°C, mean annual temperature was 11.1°C. Corals at this station therefore experience lower temperatures than at XHuinay North. Although *T. endesa* was found in significantly higher numbers at Ensenada de Las Islas, the population density of *C. huinayensis* in the Piti-Palena fjord was $2,211 \pm 180$ n/m² (Wurz, 2014) and therefore much higher. For *C. huinayensis* it was found, that abundance is much higher at stations with more stable conditions (Wendländer, 2014; Wurz, 2014). Reef building cold-water corals, such as *L. pertusa*, show also strong dependencies between their abundance and narrow environmental conditions concerning temperature and salinity. Concluding, all these are indicators for the preference of CWC for habitats exhibiting stable

11 Discussion

environmental conditions (Freiwald *et al.*, 2004). The abundance survey in both fjords showed, that *T. endesa* is able to settle at habitats, which reveal fluctuations in temperature and sea water-carbonate chemistry. The influence of changing sea water-carbonate chemistry on the metabolism of *T. endesa* regarding growth and respiration rates was examined in the present study and will be discussed in the following chapters.

11.2.3 ABUNDANCE REGARDING SUBSTRATE INCLINATION

During summer months, the input of terrestrial, organic material leads to high sedimentation rates (Jantzen *et al.*, 2013b). Corals living at shallower substrates are therefore more influenced by sedimentation than those living at steep slopes and overhangs. The distribution of *T. endesa* is related to slopes between 70° and 145°. It occurs therefore at less inclined substrates than *C. huinayensis* (>88°, Wendländer, 2014) and *D. dianthus* (>80°, Häussermann and Försterra, 2007). The analysis of abundances of *T. endesa* regarding the substrate inclination showed no significant influence. Figure 35 shows schematically an overhang, colonized by *T. endesa* and *C. huinayensis*.

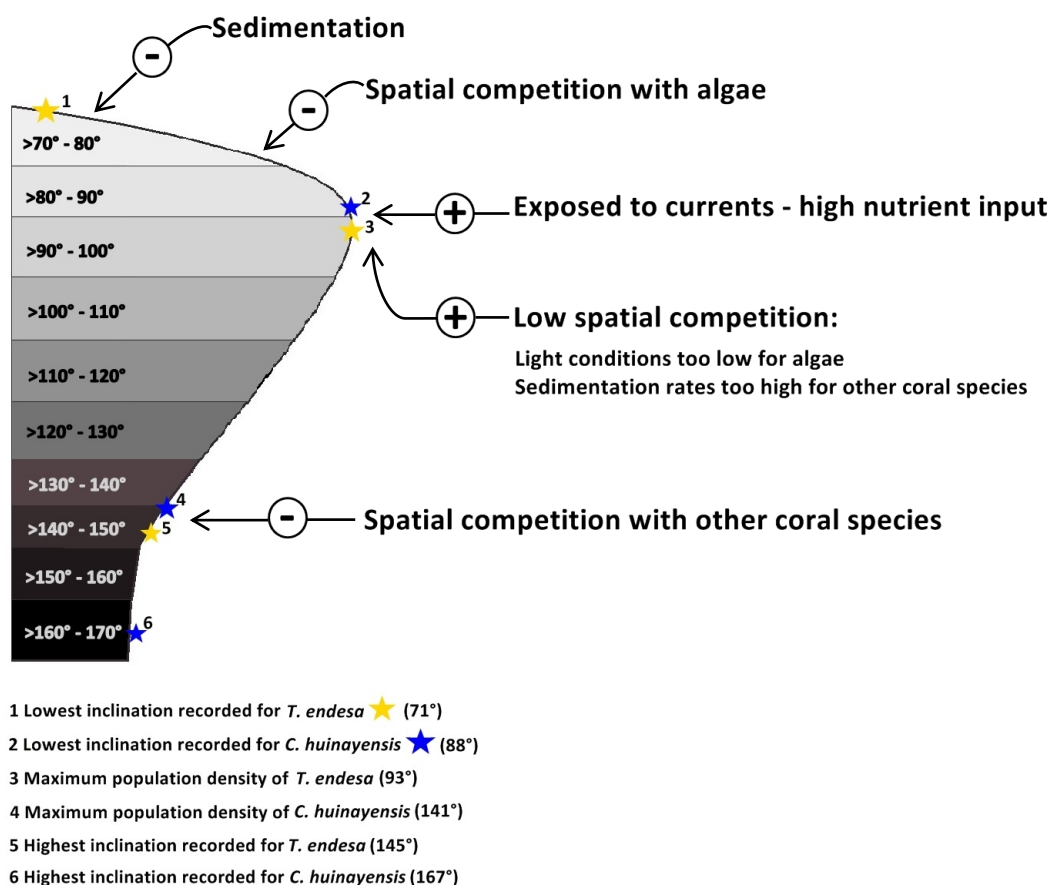


Figure 36: Schematic drawing of a rocky overhang, colonized by *T. endesa* ★ and *C. huinayensis* ★. Increased shadings of the substrate indicate increased inclination. Abiotic and biotic factors, influencing the corals at their location, are marked as being potentially positive (+) or negative (-). Data for *C. huinayensis*: Wendländer (2014).

11 Discussion

Herein it becomes visual, that although there are areas where *T. endesa* and *C. huinayensis* occur at substrates with a similar inclination – in general, they colonize at different sections of the rocky fjord walls. Within the inclination range of 70° to 90°, *T. endesa* has to cope with sedimentation particularly, but – due to the light conditions – is also in spatial competition with algae. The optimal slope for *T. endesa* to settle seems to be at an inclination of about 90° to 100°. This is also the range where the highest population densities were found (87 ± 0 at XHuinay North and 178 ± 96 at Ensenada de Las Islas). Here, the low light conditions inhibit algae settlement and reduce therefore the spatial competition. In addition, settling at this exposed position of the overhang, might lead to an increased nutrient availability for *T. endesa*. At substrates with an inclination of 130° and more the abundance of other coral species – such as *C. huinayensis* (Wendländer, 2014) – increases and therefore also the spatial competition with *T. endesa*.

11.3 MASS INCREASE

11.3.1 METHODOLOGICAL CONSIDERATIONS

CWC growth can be influenced by a number of environmental parameters such as temperature (Grigg, 1974; Matsumoto, 2007; Silverman *et al.*, 2007), flow speed (Purser *et al.*, 2010; Sokol, 2012), prey abundance (Silverman *et al.*, 2007; Purser *et al.*, 2010; Naumann *et al.*, 2011; Maier, 2013) and aragonite saturation status (Gattuso *et al.*, 1998; Silverman *et al.*, 2007; Jury *et al.*, 2009; Langdon *et al.*, 2000; Form and Riebesell, 2011). There have been already some studies on long-term growth rates of cold-water corals, but most of them took place under laboratory conditions (e.g. Form and Riebesell, 2012; Boehmer, 2013) or they were indirect estimations of the *in situ* growth rates using dating techniques such as U/Th-dating (e.g. Cheng *et al.*, 2000; Risk *et al.*, 2002). In 2011, Jantzen *et al.* (2013a) conducted an *in situ* short-term experiment in the fjord Comau, measuring the growth rate of *D. dianthus* over two weeks. There are very few long-term *in situ* measurements on growth rates of CWC (but see Jantzen *et al.*, 2014 for *D. dianthus*, Wurz, 2014 for *C. huinayensis* and Form (unpublished data) for *L. pertusa*). Therefore, to the authors' knowledge, this is one of the first experiments with direct measurements of *in situ* growth rates of a CWC and the first one for *T. endesa*. *In situ* measurements may have some flaws, such as that many undetermined factors may influence the experimental organisms and the experimental setups are more complicated. For laboratory experiments with CWC, the quality of the cultivation may have an important impact. Lartaud *et al.* (2014) reported lower budding rates for *L. pertusa* and *M. oculata* when these corals were maintained in an aquarium. Also *D. dianthus* exhibits growth rates being reduced for two thirds when measured in a laboratory and not *in situ* (Jantzen *et al.*, 2013a). A proper comparison of growth rates of corals in different studies is complicated because of different cultivation setups and divergent measuring methods, since almost all results are based on *in vitro* experiments. Therefore the *in vitro* measured growth rates of CWCs gained in other studies might be influenced or biased by cultivation artefacts and therefore underestimated (Jantzen *et al.*, 2013a). The test corals of this experiment might have been influenced in their growth rates due to the sampling procedure, the cultivation, the transport and the weight

11 Discussion

measurement. However, for *D. dianthus* it has been shown that the transport of corals to their stations was not influencing their growth rates (Jantzen *et al.*, 2013b). Furthermore, following Form *et al.* (2012) the duration of the transport should have had no impact on the growth rates either, because compared to the time span of the whole experiment its negligible. The buoyant weight technique has been proved by Davies (1989) to be a non-invasive method, having no influence on the growth rates of the scleractinian *Porites porites*. Long-term growth rates can be biased by bioeroding organisms on a micro - and macro scale (Försterra *et al.*, 2005). The bioeroding activity of marine grazers (e.g. boring Sponges and marine Gastropods) can lead to an underestimation of growth rates (Jantzen *et al.*, 2013a).

11.3.2 INFLUENCE OF CARBONATE CHEMISTRY ON *IN SITU* GROWTH RATES

Towards the mouth of the fjord Comau, the influence of the Pacific Ocean increases (Pickard, 1971) compared to XHuina North. The control groups at Lilliguapi and XHuina North showed similar growth rates of $9.82 \pm 4.38\% \text{ yr}^{-1}$ ($0.03 \pm 0.01\% \text{ d}^{-1}$) and $10.87 \pm 4.4\% \text{ yr}^{-1}$ ($0.03 \pm 0.01\% \text{ d}^{-1}$). Overall the *in situ* long-term growth rate of *T. endesa* can therefore be assumed as $10.34 \pm 4.34\% \text{ yr}^{-1}$ ($0.03 \pm 0.01\% \text{ d}^{-1}$). These values are comparable to other cold-water corals such as the solitary scleractinians *C. huinayensis* with $0.06 \pm 0.04\% \text{ d}^{-1}$ (Wurz, 2014) and *D. dianthus* with $0.04 \pm 0.02\% \text{ d}^{-1}$ (Orejas *et al.*, 2011b) and the colony-forming *Dendrophyllia cornigera* with $0.04 \pm 0.02\% \text{ d}^{-1}$ (Orejas *et al.*, 2011b). There are CWCs (i.e. *M. oculata*, $0.20 \pm 0.09\% \text{ d}^{-1}$) (Orejas *et al.*, 2011b), which can grow at rates that are comparable to those of massive growing tropical corals. Although, they do not exceed growth rates that are examined for tropical corals as for instance the branching coral *Stylophora pistillata* with $1.20 \pm 0.49\% \text{ d}^{-1}$ (Orejas *et al.*, 2011a) or the massive coral *Turbinaria reniformis* with $0.78 \pm 0.34\% \text{ d}^{-1}$ (Orejas *et al.*, 2011a).

The cross-transplantation experiment showed that specimen of *T. endesa* coming from a high pH location (Lilliguapi) being transplanted to a low pH location (XHuina North) exhibit growth rates of $10.51 \pm 1.14\% \text{ yr}^{-1}$ ($0.03 \pm 0.00\% \text{ d}^{-1}$), comparable to the control group, which stayed at the high pH location $9.82 \pm 4.38\% \text{ yr}^{-1}$ ($0.03 \pm 0.01\% \text{ d}^{-1}$). There was no significant difference in growth rates between cross-transplanted corals of XHuina North at the central part of the fjord (pH 7.66) and Lilliguapi close to the Golf of Ancud (pH 7.87). This may be an indication for the capability of *T. endesa* to cope with changes concerning the surrounding sea water pH on a physiological level. Jantzen *et al.* (2014) reported for specimens of *D. dianthus* — which were also transplanted along the natural pH gradient of Comau Fjord — growth rates of $0.05 \pm 0.03\% \text{ d}^{-1}$. For *D. dianthus* temperature and salinity are stated to affect skeletal growth rates and determine the distribution (Försterra and Häussermann, 2003; Cairns *et al.*, 2005; Försterra *et al.*, 2005). These factors should therefore also be taken into consideration when examining the causes and causalities of the *in situ* growth rates of *T. endesa*. McCulloch *et al.* (2012a) has shown that the solitary coral *Caryophyllia smithii* is capable to regulate the internal pH in its tissues up to 0.78 units above the surrounding sea water pH. This active physiological adaptation to changing pH values in the surrounding water is due to the regulation of the internal pH through Ca^{2+} -ATPase activity (McCulloch *et al.*, 2012a). However, pH elevation is suggested to be accompanied by energetic effort, leading to a reduction of energy

11 Discussion

for other physiological important processes. A decrease of sea water pH of 0.1 units led to a 10% increased energy budget (McCulloch *et al.*, 2012a).

Since *T. endesa* showed similar growth rates in environments with different pH it might also be capable of regulating its internal pH. Additionally to the pH-value of the environment, aragonite saturation and TA can influence the growth of calcifying CWCs. TA values at XHuinay North and Lilliguapi were lower than those expected for surface waters of the Southern Ocean and the equatorial upwelling Pacific (Lee *et al.*, 2006). Though, an eroding effect of waters being undersaturated with aragonite (<1) can be excluded, as Jantzen *et al.* (2013b) verified aragonite saturation levels at the sampling sites (approximately 20m water depth) in Comau Fjord between 1.5 to 2. However, if CWCs live in waters, which are undersaturated with regard of aragonite, they can be deeply impaired in their net calcification rates (McCulloch *et al.*, 2012a). *T. endesa* seems to be capable of thriving and maintaining its growth rates even under low and dynamic pH values. Therefore it might be able to adjust to future environmental conditions. With ongoing OA also the pH values inside the fjord Comau will further decrease. In the long run the accumulation of CO₂ and the resulting shift of the aragonite saturation level may still lead to an eroding effect on coral skeletons even if they are capable to operate biomineralisation in low pH environments. Following McCulloch *et al.* (2012a) this will limit the distribution of CWCs in the deep regions of the oceans as it will shift the calcite compensation depth to shallower waters.

11.4 RESPIRATION RATES

11.4.1 METHODOLOGICAL CONSIDERATIONS

The usage of closed incubation chambers and optical oxygen microsensors for high resolution recording of decreasing oxygen concentrations has been approved for marine invertebrates in general (Gatti, 2002) and cold-water corals in specific (e.g. Dodds *et al.*, 2007; Boehmer, 2013; Wendländer, 2014; Wurz, 2014). Despite its high precision and capacity to detect possible fluctuations in respiration rates over time, the experimental setup for this measurement is quite complicated. This might lead to problems in the implementations of the measurement, particularly during field trips and ship cruises. For that reason, the present study compared the results of the automatical measurement in respiration chambers with a manual method. The manual method cannot detect eventual fluctuations during the incubation time, as it only considers the delta in oxygen concentration of start and end values. Its practical applicability, on the other hand, is much better. The present study showed that the oxygen decrease within the respiration chambers, measured with the automatical method, was consistent and linear. Therefore, only start and end values of oxygen saturation were used for the analysis. Furthermore, measurements with both methods resulted in data that showed no statistically difference. Varieties in respiration rates can be assumed to be a result of variations of the individual experimental specimen. In conclusion, the manual method is, at least for respiration measurements of *T. endesa*, a valid method and can be used for further experiments. Respiration measurements took place in natural sea water, sampled at the respective sampling sites for

11 Discussion

T. endesa. That way, the conditions during the measurement were as close as possible to *in situ* conditions, especially concerning the carbonate chemistry. Temperatures were constant during the measurements and matched with the ambient temperatures at the sampling stations ($12.5 \pm 0.5^\circ\text{C}$). This was important as Dodds *et al.* (2007) showed that temperature has a measurable effect on the respiration rates of CWCs. Previous studies on other solitary CWCs showed the high relevance of food availability and ingestion rate (Naumann *et al.*, 2011; Maier, 2013) on respiration rates. Correlations between respiration rates and increased food densities, resulting in an enhancing effect on oxygen uptake have been shown for *D. dianthus* (Maier, 2013) and *L. pertusa* (Larsson *et al.*, 2013). Using artificial seawater for respiration measurements might therefore reduce a potential treatment artefact, as the amount of nourishment in the water can be controlled. However, regarding CO_2 species and alkalinities, the chemical composition of artificial seawater can differ a lot from natural seawater (Atkinson, 1997). The influence of the ambient carbonate chemistry on the physiology of *T. endesa* was one of the main topics of the recent study. Therefore it was substantial to measure the influence of the carbonate chemistry at conditions as natural as possible, thus in natural, ambient seawater. The measurement interval of 12 hours was chosen in order to ensure normoxic conditions, as Dodds *et al.* (2007) showed that oxygen consumption rates of the CWC *L. pertusa* were not constant when the experimental conditions were out of the normoxic range. All previous measurements of respiration rates of CWCs in the fjord Comau were part of laboratory long-term experiments (e.g. Boehmer, 2013; Wurz, 2014). Herein corals were cultivated over several weeks in an aquaria setup and measured in periodical intervals. Contrary to that, in the present experiment, *T. endesa* was not cultivated before the measurement of respiration rates. Moreover, measurements took only place once, directly after the retrieve from the *in situ* conditions. Therefore, possible treatment artefacts due to the cultivation in other experiments have to be considered when comparing respiration rates from laboratory experiments with the present results. Likewise the sampling process of *T. endesa* may have had an influence on the experimental specimen and therefore affect the respiration rates. For both types of respiration measurements – the manual method (e.g. Faxneld *et al.*, 2010; Smith *et al.*, 2013) and the automatical method (e.g. Boehmer, 2013; Wendländer, 2014; Wurz, 2014), the measurements in the framework of this study followed already established procedures. Hence, the obtained results can be assumed to be realistic respiration rates of *T. endesa*.

11.4.2 INFLUENCE OF CARBONATE CHEMISTRY ON RESPIRATION RATES

The present study examined the *in situ* effects of low sea water pH values on the *in vitro* respiration rates of *T. endesa*. This allows a statement on the physiological reactions of this CWC towards the present environmental conditions. In scleractinians, an increased respiration rate is an indicator for stress (Telesnicki *et al.*, 1995). Specimen of *T. endesa* at XHuinay North, living under low pH conditions (7.66 ± 0.04) showed no significant difference in respiration rates ($7.16 \pm 4.23 \mu\text{Mol O}_2 \times \text{cm}^2 \times \text{d}^{-1}$) to those at Lilliguapi under higher pH (7.87 ± 0.06) ($8.05 \pm 2.93 \mu\text{Mol O}_2 \times \text{cm}^2 \times \text{d}^{-1}$). Corals being transplanted from

12 Conclusion

high to low pH conditions showed an increase of 22% in respiration rates ($9.88 \pm 4.52 \mu\text{Mol O}_2 \times \text{cm}^2 \times \text{d}^{-1}$) compared to their control group ($8.05 \pm 2.93 \mu\text{Mol O}_2 \times \text{cm}^2 \times \text{d}^{-1}$), although this effect was not statistically significant. As already mentioned in Chapter 10.3.2 some scleractinians are capable of regulating their internal pH (McCulloch *et al.*, 2012a), an active process, which is energy demanding. A decrease in sea water pH of 0.1 results in a 10% increased energy demand (McCulloch *et al.*, 2012b). Slightly higher respiration rates of *T. endesa* ($9.88 \pm 4.52 \mu\text{Mol O}_2 \times \text{cm}^2 \times \text{d}^{-1}$) at lower pH than at higher pH ($8.05 \pm 2.93 \mu\text{Mol O}_2 \times \text{cm}^2 \times \text{d}^{-1}$) could therefore be explained by an additional energy demand of 22% for regulating the internal pH. Wurz (2013) measured comparable respiration rates for *C. huinayensis* at low pH (7.6) with $7.24 \pm 1.74 \mu\text{mol O}_2 \times \text{cm}^2 \times \text{d}^{-1}$. However at high pH (7.8) respiration rates of *C. huinayensis* were much lower ($3.69 \pm 0.80 \mu\text{mol O}_2 \times \text{cm}^2 \times \text{d}^{-1}$) compared to *T. endesa* in the present experiment. Although, he also found no significant difference in respiration rates between corals cultivated at a pH of 7.6 and pH 7.8. For *C. huinayensis* the decrease in sea water pH from 7.8 to 7.6 seems to be more energy demanding than for *T. endesa* as it resulted in increased respiration rates of 140%. Also *D. dianthus* showed no significant difference in respirations rates under lowered pH values (Boehmer, 2013). But for this experiment it should be noted, that corals were examined at a pH of 7.84 ± 0.08 and 8.12 ± 0.09 . So the experimental conditions were much less acidic than in the present study. In any way it is remarkable that the respiration rates of *D. dianthus* were more than threefold higher than those of *T. endesa*, being $23.71 \pm 7.56 \mu\text{mol O}_2 \times \text{cm}^2 \times \text{d}^{-1}$ at a pH of 7.84 ± 0.08 and $22.07 \pm 15.07 \mu\text{mol O}_2 \times \text{cm}^2 \times \text{d}^{-1}$ at pH of 8.12 ± 0.09 (Boehmer, 2013).

12 CONCLUSION

The CWC *T. endesa*, thriving in the Patagonian fjord region, has the potential to colonize habitats that are influenced by daily and seasonally fluctuations and that are foreseen to undergo more severe changes in the future. As *T. endesa* is abundant in two different fjord systems it seems to have the capability and ecological virility to adapt to different environmental conditions. The inclination of the settlement substrate (shallow limit: 71°; maximum population density at 93°) might be a hint for its ability to sustain sedimentation and to have herein an advantage over the accompanied species *C. huinayensis* (shallow limit: 88°, maximum population density at 141°; Wendländer, 2014) and *D. dianthus* (shallow limit: 80°; Häussermann and Försterra, 2007). In Comau Fjord it experiences already today ambient sea water conditions that are predicted for the future oceans of the end of this century. The examination of *in situ* mass increase and *in vitro* respiration rates of *T. endesa* revealed that alongside with *C. huinayensis* and *D. dianthus* it is capable to maintain its capability of calcification in acidified waters. *T. endesa* seems to stay physiologically potent by probably developing adaptation mechanisms such as internal pH up-regulation (McCulloch *et al.*, 2012b).

In summary, the *T. endesa* generally seems to cope with lowered sea water pH, but this might be associated with energetic effort. Moreover, a further decrease of 0.4 units in sea water pH and rising temperatures of at least 2°C are predicted until the end of the century (Hoegh-Guldberg *et al.*, 2007). Resulting in highly lowered aragonite saturation states, this will endanger cold - and warm-water corals as their habitats will be in regions that will be undersaturated with respect to aragonite (Maier *et al.*, 2013). All organisms of the benthic habitat associated with CWCs might be threatened by the proceeding climate change and ocean acidification and in addition by expanding fisheries in the Chilean Fjord region (Häussermann *et al.*, 2007). Following the argumentation of Försterra *et al.* (2003), species of the endemic and highly diverse community could be irretrievably lost before even been investigated. Therefore, it is indispensable to keep up the investigations on ecological processes and dependencies of this unique biocenosis to promote the endeavors for legal protection of CWC habitats (Reed, 2002).

13 OUTLOOK

Likewise the present results for *T. endesa*, former cross-transplantation experiments with *D. dianthus* (Jantzen *et al.*, 2013a) and *C. huinayensis* (Wurz, 2014) showed the capability of CWCs to grow and maintain their physiological virility along a natural pH gradient in the fjord Comau. However, the species specific responses to abiotic environmental factors might be different. Therefore, the extrapolation and prediction of physiological responses of different species is of limited suitability. In order to verify the determined knowledge of *in situ* growth and respiration rates of *T. endesa*, experiments could be repeated in the controlled conditions of a laboratory experiment. For a more detailed look on the calcification processes of *T. endesa* and the mechanisms, which are involved in the uptake of inorganic carbon, direct measurements of Ca^{2+} , pH and O_2 on the surface and inside the polyp could be conducted with microsensors (following Revsbech, 1995). Several studies also examined the influence of biotic factors on the respiration rates of CWCs. The food availability and ingestion rate (Naumann *et al.*, 2011; Maier, 2013) can have traceable influences. An additional analysis on ingestion rates, food quality and food availability, would provide an indication for the reliability of calcification rates. This would be feasible in a laboratory experiment, where the food quality and supply can be controlled.

Global warming can increase respiration rates of corals as it has been shown by Dodds *et al.* (2007) and enhance coral growth (Silvermann *et al.*, 2007). Therefore, further experiments should also investigate the influence of changing or increasing temperatures, respectively.

In order to describe the environmental conditions to which *T. endesa* is subject to, more oceanographic investigations are needed. As measurements of the physical parameters pH, salinity and oxygen usually take place only in a narrow time window once a year, not possible so far to predicate fluctuations and thus changes of abiotic factors in the course of the year. To have a more detailed understanding of the influence of the carbonate system on the physiology of *T. endesa*, it is necessary to know fluxes and fluctuations for the whole year. Therefore, samples must be taken in regular intervals if not even logged constantly with aid of permanent installed data loggers.

14 ACKNOWLEDGEMENTS

I would like to thank Prof. Dr. Ulf Riebesell for correcting and judging this Master thesis. Thank you, Dr. Armin Form and Janina Büscher, not only for correcting this work, but also for enkindling my fascination for cold-water corals.

Especially, I would like to thank Dr. Jürgen Laudien, who gave me the opportunity to do my thesis on *Tethocyathus endesa* under his supervision. You gave me the chance to take part in an awesome diving expedition to the Chilean fjord region – an unique experience and adventure for which I am very thankful. Thanks particularly for your confidence and encouragement!

In this regard, many thanks to everyone at the Huinay Scientific Field Station, especially Dr. Vreni Häussermann, Günther (Fossi) Försterra, Ulo Pörschmann and Kaitlyn (Katie) McConnell.

Also to all the lovely people at the Reserva Añihue, to mention particularly Felipe Gonzáles-Díaz and Thomas Heran Arce. I also want to thank Erik Wurz, Henry Göhlich, Christopher Nowak and Svantje Gottschlich for your preparatory work in 2014 - without you, my experiment could not have taken place.

Special thanks to Maximilian (Max) Neffgen and Felix Roßbach - it was a pleasure to work with you as a diving team. Thank you for all the night shifts, helping hands and pep talk!

Thank you Roland Friedrich and the Scientific Diving Center at the CAU Kiel, your profound instruction qualified me for taking my samples independently and to work as proper scientific diver.

I am especially thankful to my family, not only for your general support, but particularly for always encouraging me with my ambition to study and become a marine biologist.

‘For most of history, man has had to fight nature to survive; in this century he is beginning to realize that, in order to survive, he must protect it.’

(Jacques-Yves Cousteau)

15 REFERENCES

- Atkinson M.J., Bingman C. (1997) Elemental composition of commercial sea salts, *Journal of Aquaculture and Aquatic Sciences*, 8, 39
- Bialek E.L. (1966) Special publication, Handbook of Oceanographic tables, Oceanographic Analysis Division Marine Science Department, U.S. Naval Oceanographic Office Washington D.C., 435pp.
- Boehmer A. (2013) Response of the cold-water coral *Desmophyllum dianthus* to future CO₂ concentrations, Alfred Wegener Institute Helmholtz Centre for Polar and Marine Research, Bremerhaven and Senckenberg am Meer, German Centre for Marine Biodiversity Research, Wilhelmshaven, Master-Thesis 69 pp.
- Breedy O., Cairns S.D., Häussermann V. (2015) A new alcyonacean octocoral (Cnidaria, Anthozoa, Octocorallia) from Chilean fjords, *Zootaxa*, 3919, 327-334
- Brewer P.G., Bradshaw A.L., Williams R.T. (1986) Measurements of total carbon dioxide and alkalinity in the North Atlantic Ocean in 1981, *The Changing Carbon Cycle: A Global Analysis*, edited by J.R. Trabalka and D.E. Reichle, Springer, New York, 348-370
- Bustamante, M. S. (2009) The southern Chilean fjord region: oceanographic aspects, Marine benthic fauna of Chilean Patagonia, Santiago: *Nature In Focus*, 53-60
- Cairns S.D., Häussermann V., Försterra G. (2005) A review of the Scleractinia (Cnidaria: Anthozoa) of Chile, with the description of two new species, *Zootaxa*, 1018, 15-46
- Cairns S.D. (2007) Deep-water corals: an overview with special reference to diversity and distribution of deep-water scleractinian corals, *Bulletin of Marine Science*, 81, 311-322
- Caldeira K., Wickett M.E. (2003) Anthropogenic carbon and ocean pH, *Nature*, 425, 365
- Chalker B.E., Taylor D.L. (1975) Light-enhanced calcification, and the role of oxidative phosphorylation in calcification of the coral *Acopora cervicornis*. *Proceedings of the Royal Society*, 190, 323-331
- Cheng H., Adkins J., Edwards R.L., Boyle E.A. (2000) U-Th dating of deep-sea corals, *Geochimica et Cosmochimica Acta*, 64, 2401-2416
- Comeau S., Gorsky G., Jeffree R., Teyssie J.L., Gattuso J.P. (2009) Impact of ocean acidification on a key Arctic pelagic mollusc (*Limacina helicina*), *Biogeosciences*, 6, 1877-1182
- Davis P.S. (1989) Short-term growth measurements of corals using an accurate buoyant weighting technique, *Marine Biology*, 101, 389-462
- Davies A.J., Guinotte J.M. (2011) Global habitat suitability for framework-forming cold-water corals, *PLoS ONE*, 6, e18483
- Diercks S., Laudien J., Roßbach F., Häussermann V., Försterra G. (2015a) Total alkalinity measured at time series station Lilliguapi, Patagonia, Chile, Alfred Wegener Institute Helmholtz Center for Polar and Marine Research, Bremerhaven, doi:10.1594/PANGAEA.846927

15 References

- Diercks S., Laudien J., Roßbach F., Häussermann V., Försterra G. (2015b) Total alkalinity measured at time series station X-Huinay North, Patagonia, Chile, Alfred Wegener Institute Helmholtz Center for Polar and Marine Research, Bremerhaven, doi:10.1594/PANGAEA.846928
- Diercks S., Laudien J., Roßbach F., Häussermann V., Försterra G. (2015c) Total alkalinity measured at time series station Anihue, Patagonia, Chile, Alfred Wegener Institute Helmholtz Center for Polar and Marine Research, Bremerhaven, doi:10.1594/PANGAEA.846925
- Dodds L.A., Roberts J.M., Taylor A.C., Marubini F. (2007) Metabolic tolerance of the cold-water coral *Lophelia pertusa* (Scleractinia) to temperature and dissolved oxygen change, *Journal of Experimental Marine Biology and Ecology*, 349, 205-214
- Erez, J., Reynaud, S., Silverman, J., Schneider, K., Allemand, D. (2011) Coral calcification under ocean acidification and global change, *Coral reefs: an ecosystem in transition*, Springer Netherlands, 151-176
- Fabricius K.E., Langdon C., Uthicke S., Humphrey C., Noonan S., Death G., Okazaki R., Muehllehner N., Glas M.S., Lough J.M. (2011) Losers and winners in coral reefs acclimatized to elevated carbon dioxide concentrations, *Nature Climate Change*, 1, 165-169
- Faxneld S., Jörgensen T.L., Tedengren M. (2010) Effects of elevated water temperature, reduced salinity and nutrient enrichment on the metabolism of the coral *Turbinaria mesenterina*, *Estuarine, Coastal and Shelf Science*, 88, 482-487
- Feely R.A., Sabine C.L., Lee K., Berelson W., Kleypas J., Fabry V.J., Millero F.J. (2004) Impact of anthropogenic CO₂ on the Ca CO₃ system in the oceans, *Science*, 305, 362-366
- Fillinger L., Richter C. (2013) Vertical and horizontal distribution of *Desmophyllum dianthus* in Comau Fjord, Chile: a cold-water coral thriving at low pH, *PeerJ*, 1, 194
- Form A.U., Riebesell U. (2012) Acclimation to ocean acidification during long-term CO₂ exposure in the cold-water coral *Lophelia pertusa*, *Global Change Biology*, 18, 843-853
- Försterra G., Häussermann V. (2003) First report on large scleractinian (Cnidaria: Anthozoa) accumulations in cold-temperate shallow water of south Chilean fjords, *Zoologische Verhandelingen (Leiden)*, 345 pp.
- Försterra G., Beuck L., Häussermann V., Freiwald A. (2005) Shallow-water *Desmophyllum dianthus* (Scleractinia) from Chile: characteristics of the biocoenoses, the bioeroding community, heterotrophic interactions and (paleo)-bathymetric implications, *Cold-water corals and Ecosystems*, 937-977
- Freiwald A., Fossa J.H., Grehan A., Koslow T., Roberts J.M. (2004) Cold-water coral reefs: Out of sight – no longer out of mind, UNEP-WCMC, Cambridge, UK, 86 pp.
- Friedlander A.M., Ballestros E., Beets J., Berkenpas E., Gaymer C.F., Gorny M., Sala E. (2013) Effects of isolation and fishing on the marine ecosystems of Easter Island and Salas y Gómez, Chile, *Aquatic Conservation: Marine and Freshwater Ecosystems*, 23, 515-531
- Galea H., Häussermann V., Försterra G. (2007) Hydrozoa, fjord Comau, Check list 3, 159-167
- Gatti S., Brey T., Müller W.E.G., Heilmeyer O., Holst G. (2002) Oxygen microoptodes: a new tool for oxygen measurements in aquatic animal ecology, *Marine Biology*, 140, 1075-1085
- Gattuso J-P., Frankignoulle M., Bourge I., Romaine S., Buddemeier R.W. (1998) Effect of calcium carbonate saturation of sea water on coral calcification, *Global and Planetary Change*, 18, 37-46
- Glynn P.W. (1993) Coral reef bleaching: ecological perspectives, *Coral Reefs*, 12, 1-17

15 References

- Goreau T.F. (1992) Bleaching and reef community change in Jamaica: 1951-1991, *American Zoologist*, 32, 683-695
- Gran G. (1952) Determination of the equivalence point in potentiometric titrations, Part II, *The Analyst*, 77, 661-671
- Grigg R.W. (1974) Growth rings: annual periodicity in two gorgonian corals, *Ecology*, 55, 876-881
- Guinotte J.M., Orr J., Cairns S., Freiwald A., Morgan L., George R. (2006) Will human-induced changes in sea water chemistry alter the distribution of deep-sea scleractinian corals? *Frontiers in Ecology and the Environment*, 1(4), 141-146
- Häussermann V., Försterra G. (2007) Large assemblages of cold-water corals in Chile: a summary of recent findings and potential impacts, *Conservation and adaptive management of seamount and deep-sea coral ecosystems*, Editors: George, R.Y., Cairns S.D., eds., Rosenstiel, School of Marine and Atmospheric Science, University of Miami.
- Hilmi N., Allemand D., Dupont S., Safa A., Haraldsson G., Nunes P.A., Moore C., Hattam C., Reynaud S., Hall-Spencer J.M., Fine M., Turley C., Jeffree R., Orr J., Munday P.L., Cooley S.R. (2013) Towards improved socio-economic assessments of ocean acidification's impacts, *Marine Biology*, 160, 1773-1787
- Hoegh-Guldberg O. (1999) Climate change, coral bleaching and the future of the world's coral reefs, *Marine Freshwater Research*, 50, 839-866
- Hoegh-Guldberg O., Mumby P.J., Hooten A.J., Steneck R.S., Greenfield P., Gomez E., Harvell C.D., Sale P.F., Edwards A.J., Caldeira K., Knowlton N., Eakin C.M., Iglesias-Prieto R., Muthiga N., Bradbury R.H., Dubi A., Hatzioios M.E. (2007) Coral Reefs Under Rapid Climate Change and Ocean Acidification, *Science*, 318, 1737-1742
- Häussermann V. (2004): Neue integrative Ansätze für das Sammeln, Bearbeiten und Beschreiben skelettloser Hexacorallia am Beispiel chilenischer Seeanemonen, Dissertation, LMU München: Fakultät für Biologie, 314 pp.
- Häussermann V., Försterra G. (2007) Large assemblages of cold-water corals in Chile: a summary of recent findings and potential impacts, George R. Y. and S. D. Cairns, eds. *Conservation and adaptive management of seamount and deep-sea coral ecosystems*, Rosenstiel School of Marine and Atmospheric Science, University of Miami, Miami, 324 pp.
- Häussermann V., Försterra G., Plotnek E. (2012) Sightings of marine mammals and birds in the Comau Fjord, Northern Patagonia, between 2003 and mid 2012, *Spixiana*, 35, 161-288
- Hennige S.J., Wicks L.C., Kamenos N.A., Bakker D.C., Findlay H.S., Dumousseaud C., Roberts J.M. (2014) Short-term metabolic and growth responses of the cold-water coral *Lophelia pertusa* to ocean acidification, *Deep-Sea Research II*, 27-35
- Hoegh-Guldberg O., Mumby P.J., Hooten A.J., Steneck R.S., Greenfield P., Gomez E., Harvell C.D., Sale P.F., Edwards A.J., Caldeira K., Knowlton N., Eakin C.M., Iglesias-Prieto R., Muthiga N., Bradbury R.H., Dubi A., Hatzioios M.E. (2007) Coral reefs under rapid climate change and ocean acidification, *Science*, 318, 1737-1742
- Hutchins D.A., Mulholland M.R., Fu F.-X. (2009) Nutrient cycles and marine microbes in a CO₂-enriched ocean, *Oceanography*, 22, 128-145

15 References

- IPCC (2013) Climate Change 2013: The Physical Science Basis, Contribution of Working Group I to the Fifth Assessment, Report of the Intergovernmental Panel on Climate Change [Stocker T.F., Qin D., Plattner G.-K., Tignor M., Allen S.K., Boschung J., Nauels A., Xia Y., Bex V, Midgley P.M. (eds.)], Cambridge University Press, Cambridge, United Kingdom and New York, NY, USA, 1535 pp.
- IPCC (2014) Climate Change 2014: Impacts, Adaptation, and Vulnerability, Part A: Global and Sectoral Aspects. Contribution of Working Group II to the Fifth Assessment Report of the Intergovernmental Panel on Climate Change [Field, C.B., V.R. Barros, D.J. Dokken, K.J. Mach, M.D. Mastrandrea, T.E. Bilir, M. Chatterjee, K.L. Ebi, Y.O. Estrada, R.C. Genova, B. Girma, E.S. Kissel, A.N. Levy, S. MacCracken, P.R. Mastrandrea, and L.L. White (eds.)], Cambridge University Press, Cambridge, United Kingdom and New York, NY, USA, 1132 pp.
- Jokiel R.L., Maragos J.E., Franzisket L. (1978) Coral growth: buoyant weight technique, *Monographs Oceanography Methodology (UNESCO)*, 5, 529-542
- Jantzen C., Häussermann V., Försterra G., Laudien J., Richter C. (2011) The cold water coral *Desmophyllum dianthus* grows along a pH gradient in the Comau Fjord (Patagonia, Chile) , Youmares 2 conference, Bremerhaven 2011
- Jantzen C., Laudien J., Sokol S., Försterra G., Häussermann V., Kupprat F., Richter C. (2013a) In situ short-term growth rates of a cold-water coral, *Marine and Freshwater Research*, 64, 631-641
- Jantzen C., Häussermann V., Försterra G, Laudien J., Ardelan M., Maier S., Richter C. (2013b) Occurrence of a cold-water coral along natural pH gradients (Patagonia, Chile), *Marine Biology*, 160, 2597-2607
- Jantzen C., Nowak C., Laudien J., McConnell K., Häussermann V. (2014) Long-term *in situ* growth rate adaptability of a cold-water coral in a natural pH gradient, Youmares 5 conference, Stralsund 2014
- Jury C., Whitehead R., Szmant A. (2009) Effects of variations in carbonate chemistry on the calcification rates of *Madracis auretenra* (*Madracis mirabilis* sensu Wells, 1973): bicarbonate concentrations best predict calcification rates, *Global Change Biology*, 16, 1632-1644
- Kanwisher J.W., Wainwright S.W. (1967) Oxygen balance in some reef corals, *Biological Bulletin*, 133, 435-438
- Kleypas J.A., Buddemeier R.W., Archer D., Gattuso J.P., Langdon C., Opdyke B.N. (1999) Geochemical consequences of increased atmospheric carbon dioxide on coral reefs, *Science*, 284, 118-120
- Kurihara H. (2008) Effects of CO₂-driven ocean acidification on the early developmental stages of invertebrates, *Marine Ecology Progress Series*, 373, 275-284
- Langdon C., Takahashi T., Sweeney C., Chipman D., Goddard J., Marubini F., Aceves H., Barnett H., Atkinson M. (2000) Effect of calcium carbonate saturation state on the calcification rate of an experimental reef, *Global Biogeochemical Cycles*, 14, 639-654
- Langdon, C., Atkinson M.J. (2005) Effect of elevated pCO₂ on photosynthesis and calcification of corals and interactions with seasonal change in temperature/irradiance and nutrient enrichment, *Journal of Geophysical Research: Oceans* (1978-2012), 110.C9
- Larsson A.I., Lundälv T., van Oevelen D. (2013) Skeletal growth, respiration rate and fatty acid composition in the cold-water coral *Lophelia pertusa* under varying food conditions, *Marine Ecology Progress Series*, 483, 169-184

15 References

- Lartaud F., Pareige S., de Rafelis M., Feuillassier L., Bideau M., Peru E., DelaVega E., Nedoncelle K., Romans P., LeBris N. (2014) Temporal changes in the growth of two Mediterranean cold-water coral species, *in situ* and in aquaria, *Deep-Sea Research II*, 99, 64-70
- Laudien J., Häussermann V., Försterra G., Göhlich H. (2014): Physical oceanographic profiles of seven CTD casts from Gulf of Ancud into Comau Fjord in 2014, Alfred Wegener Institute, Helmholtz Center for Polar and Marine Research, Bremerhaven, doi:10.1594/PANGAEA.832187
- Lee K., Tong L.T., Millero F.J., Sabine C.L., Dickson A.G., Goyet C., Park G., Wanninkhof R., Feely R.A., Key R.M. (2006) Global relationships of total alkalinity with salinity and temperature in surface waters of the world's oceans, *Geophysical Research Letters*, 33, 19
- Maier C., Schubert A., Berzunza Sánchez M.M., Weinbauer M.G., Watremez P., Gattuso J.P. (2013) End of the century pCO₂ levels do not impact calcification in Mediterranean cold-water corals, *PLoS ONE*, 8, e62655
- Maier S. (2013) Energy budget of a scleractinian cold-water coral (*Desmophyllum dianthus*), Comau Fjord, Chile, Master thesis, University of Bremen, 110pp.
- Matsumoto A.K. (2007) Effects of low water temperature on growth and magnesium carbonate concentrations in the cold-water gorgonian *Primnoa pacifica*, *Bulletin of Marine Science*, 81, 423-435
- McCulloch M., Falter J., Trotter J., Montagna P. (2012a) Coral resilience to ocean acidification and global warming through pH up-regulation, *Nature Climate Change Letter*, 2, 623-627
- McCulloch M., Trotter J., Montagna P., Falter J., Dunbar R., Freiwald A., Försterra N., Lopez Correa M., Maier C., Rüggeberg A., Taviani M. (2012b) Resilience of cold-water scleractinian corals to ocean acidification: Boron isotopic systematics of pH and saturation state up-regulation, *Geochimica Et Cosmochimica Acta*, 87, 21-34
- Millero, F. J., Lee K., Roche M. (1998) Distribution of alkalinity in the surface waters of the major oceans, *Marine Chemistry*, 60, 111-130
- Millero F.K. (2006) *Chemical oceanography*, 3rd edition, CRC, Boca Raton, 571pp.
- Muñoz P., Sellanes J., Villalobos K., Zapata-Hernández G., Mayr C., Araya K. (2014) Geochemistry of reduced fluids from shallow cold vents hosting chemosynthetic communities (Comau Fjord, Chilean Patagonia, ~ 42° S), *Progress in Oceanography*, 129, 159-169
- Naumann M. S., Orejas C., Wild C., Ferrier-Pages C. (2011) First evidence for zooplankton feeding sustaining key physiological processes in a scleractinian cold-water coral, *Journal of Experimental Biology*, 214 (21), 3570-3576
- Orejas, C., Ferrier-Pagès C., Reynaud S., Tsounis G., Allemand D., Gili J.-M. (2011a) Experimental comparison of skeletal growth rates in the cold-water coral *Madrepora oculata* Linnaeus, 1758 and three tropical scleractinian corals, *Journal of Experimental Marine Biology and Ecology*, 405, 1-5
- Orejas C., Ferrier-Pagès C., Reynaud S., Gori A., Beraud E., Tsounis G., Allemand D., Gili J.-M. (2011b) Long-term growth rates of four Mediterranean cold-water coral species maintained in aquaria, *Marine Ecology Progress Series*, 429, 57-65

15 References

- Orr J.C., Fabry V.J., Aumont O., Bopp L., Doney S.C., Feely R.M., Gnanadesikan A., Gruber N., Ishida A., Joos F., Key R.M., Lindsay K., Maier-Reimer E., Matear R., Monfray P., Mouchet A., Najjar R.G., Plattner G., Rodgers K.B., Sabine C.L., Sarmiento J.L., Schlitzer R., Slater R.D., Totterdell I.J., Weirig M., Yamanaka
- Y., Yool A. (2005) Anthropogenic ocean acidification over the twenty-first century and its impact on calcifying organisms, *Nature*, 437, 681-686
- Palma S., Silva N. (2004) Distribution of siphonophores, chaetognaths, euphausiids and oceanographic conditions in the fjords and channels of southern Chile, *Deep-Sea Research Part II*, 51, 513-535
- Pantoja S., Iriarte J.L., Daneri G. (2011) Oceanography of the Chilean Patagonia, *Continental Shelf Research*, 31, 149-153
- Pickard G.L. (1971) Some physical oceanographic features of inlets of Chile, *Journal of the Fisheries Research Board of Canada*, 28, 1077-1106
- Pörtner H.O. (2008) Ecosystem effects of ocean acidification in times of ocean warming: a physiologist's view, *Marine Ecology Progress Series*, 373, 203-217
- Purser A., Larsson A.I., Thomsen L., von Oevelen D. (2010) The influence of flow velocity and food concentration on *Lophelia pertusa* (Scleractinia) zooplankton capture rates, *Journal of Experimental Marine Biology and Ecology*, 395, 55-62
- Reed J.K. (2002) Deep-water *Oculina* coral reefs of Florida: biology, impacts, and management, *Hydrobiologia*, 471, 43-55
- Reichel L. (2012) Succession of benthic hard bottom communities in the shallow sublittoral of Comau Fjord, Chile, Master-thesis: Christian-Albrechts-Universität zu Kiel, 63 pp.
- Revsbech N. P. (1995) Microenvironment and photosynthesis of zooxanthellae in scleractinian corals studied with microsensors for O₂, pH and light, *Marine ecology progress series*, 117, 159-172
- Reynaud-Vaganay S., Juillet-Leclerc A., Jaubert J., Gattuso J-P. (2001) Effect of light on skeletal $\delta_{13}\text{C}$ and $\delta_{18}\text{O}$, and interaction with photosynthesis, respiration and calcification in two zooxanthellate scleractinian corals, *Palaeogeography, Palaeoclimatology, Palaeoecology*, 175, 393-404
- Ries J.B., Cohen A.L., McCorkle D.C. (2009a) Marine calcifiers exhibit mixed responses to CO₂-induced ocean acidification, *Geology*, 37, 1131-1134
- Ries J.B., Cohen A.L., McCorkle D.C. (2009b) A nonlinear calcification response to CO₂-induced ocean acidification by the coral *Oculina arbuscula*, *Geology*, 37, 1057-1152
- Risk M.J., Heikoop J.M., Snow M.G., Beukens R. (2002) Lifespans and growth patterns of two deep-sea corals: *Primnoa resedaeformis* and *Desmophyllum cristagalli*. *Hydrobiologia*, 471, 125-131
- Roberts J. M., Wheeler A. J., Freiwald A. (2006) Reefs of the deep: The biology and geology of cold water coral ecosystems, *Science*, 312 (5773), 543-547
- Roberts J. M., Wheeler A. J., Freiwald A. (2006) Reefs of the deep: The biology and geology of cold water coral ecosystems, *Science*, 312(5773), 543-547

15 References

- Roberts J.M., Wheeler A.J., Freiwald A., Cairns S. (2009) Cold-water corals – The Biology and Geology of Deep-Sea Coral Habitats, Cambridge University Press, The Edinburgh Building, Cambridge CB2 8RU, United Kingdom
- Rosa R., Seibel B.A. (2008) Synergistic effects of climate-related variables suggest future physiological impairment in an oceanic predator, *Proceeding of the National Academy of Sciences, USA* 105, 20776-20780
- Schumann R. (2012) Online Unterlagen, Methodenbeschreibungen und Arbeitsanleitungen Sauerstoffsättigung, Universität Rostock - Biologische Station Zingst, URL: <http://www.bsz.uni-rostock.de/stationslehre/lernmaterial/> (date: 13.11.2015)
- Silva N. (2008) Dissolved oxygen, pH and nutrients in the austral Chilean channels and fjords, *Comité Oceanográfico Nacional – Pontificia Universidad Católica de Valparaíso, Valparaíso*, 37-43
- Silverman J., Lazar B., Erez J. (2007) The effect of aragonite saturation, temperature and nutrients on the community calcification rate of a coral reef, *Journal of Geophysical Research (1978–2012)*, 112.C5
- Smith J.E., Price N.N., Nelson C.E., Haas A.F. (2013) Coupled changes in oxygen concentration and pH caused by metabolism of benthic coral reef organisms, *Marine Biology*, 160, 2437-2447
- Sokol S. (2012) The influence of heterotrophy and flow on calcification of the cold-water coral *Desmophyllum dianthus*, Diploma thesis, Christian-Albrechts-University of Kiel, 95 pp.
- Stolzenberger-Ramirez A. (2010) URL: <http://www.geodsz.com/deu/d/Korallen>, (date: 13.11.2015)
- Telesnicki G. J., Goldberg W. M. (1995) Effects of turbidity on the photosynthesis and respiration of two South Florida reef coral species, *Bulletin of Marine Science*, 57(2), 527-539
- Thresher R.E., Tilbrook B., Fallon S., Wilson N.C., Adkins J. (2011) Effects of chronic low carbonate saturation levels on the distribution, growth and skeletal chemistry of deep-sea corals and other seamount megabenthos, *Marine Ecology Progress Series*, 442, 87-99
- Valle-Levinson A., Sarkar N., Sanay R., Soto D., León J. (2007) Spatial structure of hydrography and flow in a Chilean fjord, *Estuario Reloncavi, Estuaries and Coasts*, 30, 113-126
- Venn A., Tambutté E., Holcomb M., Allemand D., Tambutté S. (2011) Live tissue imaging shows reef corals elevate pH under their calcifying tissue relative to sea water, *PLoS ONE*, 6, e20013
- Vila A.R., Falabella V., Gálvez M., Fariás A., Droguett D., Saavedra B. (2015) Identifying high-value areas to strengthen marine conservation in the channels and fjords of the southern Chile ecoregion, *Oryx*, doi:10.1017/S0030605314000908
- Wolf-Gladrow D.A., Zeebe R.E., Klaas C., Körtzinger A., Dickson A.G. (2007) Total alkalinity: The explicit conservative expression and its application to biogeochemical processes, *Marine Chemistry*, 106, 287-300
- Wurz E. (2014) Autökologie der Kaltwassersteinkoralle *Caryophyllia huinayensis* aus der patagonischen Fjordregion, Master Thesis: Universität Rostock, 73 pp.
- Wendländer N. (2014) Bachelor-Thesis: Abundance, Clearance Rate and Respiration of the Chilean cold-water coral *Caryophyllia huinayensis*, Bachelor-Thesis: Christian-Albrechts-University of Kiel, 50 pp.

16 APPENDIX

Appendix 1: Logged temperature [°C]

Table A1.1: Logged temperature [°C] at XHuinay North (Feb. 2014-Feb. 2015), depth: 20m

Month	Average temperatures [°C]	SD [°C]
February 2014	11.57	± 0.54
March 2014	12.64	± 0.89
April 2014	11.98	± 0.53
May 2014	11.60	± 0.39
June 2014	11.16	± 0.16
July 2014	10.99	± 0.14
August 2014	10.55	± 0.15
September 2014	10.74	± 0.08
October 2014	11.09	± 0.43
November 2014	11.22	± 0.40
December 2014	11.56	± 0.77
January 2015	11.39	± 0.51
February 2015	11.52	± 0.50

Table A1.2: Logged temperature [°C] at Lilliguapi (February 2014-January 2015), depth: 20m

Month	Average temperatures [°C]	SD [°C]
February 2014	12.85	± 0.93
March 2014	12.77	± 0.71
April 2014	11.96	± 0.29
May 2014	11.42	± 0.18
June 2014	10.80	± 0.21
July 2014	10.50	± 0.20
August 2014	10.41	± 0.17
September 2014	10.80	± 0.10
October 2014	11.21	± 0.37
November 2014	11.51	± 0.38
December 2014	12.22	± 0.92
January 2014	12.14	± 0.55

Table A1.3: Logged temperature [°C] at Ensenada de Las Islas (February 2014-January 2015), depth: 22m

Month	Average temperatures [°C]	SD [°C]
February 2014	12.16	± 0.40
March 2014	12.23	± 0.60
April 2014	11.61	± 0.20
May 2014	10.97	± 0.83

16 Appendix

June 2014	10.37	± 0.26
July 2014	10.07	± 0.40
August 2014	9.92	± 0.07
September 2014	10.2	± 0.04
October 2014	10.55	± 0.15
November 2014	10.9	± 0.19
December 2014	11.63	± 0.41
January 2014	12.59	± 0.72

Appendix 2: pH

Table A2.1: Manually pH measurements at Lilliguapi and XHuinay North

Date	Location	pH	SD
30.01.2015	Lilliguapi	7.90	± 0.01
30.01.2015	Lilliguapi	7.92	± 0.01
05.02.2015	Lilliguapi	7.90	± 0.01
21.02.2015	Lilliguapi	7.85	± 0.04
23.02.2015	Lilliguapi	7.77	± 0.01
25.01.2015	XHuinay North	7.72	± 0.00
29.01.2015	XHuinay North	7.72	± 0.04
31.01.2015	XHuinay North	7.63	± 0.01
31.01.2015	XHuinay North	7.63	± 0.00
31.01.2015	XHuinay North	7.66	± 0.00
01.02.2015	XHuinay North	7.68	± 0.01
08.02.2015	XHuinay North	7.68	± 0.01
24.02.2015	XHuinay North	7.60	± 0.01

Table A2.2: Statistical report for ANOVA of manually measured pH values at Lilliguapi and XHuinay North

Residuals:					
	Min	1Q	Median	3Q	Max
	- 0.098	-0.035	0.015	0.032	0.055
Coefficients:					
	Estimate	Std. Error	t value	Pr(> t)	
(Intercept)	7.86800	0.02251	349.461	2e-16	
Lilliguapi/XHuinay North	-0.20300	0.02870	-7.073	2.06e-5	
Residual standard error:	0.05034 on 11 degrees of freedom				
Multiple R-squared:	0.8198		Adjusted R-squared: 0.8034		
F-statistic:	50.03 on 1 and 11 DF		p- value:	2.064e-5	

Appendix 3: Total Alkalinity**Table A3.1:** Total Alkalinity at XHuinay North, Lilliguapi and Ensenada de Las Islas in mmol l⁻¹

Date	Location	Average TA [mmol l ⁻¹]
26.01.2015	XHuinay North	2.288
28.01.2015	XHuinay North	2.273
29.01.2015	XHuinay North	2.206
01.02.2015	XHuinay North	2.220
08.02.2015	XHuinay North	2.226
20.02.2015	XHuinay North	2.233
28.01.2015	Lilliguapi	2.192
30.01.2015	Lilliguapi	2.210
04.02.2015	Lilliguapi	2.229
21.02.2015	Lilliguapi	2.243
18.02.2015	Ensenada de Las Islas	2.182

Table A3.2: Statistical report for ANOVA of Total Alkalinity values at XHuinay North and Lilliguapi

Residuals:					
	Min	1Q	Median	3Q	Max
	-0.036500	-0.020637	-0.008025	0.019700	0.055900
Coefficients:					
	Estimate	Std. Error	t value	Pr(> t)	
(Intercept)	2.18550	0.007955	278.893	<2 e ⁻¹⁶	
Lilliguapi/XHuinay North	0.022350	0.010270	2.176	0.0381	
Residual standard error:	0.02756 on 28 degrees of freedom				
Multiple R-squared:	0.1447		Adjusted R-squared: 0.1141		
F-statistic:	4.736 on 1 and 28 DF		p- value:		0.0318

Table A3.3: Statistical report for ANOVA of TA values at XHuinay North and Ensenada de Las Islas

Residuals:					
	Min	1Q	Median	3Q	Max
	- 0.0365	-0.0203	-0.0077	0.0090	0.0559
Coefficients:					
	Estimate	Std. Error	t value	Pr(> t)	
(Intercept)	2.240900	0.006999	320.164	<2 e ⁻¹⁶	
XHuinay North/Ensenada de Las Islas	-0.058467	0.018518	-3.157	0.00519	
Residual standard error:	0.0297 on 19 degrees of freedom				
Multiple R-squared:	0.3441		Adjusted R-squared: 0.3096		
F-statistic:	9.968 on 1 and 19 DF		p- value:		0.005188

Table A3.4: Statistical report for ANOVA of TA values at Lilliguapi and Ensenada de Las Islas

Residuals:					
	Min	1Q	Median	3Q	Max
	- 0.033450	-0.008800	-0.001833	0.010950	0.025850
Coefficients:					
	Estimate	Std. Error	t value	Pr(> t)	
(Intercept)	2.218550	0.005408	410.223	<2 e ⁻¹⁶	
Lilliguapi/Ensenada de Las Islas	-0.036117	0.012093	-2.987	0.0105	
Residual standard error:	0.01873 on 13 degrees of freedom				
Multiple R-squared:	0.4069		Adjusted R-squared: 0.3613		
F-statistic:	8.92 on 1 and 13 DF		p- value:		0.01051

Appendix 4: Abundance and substrate inclination**Table A4.1:** Abundance in different depth zones at XHuinay North

Location	Depth [m]	Individuals / Sampling frame	n / m ²	Substrate Inclination [°]
XHuinay North	16	3	52	71
XHuinay North	16	2	35	74
XHuinay North	16	2	35	77
XHuinay North	16	1	17	102
XHuinay North	16	2	35	105
XHuinay North	16	6	104	106
XHuinay North	16	4	69	109
XHuinay North	16	1	17	113
XHuinay North	16	13	225	113
XHuinay North	16	1	17	115
XHuinay North	16	2	35	116
XHuinay North	16	5	87	119
XHuinay North	16	5	87	120
XHuinay North	16	2	35	121
XHuinay North	16	3	52	122
XHuinay North	16	4	69	123
XHuinay North	16	2	35	125
XHuinay North	16	3	52	126
XHuinay North	19	2	35	104
XHuinay North	19	1	17	109
XHuinay North	19	5	87	110
XHuinay North	19	9	156	111
XHuinay North	19	5	87	111
XHuinay North	19	1	17	111
XHuinay North	19	4	69	113
XHuinay North	19	9	156	115

16 Appendix

XHuinay North	19	4	69	116
XHuinay North	19	2	35	116
XHuinay North	19	5	87	116
XHuinay North	19	2	35	117
XHuinay North	19	5	87	120
XHuinay North	22	4	69	79
XHuinay North	22	5	87	91
XHuinay North	22	5	87	103
XHuinay North	22	7	121	106
XHuinay North	22	3	52	108
XHuinay North	22	2	35	110
XHuinay North	22	10	173	110
XHuinay North	22	6	104	111
XHuinay North	22	6	104	112
XHuinay North	22	3	52	113
XHuinay North	22	2	35	113
XHuinay North	22	6	104	114
XHuinay North	22	6	104	114
XHuinay North	22	3	52	115
XHuinay North	22	2	35	117
XHuinay North	22	7	121	117
XHuinay North	22	2	35	122
XHuinay North	22	2	35	144
XHuinay North	22	2	35	145
XHuinay North	22	5	87	145
XHuinay North	25	2	35	104
XHuinay North	25	4	69	105
XHuinay North	25	2	35	108
XHuinay North	25	2	35	110
XHuinay North	25	5	87	111
XHuinay North	25	3	52	111
XHuinay North	25	2	35	112
XHuinay North	25	1	17	114
XHuinay North	25	6	104	114
XHuinay North	25	4	69	114
XHuinay North	25	1	17	117
XHuinay North	25	3	52	117
XHuinay North	25	2	35	118
XHuinay North	25	12	208	119
XHuinay North	25	5	87	119
XHuinay North	25	1	17	121
XHuinay North	25	4	69	123
XHuinay North	25	8	139	124
XHuinay North	25	9	156	126
XHuinay North	25	5	87	128

16 Appendix

XHuinay North	25	3	52	131
---------------	----	---	----	-----

Table A4.2: Abundance in different depth zones at Ensenada de Las Islas

Location	Depth [m]	Individuals / Sampling frame	n / m ²	Substrate Inclination [°]
Ensenada de Las Islas	21	12	208	84
Ensenada de Las Islas	21	8	139	90
Ensenada de Las Islas	21	17	295	93
Ensenada de Las Islas	21	12	208	97
Ensenada de Las Islas	21	11	191	103
Ensenada de Las Islas	21	15	260	106
Ensenada de Las Islas	21	6	104	107
Ensenada de Las Islas	21	6	104	108
Ensenada de Las Islas	21	17	295	108
Ensenada de Las Islas	21	9	156	108
Ensenada de Las Islas	21	8	139	110
Ensenada de Las Islas	21	9	156	111
Ensenada de Las Islas	21	6	104	113
Ensenada de Las Islas	21	4	69	113
Ensenada de Las Islas	21	6	104	113
Ensenada de Las Islas	21	3	52	114
Ensenada de Las Islas	21	8	139	115
Ensenada de Las Islas	21	8	139	118
Ensenada de Las Islas	24	8	139	112
Ensenada de Las Islas	24	5	87	112
Ensenada de Las Islas	24	10	173	112
Ensenada de Las Islas	24	5	87	113
Ensenada de Las Islas	24	7	121	113
Ensenada de Las Islas	24	9	156	114
Ensenada de Las Islas	24	7	121	114
Ensenada de Las Islas	24	7	121	114
Ensenada de Las Islas	24	2	35	115
Ensenada de Las Islas	24	8	139	115
Ensenada de Las Islas	24	1	17	115
Ensenada de Las Islas	24	8	139	115
Ensenada de Las Islas	24	8	139	116
Ensenada de Las Islas	24	9	156	119
Ensenada de Las Islas	24	8	139	119
Ensenada de Las Islas	24	7	121	122
Ensenada de Las Islas	27	8	139	71
Ensenada de Las Islas	27	8	139	77
Ensenada de Las Islas	27	15	260	79
Ensenada de Las Islas	27	8	139	81
Ensenada de Las Islas	27	8	139	88
Ensenada de Las Islas	27	9	156	88

16 Appendix

Ensenada de Las Islas	27	4	69	96
Ensenada de Las Islas	27	9	156	100
Ensenada de Las Islas	27	4	69	102
Ensenada de Las Islas	27	13	225	110

Table A4.3: Statistical report for ANOVA of abundance of *T. endesa* in 21/22m depth at Ensenada de Las Islas and XHuinay North

Residuals:					
	Min	1Q	Median	3Q	Max
	-107.000	-32.733	-6.733	28.267	136.000
Coefficients:					
	Estimate	Std. Error	t value	Pr(> t)	
(Intercept)	159.00	13.22	12.024	3.3e-13	
Ensenada de Las Islas/XHuinay North	-83.27	19.61	- 4.245	0.000184	
Residual standard error:	56.1 on 31 degrees of freedom				
Multiple R-squared:	0.3677		Adjusted R-squared: 0.3473		
F-statistic:	18.02 on 1 and 31 DF		p- value:		0.0001839

Appendix 5: Mass Increase

Table A5.1: Mass increase (mg y^{-1} and $\% \text{d}^{-1}$). Treatments: L and X (Controls), LtoX (transplanted from high to low pH), XtoL (transplanted from low to high pH).

Sample	Treatment	Increase [mg yr^{-1}]	Increase [$\% \text{d}^{-1}$]
L5	L	76.64	0.02
L8	L	73.23	0.04
L12	L	49.41	0.02
L13	L	41.49	0.02
L14	L	63.76	0.03
L15	L	67.40	0.03
L17	L	28.56	0.01
L18	L	100.60	0.04
L19	L	42.01	0.02
L88	L	61.01	0.02
L99	L	112.11	0.05
L1	L to X	84.38	0.03
L4	L to X	74.53	0.03
L6	L to X	70.40	0.03
L7	L to X	56.95	0.03
L11	L to X	61.09	0.03

16 Appendix

L16	L to X	71.98	0.03
X4	X	33.22	0.01
X5	X	58.29	0.02
X6	X	83.69	0.04
X7	X	124.11	0.05
X10	X	62.69	0.03
X13	X	55.35	0.02
X14	X	59.50	0.02
X16	X	96.44	0.04
X19	X	60.31	0.02
X33	X	66.85	0.02
X12	X	108.58	0.05
X1	X to L	61.64	0.03
X2	X to L	88.54	0.03
X3	X to L	34.83	0.02
X9	X to L	46.40	0.01
X11	X to L	36.24	0.02
X15	X to L	27.18	0.01
X17	X to L	34.39	0.01
X20	X to L	95.68	0.03

Appendix 6: Respiration rates (RR)

Table A6.1: Correlation of Dry Mass and calyx surface area

Dry Mass [g]	Calyx surface area [cm ²]
0.31	2.20
0.56	2.20
0.60	2.36
0.38	2.20
0.22	1.88
0.36	1.88
1.42	2.83
0.62	2-20
0.20	1.57
0.43	2.04

Table A6.2: Respiration rates [$\mu\text{Mol} \times \text{O}_2 \times \text{cm}^{-2} \times \text{d}^{-1}$] measured via handheld Luminescent/Optical Dissolved Oxygen Probe

Sample	Treatment	RR [$\mu\text{Mol} \times \text{O}_2 \times \text{cm}^{-2} \times \text{d}^{-1}$]	SD [$\mu\text{Mol} \times \text{O}_2 \times \text{cm}^{-2} \times \text{d}^{-1}$]
L19	L	9.54	± 0.61
L13	L	11.20	± 0.85
L5	L	7.67	± 0.00
L15	L	6.37	± 0.10

L99	L	12.45	± 0.11
L1	LtoX	11.71	± 0.08
L2	LtoX	18.10	± 0.10
L6	LtoX	9.95	± 0.10
L16	LtoX	6.37	± 0.13
L4	LtoX	10.29	± 0.10
L11	LtoX	8.87	± 0.13
L88	LtoX	15.94	± 0.17
L17	LtoX	7.13	± 0.11
L18	LtoX	6.76	± 0.11
X4	X	15.84	± 0.11
X14	X	14.22	± 0.10
X12	X	3.33	± 0.18
X10	X	6.26	± 0.11
X7	X	9.23	± 0.11
X16	X	7.25	± 0.13
X20	X	8.54	± 0.10
X17	X	5.21	± 0.10
X15	X	4.15	± 0.09
X3	XtoL	7.76	± 0.13
X2	XtoL	6.72	± 0.10

Table A6.3: Respiration rates [$\mu\text{Mol} \times \text{O}_2 \times \text{cm}^{-2} \times \text{d}^{-1}$] measured via optodes and respiration chambers

Sample	Treatment	RR [$\mu\text{Mol} \times \text{O}_2 \times \text{cm}^{-2} \times \text{d}^{-1}$]	SD [$\mu\text{Mol} \times \text{O}_2 \times \text{cm}^{-2} \times \text{d}^{-1}$]
L14	L	6.15	± 0.13
L8	L	7.61	± 0.12
L12	L	3.38	± 0.10
L7	LtoX	11.60	± 0.14
L10	LtoX	1.99	± 0.10
X13	X	9.32	± 0.17
X33	X	5.51	± 0.07
X5	X	8.29	± 0.15
X19	X	1.27	± 0.32
X6	X	1.78	± 0.34
X9	XtoL	10.22	± 0.09
X8	XtoL	7.61	± 0.95

17 DECLARATION OF ACADEMIC INTEGRITY

(SELBSTSTÄNDIGKEITSERKLÄRUNG)

Hiermit erkläre ich, dass ich die vorliegende Arbeit selbstständig und ohne fremde Hilfe angefertigt und keine anderen als die angegebenen Quellen und Hilfsmittel verwendet habe. Die eingereichte schriftliche Fassung der Arbeit entspricht der auf dem elektronischen Speichermedium.

Weiterhin versichere ich, dass diese Arbeit noch nicht als Abschlußarbeit an anderer Stelle vorgelegen hat.

I hereby declare that I have completed the available thesis in my own and have not used any other than the stated sources and aids. The submitted written version corresponds to the electronic one.

Furthermore, I assure that this thesis has not been presented as final assignment somewhere else.

Ort / place, Datum / date

Unterschrift / signature